A COMPARATIVE STUDY ON SILICON, GERMANIUM AND SILICON CARBIDE BASED POWER MOSFET AND PiN DIODE

by

TANVIR YOUSUF SHOHAG

KAZI MAHAMUD AL MASUM

BACHELOR OF SCIENCE IN ELECTRICAL AND ELECTRONIC ENGINEERING

Department of Electrical and Electronic Engineering
INTERNATIONAL ISLAMIC UNIVERSITY CHITTAGONG

APRIL 2022

A COMPERATIVE STUDY ON SILICON, GERMANIUM AND SILICON CARBIDE BASED POWER MOSFET AND PiN DIODE

by

TANVIR YOUSUF SHOHAG

KAZI MAHAMUD AL MASUM

A thesis
submitted as partial fulfilment of the requirement for the degree of

BACHELOR OF SCIENCE IN ELECTRICAL AND ELECTRONIC ENGINEERING

Department of Electrical and Electronic Engineering
INTERNATIONAL ISLAMIC UNIVERSITY CHITTAGONG

APRIL 2022

CERTIFICATE OF APPROVAL

The thesis entitled as "**A Comparative Study on Silicon, Germanium and Silicon Carbide Based Power MOSFET And PiN Diode**" submitted by **Tanvir Yousuf Shohag**, bearing Matric ID. **ET-161027** and **Kazi Mahamud Al Masum**, bearing Matric ID. **ET-161030** of session **Spring 2016**, to the Department of Electrical and Electronic Engineering, International Islamic University Chittagong, has been accepted as satisfactory in partial fulfilment of the requirements for the degree of Bachelor of Science in Engineering and approved for the examination held on **16 April, 2022**.

____

Supervisor
Engr. Md. Shahid Ullah
Assistant Professor,
Department of Electrical and Electronic Engineering
International Islamic University Chittagong.

DECLARATION

It is hereby declared that this work has been done by us and no portion of the work contained in this thesis/project has been submitted elsewhere for the award of any degree or diploma.

____

Tanvir Yousuf Shohag

____

Kazi Mahamud Al Masum

ACKNOWLEDGMENT

All praises and thanks to Allah (SWT), the Lord of the world, the most Beneficent, without Whose mercy it would not be possible for us to complete this thesis.

After that, we deeply acknowledge our sense of gratitude and sincere appreciation to our honourable thesis supervisor, Engr. Md. Shahid Ullah, Assistant Professor, Department of EEE, IIUC for his continuous support, encouragement, and suggestions throughout the whole time of the thesis. It was quite impossible to continue with the thesis work without his kind guidance. He was very helpful and ever affectionate to endure the mistakes we had committed several times during the work and always encouraged us by correcting our approaches.

Then, we are also thankful to the faculty members of our department for their kind support in this regard, especially to our undergrad advisor, Engr. Md. Lokman Hossain, Lecturer, Department of EEE, IIUC. We also owe to all those authors and researchers whose work we used in designing the research and in preparing this thesis.

Finally, we can't emphasize enough to express our heartiest gratitude to our beloved parents, family, close friends and well-wishers for their eternal support and inspiration, which are the continuous source of strength for accomplishing and being consistent all the time in this journey.

Authors

ABSTRACT

Improving switching characteristics is one of the ongoing challenges for all power electronics devices like- transistors, MOSFETs, diodes. For overcoming this particular challenge, researchers have been working on its internal structures, setups as well as several material-based studies. In this study, the switching characteristics of MOSFETs and PiN diodes have been analysed. For the MOSFET, the DC characteristics are shown after changing its base materials by Si, Ge and SiC but the overall study and simulation setups were kept as usual. Among the three, the Ge based MOSFET shows comparatively better response than the MOSFETs of Si and SiC based in terms of its turn on voltage and output characteristics. Same type of materials-based study were done for the PiN diodes. The Ge based PiN diode depicts better forward recovery time as well as forward recovery voltage than for the others two materials. This study describes briefly about the outcomes from the three MOSFETs along with the three PiN diodes.

TABLE OF CONTENTS

LIST OF FIGURES

LIST OF TABLES

LIST OF ABBREVIATIONS

Si	Silicon
SiC	Silicon Carbide
Ge	Germanium
MOSFET	Metal Oxide Semiconductor- Field Effect Transistor
GaN	Gallium Nitride
GaAs	Gallium Arsenide
WBG	Wide-Bandgap
IGBT	Insulated-Gate Bipolar Transistor
JFET	Junction-Gate Field-Effect Transistor
MOS	Metal-Oxide Semiconductor
V_{Fr}	Forward Recovery Voltage
V_{Rr}	Reverse Recovery Voltage
V_d	Drain Voltage
V_g	Gate Voltage
V_s	Source Voltage
SOI	Silicon-on -Insulator
nMOS	n-Channel Metal-Oxide Semiconductor
pMOS	p-Channel Metal-Oxide Semiconductor

CHAPTER 1
INTRODUCTION

1.1 Introduction

Solid-state electronics, also known as power electronics, are used to control and convert electrical power. Semiconductors are important in power electronics evaluation because they provide higher efficiency, higher power density, and lower cost in an integrated system [1].

The age of Si power devices spanned the last half-century. For example, Si MOSFETs with a trench gate structure is popular for applications below 600 V. On the other hand, super junction Si MOSFETs and Si insulated gate bipolar transistors (IGBTs) are preferred for 600 V to 6.5 kV, and the Si IGBT practical operating temperature is below 173°C [2]. Si devices, on the other hand, have some performance limitations, such as lower switching frequency, switching speed, operational temperature and voltage, and so on. Wide band gap (WBG) materials, such as silicon carbide (SiC) and gallium nitrate (GaN), have emerged as a breakthrough for power device applications [2]. **Fig. 1** depicts the reasons why Si should be phased out of the power electronics industry.

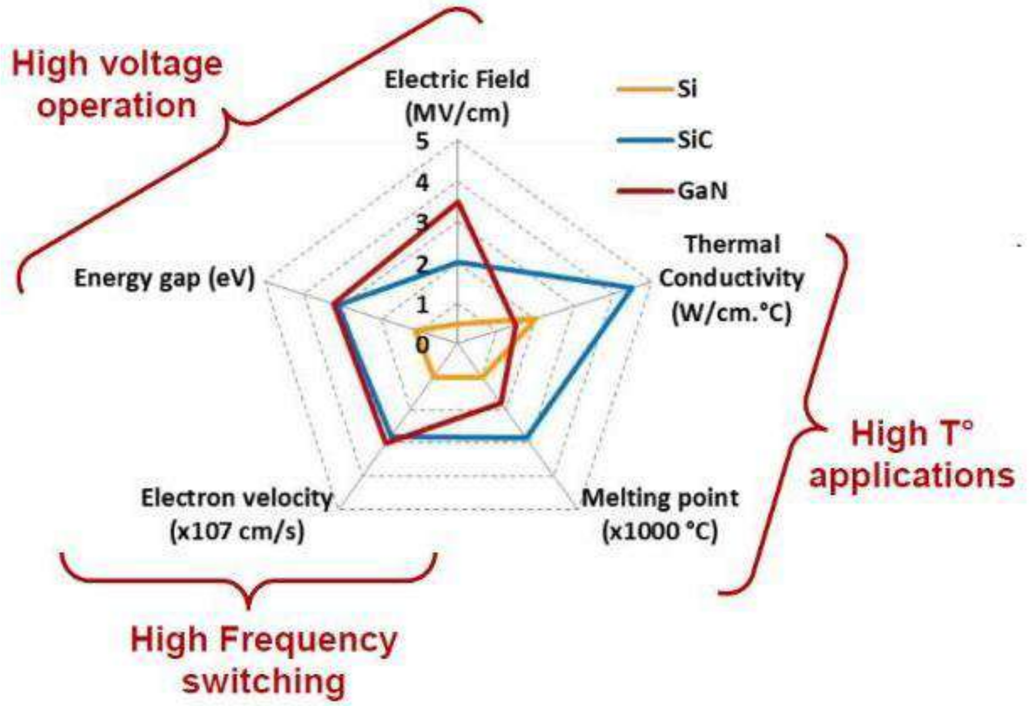

Fig. 1. Comparison of Material attributes among Si, SiC and GaN with a range of 0 to 5 [2]

After the age of Si as a wide-bandgap semiconductor material, SiC began to play a crucial but popular role in the evolution process of this industry for the last two decades, with Ge also becoming popular in some aspects [1], [3]–[5]. The switching characteristics of power switches such as power diodes, MOSFETs, IGBTs, and BJTs are another important aspect of this topology [1], [5].

Power MOSFETs and their overall performance with various materials and MOSFET structures have been the subject of extensive research [5]–[8]. In some aspects, SiC devices have an 80% lower switching loss than Si devices, prompting the development of a hybrid application of Si-IGBT and SiC-MOSFET [9]. The SiC MOSFET performed better than the Si-MOSFET in terms of on-resistance and high-temperature applications [7]. Junction Field-effect Transistors (JFET) research has been done using various materials such as Si, SiC, and others to overcome MOSFET's challenges [10]. The total ionization dose degrades the MOSFET's oxide layer, resulting in a change in threshold voltage and current rating, according to the researchers [11]. A MOSFET's DC characteristics under optical illumination were also studied [12]. The majority of this type of research uses Si, SiC, GaAs, GaN, and other similar materials, but other materials such as Ge have also been used [10].

However, after varying the semiconductor materials by Si, Ge, and SiC, the DC characteristics of MOSFETs for specific parameter settings are discussed in this paper. Using the COMSOL Multiphysics simulation software, the responses of the three MOSFETs based on Si, Ge, and SiC were simulated sequentially in terms of electron concentration, hole concentration, electric potentials, transfer characteristics, and output characteristics. Throughout the study, it was discovered that the Ge MOSFET outperforms the other two in certain methodologies, despite Si and SiC's dominance [3], [7]. Besides, There are many researches done on low and high-power diodes such as PN junction diode, Schottky, JBS, and PiN diodes in different aspects [13]–[16]. The forward and reverse recovery of different PiN diodes have also been studied several years how to reduce the recovery time and power loss along with using different semiconductor materials [17]–[20]. In this study, we discussed about the switching and recovery characteristics of PiN diode for Si, Ge and SiC materials.

1.2 Basics of n-type MOSFET

1.2.1 MOSFET’s Structure

MOSFETs are a type of Field-effect Transistors that have oxide insulation in the gate metal. Because of its advantages over other types of MOSFET, the enhancement type MOSFET with n-channel is more popular, and its construction is shown in **Fig. 2**[6].

An nMOS is a voltage-controlled device with highly n-type doped source and drain regions, as well as a p-type doped body region, and four types of terminals: source(S), drain(D), gate(G), and body(B) [6].

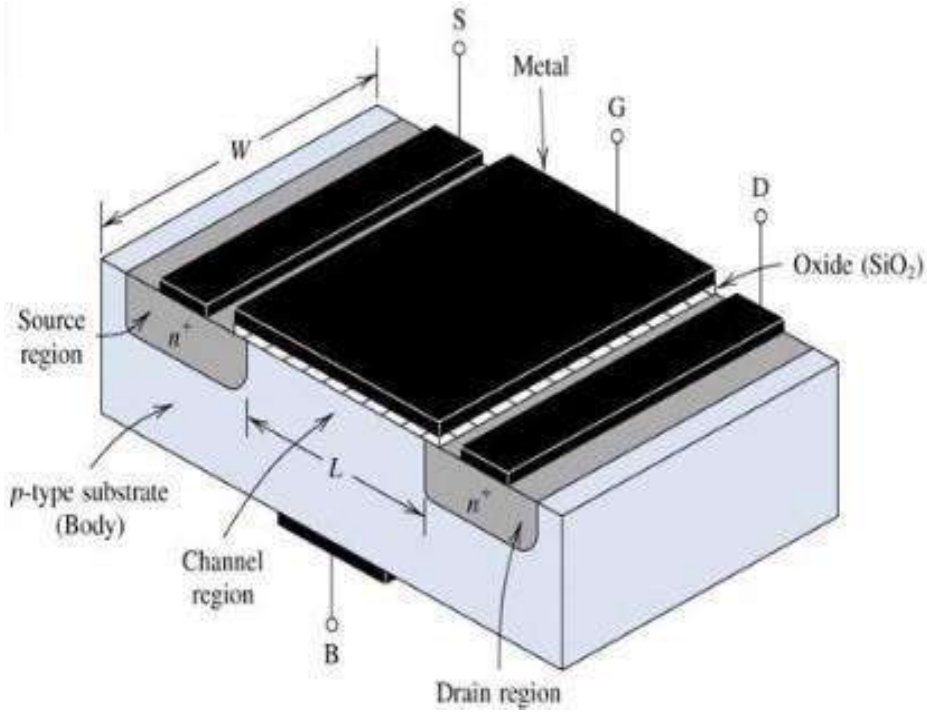

2

Fig. 2. An n-type enhancement MOSFET from the perspective view [21]**.**

1.2.2 N-type MOSFET’s switching and its DC Characteristics

Because both the source and the body are grounded, the gate-to-source voltage (V_{gs}) is in charge of creating the channel between the source and the drain, as well as controlling the threshold voltage (V_t), which causes the channel to start creating, and finally, the drain-to-source voltage (V_{ds}) is in charge of controlling the terminal current (I_d) [22].

Fig. 3 depicts the output characteristics curve of a basic nMOS with the triode and saturation region [21], [22]. Besides, the threshold voltage of the MOSFET can be understood from the figure.

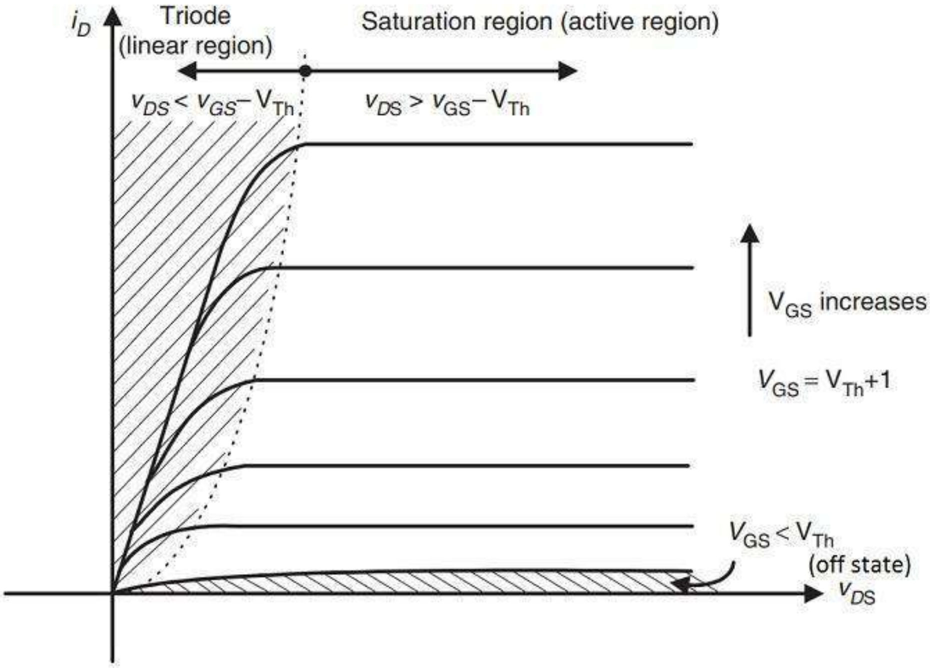

Fig. 3. Output characteristics of an enhancement n-type MOSFET [22]**.**

1.3 Basics of PIN Diode

1.3.1 PIN Diode's Structure

Like any other normal diode, the PiN diode has a highly doped P^+ region is separated by an intrinsic region from the N^+ region, as **Fig. 4(a)** [23].

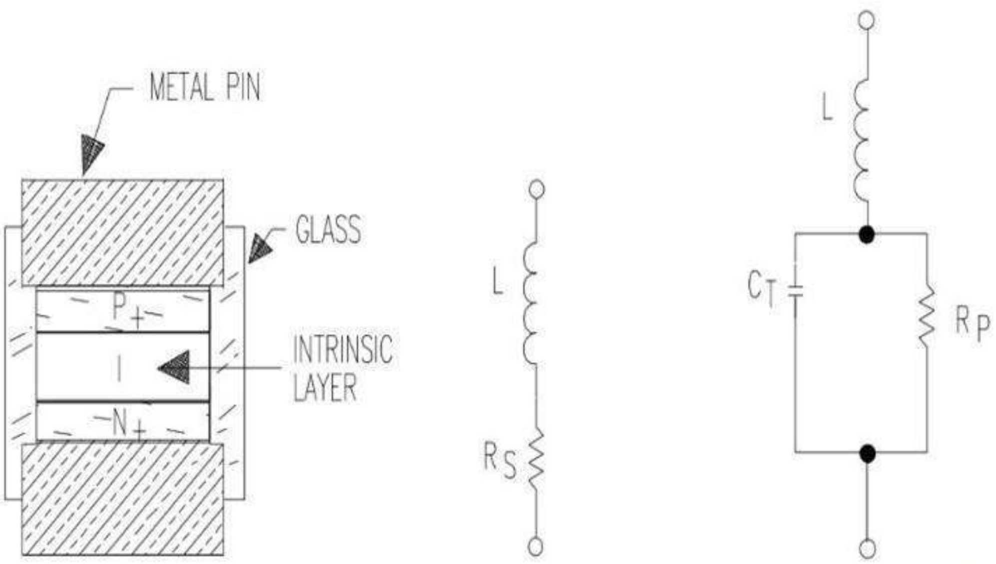

(a) Cross section **(b) Forward Biasing** **(c) Reverse Biasing**

Fig. 4. Structure and biasing conditions of a PiN diode, (a) Cross section (b) Forward Biasing (c) Reverse Biasing [23]

The intrinsic region is injected with holes and electrons during the forward-biased condition. In the intrinsic region, these electrons and holes can't recombine instantly, but rather has a certain amount of lifespan (τ). However, there is no stored charge in the intrinsic region during the reverse-biased condition and the device functions as a Capacitance (C_T) shunted by a parallel resistance (R_P). The corresponding diagrams on forward and reverse biasing circuits are shown by **Fig. 4(b)** and **Fig. 4(c)** respectively [23], [24].

1.3.2 Switching and Recovery Characteristics of PiN Diode:

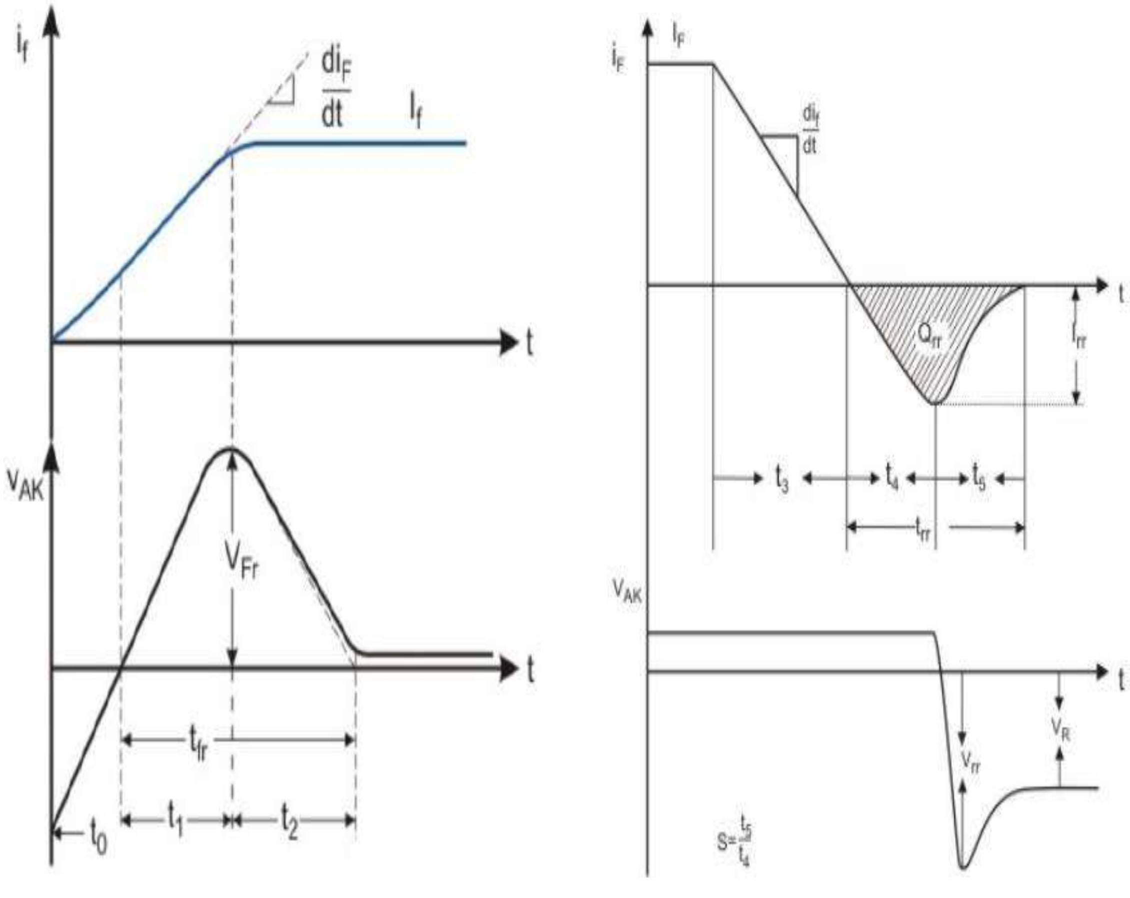

(a) Forward Recovery **(b) Reverse Recovery**

Fig. 5. Recovery characteristics of a PiN diode, (a) Forward Recovery (b) Reverse Recovery [24]

Transitioning from reverse to forward biased, power diodes need a certain amount of time when it's called turn ON. During the transition to ON state, forward diode voltage drop, V_{Fr} transiently reaches a high value due to the sudden rising rate of the forward current and after the forward recovery time, t_{fr}, the V_{Fr} reaches a steady-state value with steady but forward recovery current, If, is shown in **Fig. 5(a)** [24].

Similarly, the transition from forward to reverse biased needs a reverse recovery time, t_{rr} to reach the recovery level of reverse recovery voltage drop, V_{Rr} with reverse recovery current, I_{rr} after a sudden fall rate, which is also shown in **Fig. 5(b)** [24].

1.4 Objective

Our objective is findings on switching and DC characteristics such as transfer characteristics, output characteristics, etc. as well as carrier concentration, electric potentials of the Metal Oxide Semiconductor Field-effect Transistors (MOSFET) as well as how the forward recovery properties of a PiN diode changed after the semiconductor materials were altered by Silicon (Si), Germanium (Ge) and Silicon Carbide (SiC) material.

1.5 Thesis Outline

In this thesis, we described and discussed about our analysis in 5 chapters. The outlines of our thesis are as follows:

Chapter 1 contains the introduction. In this chapter, introduction of the thesis topic has been discussed.

Chapter 2 contains literature review. All the previous works related to this thesis has been discussed in this chapter.

Chapter 3 contains methodology where the method of developing the Comsol model has been discussed.

Chapter 4 contains result and discussion where the result of our thesis has been discussed.

Chapter 5 contains conclusion where conclusion and future work has been discussed.

1.6 Summery

After the simulation, done by COMSOL Multiphysics 5.5 Software, the DC characteristics response for the Ge based n-type MOSFET is found better than the other Si and SiC based MOSFETs for a specific geometry and other setups. And for the PiN diode of Ge gave the better forward recovery characteristics than the other two, Si and SiC based PiN diode.

CHAPTER 2
LITERATURE REVIEW

2.1 Introduction

Essentially, power devices are electronic devices that convert or control electrical power flow. Diodes, MOSFETs, BJTs, IGBTs, Thyristors, and other common power devices are commercially available and well-known. The field of power electronics encourages the device of efficient switching with high voltage, high temperature as well as high current application. On these bases, Si based power devices has been dominated the field for a long age and nowadays SiC stats to play a popular role in some aspects as well as Ge based devices [3], [5], [25], [26]. All the time, the switching characteristics of various power electronic devices plays the crucial role in its efficiency and operation [3], [5], [25]–[27].

The MOSFET (Metal Oxide Semiconductor Field-effect Transistor) is a voltage control device in which the output current, terminal current, or drain current, Id, can be controlled by changing the gate voltage V_{gs}. Besides, many researches done on low and high-power diodes such as PN junction diode, Schottky, JBS, and PiN diodes in different aspects [14], [15], [27], [28]. The forward and reverse recovery of different PiN diodes have also been studied several years how to reduce the recovery time and power loss along with using different semiconductor materials [17], [19], [20], [29]. Some researchers proposed to use the SiC based PiN diode for efficient switching [27]. Silicon-on-Insulator (SOI) PiN diode achieved faster and half of reverse recovery time needed than the conventional diode for a certain parameter [30].

2.2 Power Devices of Different Materials

Power devices are electronic devices that convert or control electrical power flow. Nowadays WBG semiconductors are becoming more popular in power devices, such as diodes, JFETs, MOSFETs, IGBTs, and thyristors, due to their higher temperature, efficiency, voltage, switching speed, and switching frequency [1]–[3].

2.3 MOSFET’s Study

Vast research has been going on power MOSFET and its overall performance with different materials and structures of MOSFET used [3], [5], [7], [10]. SiC devices show about 80% lower loss in switching than the Si devices in some aspects so that hybrid application of Si-IGBT and SiC-MOSFET was also proposed [31]. On the aspect of on-resistance and high-temperature application, the SiC MOSFET showed better performance than the Si-MOSFET [1]. For overcoming MOSFET's challenges, research on Junction Field-effect Transistors (JFET) was done by using different materials like Si, SiC, and others [10]. Researchers presented how the MOSFET's oxide layer can be degraded by the total ionization dose causing the change in threshold voltage and current rating [11]. DC characteristics of a MOSFET under optical illumination were also researched [8]. Most of these types of research are based on Si, SiC, GaAs, GaN, etc., but the other materials like Ge [10], [32].

2.4 PIN Diode's Study

There are many types of research done on low and high-power diodes such as PN junction diode, Schottky, JBS, and PiN diodes in different aspects [6], [10], [32]. The forward and reverse recovery of different PiN diodes have also been studied for several years how to reduce the recovery time and power loss along with using different semiconductor materials [18]–[20]. Some researchers proposed to use the SiC-based PiN diode for efficient switching [5], [27]. Silicon-on-Insulator (SOI) PiN diode achieved faster and half of the reverse recovery time needed than the conventional diode for certain parameters [30].

2.5 Previous Work:

2.5.1 On a future for power electronics [J. D. Van Wyk et al. (2013)]:

In 2013, J. D. Wyk et al. [2] proposed that after at least a century, power electronics technology may be approaching maturity, which, like many other technologies before it, is a significant reason to critically analyse the current state of the art and prospective future progress. It's critical to understand how and when the original driving ideology for the extraordinary development of power electronics technology emerged in this process. On the basis of a state-of-the-art assessment, it may be concluded that the historical evolution of power electronics technology is approaching the boundaries of the technology's most essential internal metrics in its current form. This indicates that the internal development process has reached a mature stage. However, it is apparent that future maturity only relates to the internal constituent technologies of power semiconductor switch and power electronic switching network technology. Emerging applications can help drive the development of the core technologies of power electronics. External power electronics constituent technologies of packaging, manufacturing, cooling, control and sensing, and environmental impact technology are not only in their infancy, but will provide enormous research, development, and application opportunities—BUT will only be driven from the outside by emerging future applications!

2.5.2 A survey of wide bandgap power semiconductor devices [J. Millan et al. (2014)]:

In 2014, J. Millan et al. [3] published his research work on WBG materials. He proposed that the unique material features of WBG open the door to a new generation of more efficient power converters in areas where Si-based systems have significant constraints, such as high temperature, high voltage, and high frequency operation. Because of the commercial availability of high-quality wafers and the maturity of the technological process, SiC and GaN are the best WBG semiconductor materials for these new power devices at the moment. Commercially accessible high voltage SiC SBDs and JBS diodes are already serious competitors to Si diodes. SiC JFETs and MOSFETs, on the other hand, will compete with Si IGBTs up to 5 kV breakdown voltages. Due to difficulties in enhancing the gate interface of SiC MOSFETs, JFETs were the first commercial SiC switches. Normally-on JFETs and normally-off hybrid cascade topologies with a normally-on SiC JFET in series with a low-voltage Si MOSFET are well-known. On the other hand, normally-off SiC JFETs still have high resistance channels that need to be addressed. Up to 1.2 kV SiC MOSFETs are now commercially available. The benefits of enhancing the SiC MOSFET are projected to be transferred to the SiC IGBT, allowing commercial development of IGBTs with breakdown voltages greater than 10 kV. The majority of GaN power devices are made with epitaxial GaN layers on Si, sapphire, or SiC substrates. GaN diodes with high voltage have been developed and are expected to be commercialized soon. Furthermore, in the recent decade, significant advancements have been made in HEMTs manufactured on GaN heterostructures. The high electron mobility values and significant 2DEG concentration make these structures appealing for high frequency switching/power applications. Despite the fact that the HEMT structure is inherently a normally-on device, numerous approaches have been devised that enable the integration of normally-off HEMTs. Up to 600 V, GaN HEMTs are already commercially accessible. Finally, for low resistance, high voltage GaN power switches, hybrid MOS-HEMT structures are being studied.

2.5.3 Review of Silicon Carbide Power Devices and Their Applications [X. She et al. (2017)]:

In 2017, X. She et al. [5] published his research on SiC based power devices and proposed that both academics and industry have paid close attention to SiC devices and power electronics systems. This study provides a comprehensive overview of the primary applications of emerging SiC technologies. The design problems and potential development trends are also discussed. SiC power conversion technologies are being adopted by industry and demonstrated in many essential applications such as solar, traction, UPS, and electric vehicles. SiC will, in conclusion, change the entire energy conversion business.

2.5.4 A Comparison between Si and SiC MOSFETs [J. Wang et al. (2020)]:

In 2020, J. Wang et al. [7] published his research work about the comparison between Si and SiC MOSFET. In this study, the on-resistance and high-temperature properties of Si and SiC power MOSFET devices are compared and the results are analysed. It must be overlooked that the experiments described above contain numerous flaws. In an electro-thermal study, for example, if the applied voltage is increased significantly and the saturation current condition emerges, the temperature of SiC power MOSFETs may rapidly rise. As a result, the condition of greater voltage and smaller scale will be investigated in future research. It is also expected to employ more advanced analytical techniques to evaluate the material structure and to investigate strategies to improve some MOSFET physical features.

2.5.5 Switching characteristics of silicon carbide power PiN diodes [A. Elasser et al. (2000)]:

In 2000, A. Elasser et al. [27] conducted an investigative analysis on switching characteristics of SiC power PiN diodes and proposed that with the SiC diode inserted, the switching reverse recovery losses are significantly decreased. Not only are IGBT losses smaller, but they also do not rise with increasing temperature, whereas Si diode losses increase dramatically. At higher temperatures, the disparity is likely to be substantially greater. At 25℃ and 150℃, SiC diode losses are an order of magnitude or lower, and IGBT losses are 3-5 times lower when the SiC diode is utilized. These findings highlight the benefits of employing SiC devices. SiC devices can function at significantly greater temperatures and have lower switching losses, voltage, and current stress. They can also function at extremely high voltages and switching frequencies. The advantages for circuit designers are enormous, particularly for applications requiring high voltages, such as X-ray tubes, high temperatures, such as those required for aircraft engine power supply, and high switching frequencies, which are employed in small converters. In hybrid motor control modules, SiC diodes can also be employed. Power converters will be able to run at high efficiency and low EMI thanks to low switching losses, low reverse recovery current, and time. However, the findings of this study demonstrate that using SiC diodes in Si IGBT switching circuits can now be advantageous due to the significant reduction in switching losses.

2.5.6 Ge MOSFETs performance: Impact of Ge interface passivation [C. H. Lee et al. (2010)]:

In 2010, C. H. Lee et al. [32] conducted a series of test experiments on the impact of Ge MOSFET interface passivation and found that using a combination of self-passivation and valency passivation, the were able to achieve the highest electron (1920 cm^2/Vs) and hole mobility (725 cm^2/Vs) in Ge MOSFETs. In n-MOSFETs, for the first time, an increase in electron mobility was recorded at low temperatures, which was enabled by a huge drop in D_{it}. In the instance of p-MOSFETs, the effects of surface orientation on hole mobility were explored, and it was discovered that Ge (110) orientation with a channel direction of <110> is a promising candidate, however thermal processing requires greater care. Ge CMOS appears to be a solid choice for technology beyond Si, according to this comprehensive analysis.

2.6 Summery

The DC characteristics response for the Ge based n-type MOSFET is determined to be better than the other Si and SiC based MOSFETs for a specified geometry and other settings after simulation using COMSOL Multiphysics 5.5 Software. And the Ge PiN diode outperformed the other two, Si and SiC based PiN diodes, in terms of forward recovery.

CHAPTER 3

METHODOLOGY AND OUTCOMES

3.1 Introduction

In this section, COMSOL Multiphysics 5.5 and 5.6 version have been used as helping tool for our analysis. The process involved in developing these models in software has been shown with proper explanation and figures. Here a n-type MOSFET model in COMSOL Multiphysics 5.5 has been used, which can give transfer characteristics, electron and hole concentrations, electric potentials and output characteristics of Si, Ge and SiC materials based MOSFET regarding voltage, current, power by varying the source, drain and gate voltage. Besides, we build a PiN diode model for findings their forward recovery characteristics such as band energy diagram, electric potential, electron concentration, forward recovery responses for Si, Ge and SiC based materials.

3.2 n-type MOSFET's Methodology for all three types

3.2.1 The Geometry and Mesh Used for three MOSFET

The geometry of the MOSFET with a width of 3µm, a depth of 0.1µm, and a height of 0.7µm is shown in **Fig. 6(a)**, and the mesh of the model is shown in **Fig. 6(b)**.

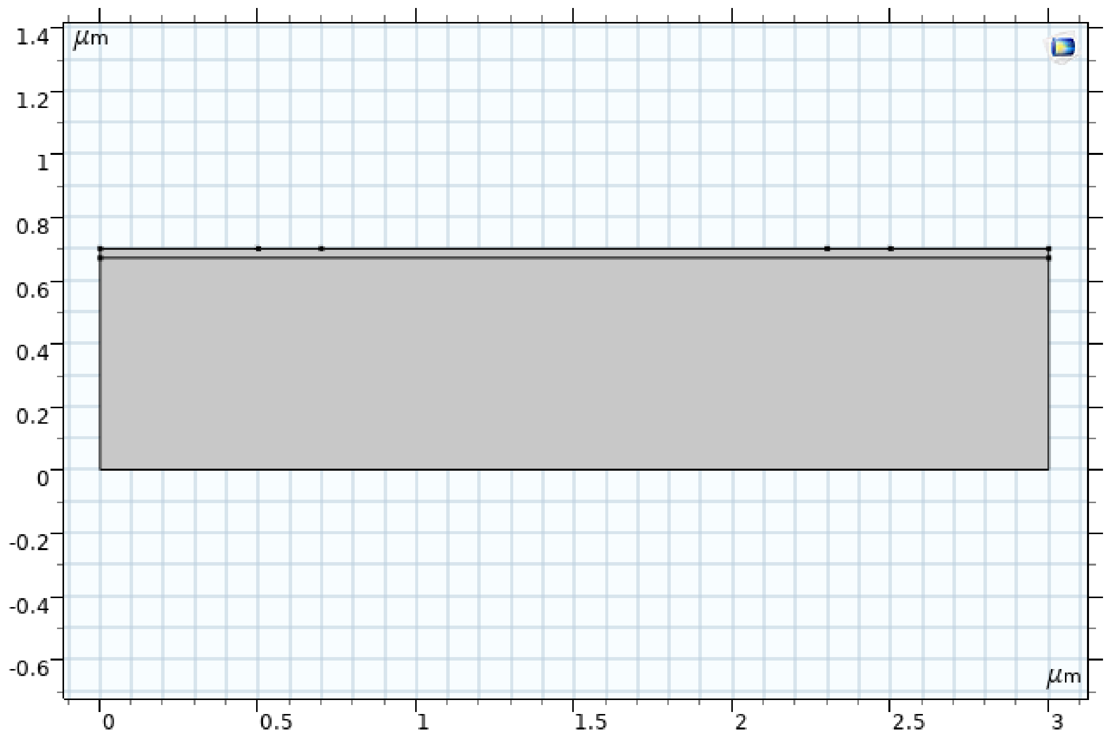

(a) Geometry of the MOSFET

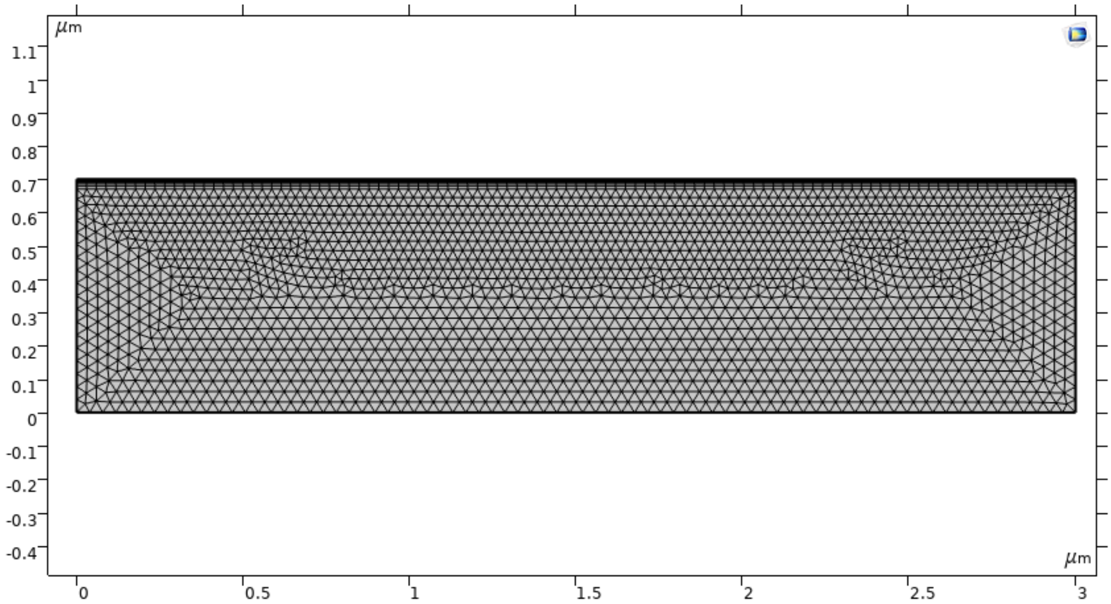

(b) Mesh design of the MOSFET

Fig. 6. Geometry and Mesh of the n-type MOSFET, (a) Geometry of the MOSFET (b) Mesh design of the MOSFET

All three Si, Ge, and SiC based MOSFETs in this paper use the same geometry and mesh as shown in **Fig. 6(a)** and **Fig. 6(b)**. As shown in **Fig. 6(a)**, the N+ Source and N+ Drain regions are both 0.03µm long and 0.5µm wide, with n-type doping of 1×10^{20} 1/cm^3. The rest of the body is p-type doped with 1×10^{17} 1/cm^3 and is considered the body region. The gate's Oxide layer is 30nm thick, with a relative permittivity of 4.5. The temperature in the simulation is set to 293.15K by default.

To observe the transfer characteristics, output characteristics, and others, the study is set up with gate voltage (V_g) for a range of 1V to 5V with an interval of 0.5V and drain voltage (V_d) for a range of 0V to 5V with an interval of 0.5V, which are represented for all three MOSFETs in the following.

3.2.2 The Simulation Structure Used for the three MOSFETs

Firstly, a low voltage as 10mV, is given in drain and a swept of study for 0 to 5V is given in gate to observe the threshold voltage of the specific geometrical n-type MOSFET for three time for three different materials. Secondly, a swept of study for 0 to 5V is given in drain to see the changes on the output characteristics. The output characteristics with different values of drain voltage as well as the transfer characteristics with different vales of gate voltage for all three MOSFETs have also been seen.

3.2.3 The properties of Materials used for the three types

In **Table 1**, the material properties applied for Si, Ge, SiC are documented. The most basic properties are included here and others are generated by COMSOL Multiphysics 5.5 simulation software. Rest of the properties are in **Appendix-I**I.

Table 1. Applied properties of the three materials [3, 5, 20, 21].

Property	Applied values for		
	Si	**Ge**	**SiC**
Relative Permittivity	11.7	16.2	9.7
Thermal conductivity [W/m.K]	131	60	450
Density [kg/m^3]	2329	5323	3200
Band gap [eV]	1.12	0.664	3.26
Electron affinity [eV]	4.05	4	3.24
Effective density of state, the conduction band [1/m^3]	2.8×10^{19}	1.04×10^{19}	1.7×10^{25}
Effective density of state, the valence band [1/m^3]	1.04×10^{19}	6.0×10^{18}	2.5×10^{25}
Mobility of the Electron [m^2/ V.s]	0.145	0.390	0.090
Mobility of the Hole [m^2/ V.s]	0.050	0.190	0.012
Electron lifetime, SRH [µs]	10	1×10^{-3}	2.5×10^{-6}
Hole lifetime, SRH [µs]	10	1×10^{-4}	5.0×10^{-7}

3.3 PIN Diode's Forward Recovery Characteristics

PiN diodes have mainly two types of switching characteristics which are forward recovery characteristics and reverse recovery characteristics. Among them, the study of the forward recovery characteristics for Si, Ge and SiC based PiN diodes have been analyse here.

3.3.1 PiN Diode's Geometry and Mesh for all three types of materials

Fig. 7(a) and **Fig. 7(b)** shows a PiN diode with an 80µm length and a cross-section area of 1×10^{-6} m^2. The geometry of the PiN diode shown in **Fig. 7(a)** and **Fig. 7(b)** is used in our study for all three types of PiN diodes: Si, Ge, and SiC. In the arc length of 70µm to 80µm, the P+ region is 10µm long with p-type doping of 1×10^{19} 1/cm^3 and the N+ region is also 10µm long with n-type doping of 1×10^{19} 1/cm^3 in the arc length of 0µm to 10µm.

(a) Geometry of the Si based PIN Diode

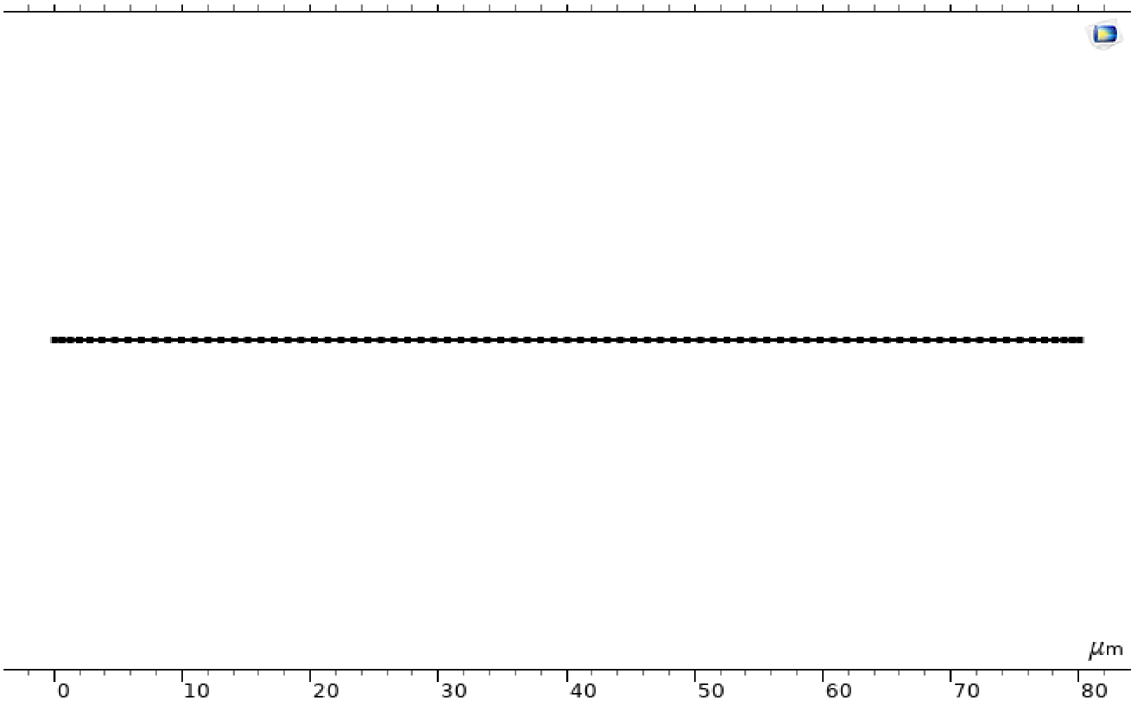

(b) Mesh design of the Si based PIN Diode

Fig. 7. Geometry and Mesh of the Si based PIN Diode, (a) Geometry of the Si based PIN Diode (b) Mesh design of the Si based PIN Diode

Finally, in the arc length of 10µm to 70µm, the intrinsic region between P+ and N+ is so low that n-type doping of 5×10^{13} 1/cm^3 is observed. And the simulation is set up with a 1×10^{-5} relative tolerance and a temperature of 193.15K.

3.3.2 The Simulation Structure for PiN Diode's Forward Recovery

The study of this paper is simulated the forward recovery of a basic PiN diode, which is driven with current density ramp rates, $\frac{dj}{dt}$ = 1×10^9 $A.cm^{-2}s^{-1}$, 2×10^9 $A.cm^{-2}s^{-1}$, 1×10^{10} $A.cm^{-2}s^{-1}$ and a fixed current density of 100 $A.cm^{-2}$. This same setup with the same geometry is used for the three PiN diodes based on Si, Ge and SiC respectively.

The right endpoint is connected to the ground and the current flows from the left. Then a ramp function along with a cut-off is applied to define the linear current ramp up to the highest on current. A study of Semiconductor Equilibrium step is applied for the beginning. After that, a study of time-dependent step is applied to observe the response of the forward recovery, with an auxiliary sweep for simulating a few different current ramp rates. The simulation is set up with the temperature of 193.15K.

3.3.3 The Properties of Materials used for Three PiN Diode

In **Table 2**, the material properties applied for Si, Ge, SiC are documented. The most basic properties are included here and others are generated by COMSOL Multiphysics simulation software. Rest of the properties are in **Appendix-II**.

Table 2. Applied properties of the three materials [24], [44], [45].

Property	Applied values for		
	Si	***Ge***	***SiC***
Relative Permittivity	11.7	16.2	10
Thermal conductivity [W/m.K]	131	60	450
Density [kg/m^3]	2329	5323	3200
Band gap [eV]	1.2	0.664	3.26
Electron affinity [eV]	4.05	4	3.24
Effective density of state, the conduction band [$1/m^3$]	2.8×10^{19}	1.04×10^{19}	1.7×10^{25}
Effective density of state, the valance band [$1/m^3$]	1.04×10^{19}	6.0×10^{18}	2.5×10^{25}
Mobility of the electron [$cm^2/V. s$]	1450	3900	900
Mobility of the hole [$cm^2/V. s$]	500	1900	120

The experimental diode is studied after being structured by Si, Ge and SiC material to observe the differences in the response.

The properties of materials given for Si-PiN, Ge-PiN, and SiC-PiN diodes are presented in **Table 2**. There are the most basic properties given here and the COMSOL Multiphysics 5.5 simulation software uses some other pre-generated properties for the materials as well.

CHAPTER 4

RESULTS AND DISCUSSIONS

4.1 n-type MOSFET's DC Characteristics

We can see the surface dopant concentration for Si, Ge and SiC based MOSFET.

4.1.1 Surface Signed Dopant Concentration

Here, the **Fig. 8(a)** shows the signed dopant concentration for Si MOSFET whereas **Fig. 8(b)** and **Fig 8(c)** shows the signed dopant concentration for Ge and SiC based MOSFET respectively.

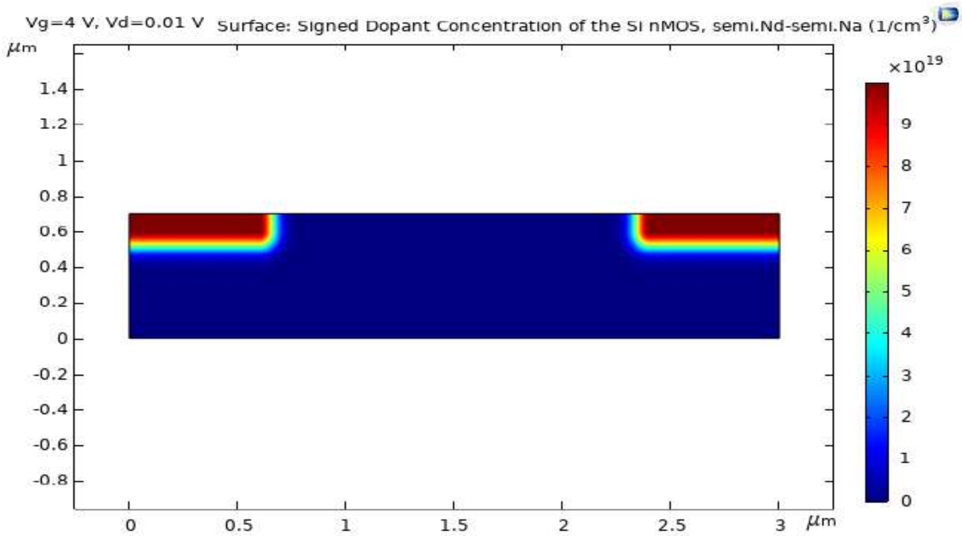

(a) For Si MOSFET

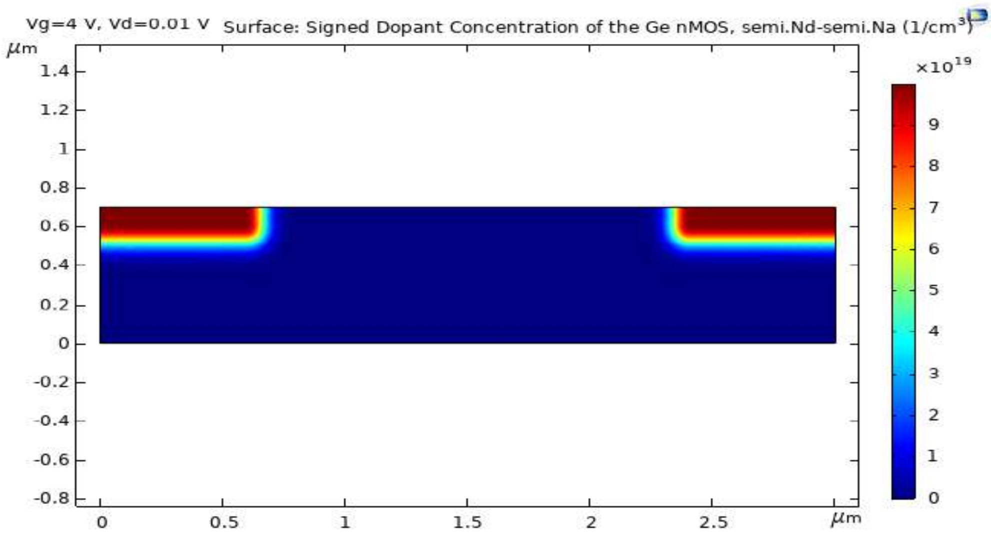

(b) For Ge MOSFET

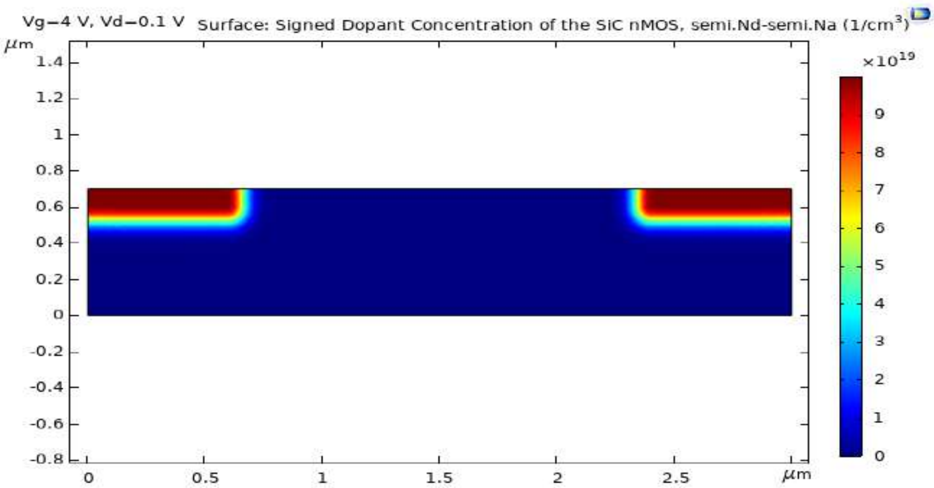

(c) For SiC MOSFET

Fig. 8. Surface Dopant Concentration of Si, Ge & SiC MOSFET when V_g = 4V & V_d =0.01V, (a) For Si MOSFET (b) For Ge MOSFET (c) For SiC MOSFET

Almost similar type of signed dopant concentration is found for the three MOSFETs. The Source and the drain are highly n-type doped with the concentration as 10×10^{19} 1/cm^3. Due to very low amount of drain voltage as 10mV, there are charges are flowing through the channel. The channel and body part of the MOSFETs have the signed dopant concentration of near to zero. Rest of the output of signed dopant concentration are in **Appendix-I.**

4.1.2 Transfer Characteristics

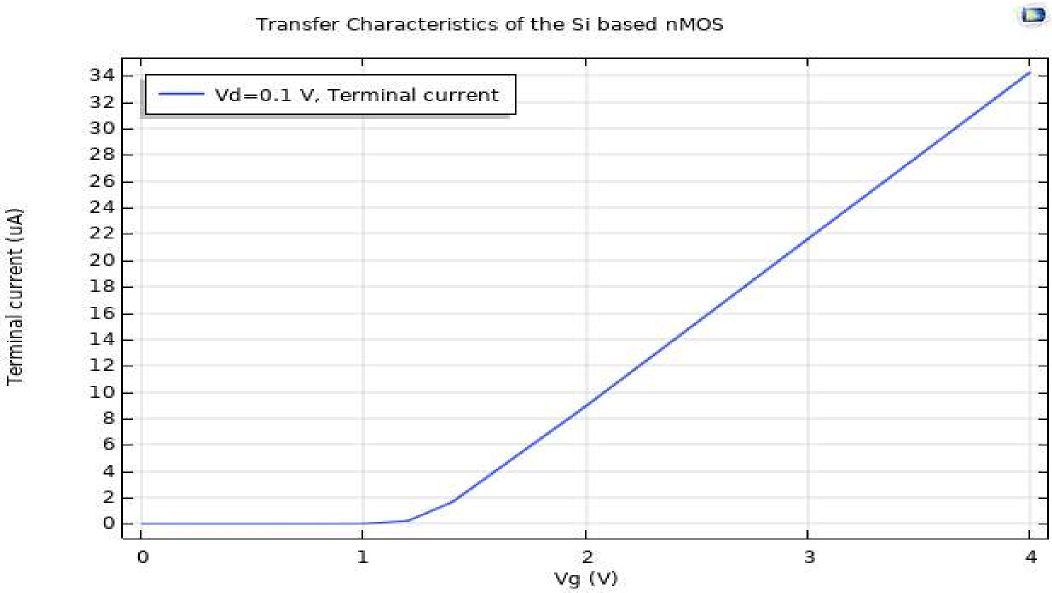

(a) For Si MOSFET

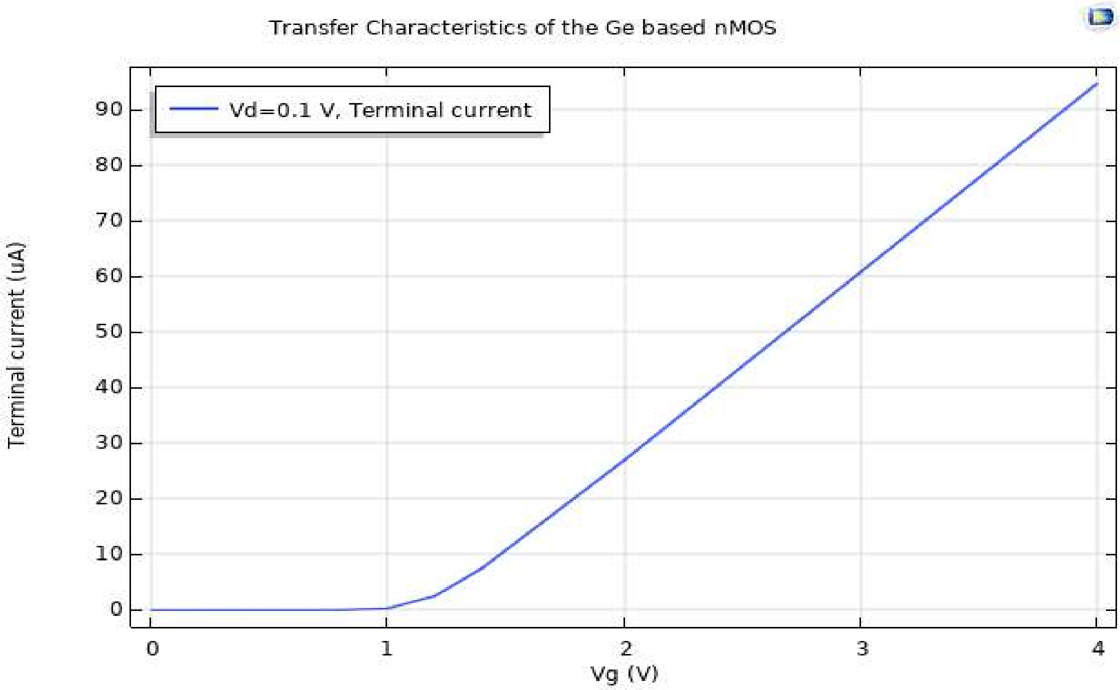

(b) For Ge MOSFET

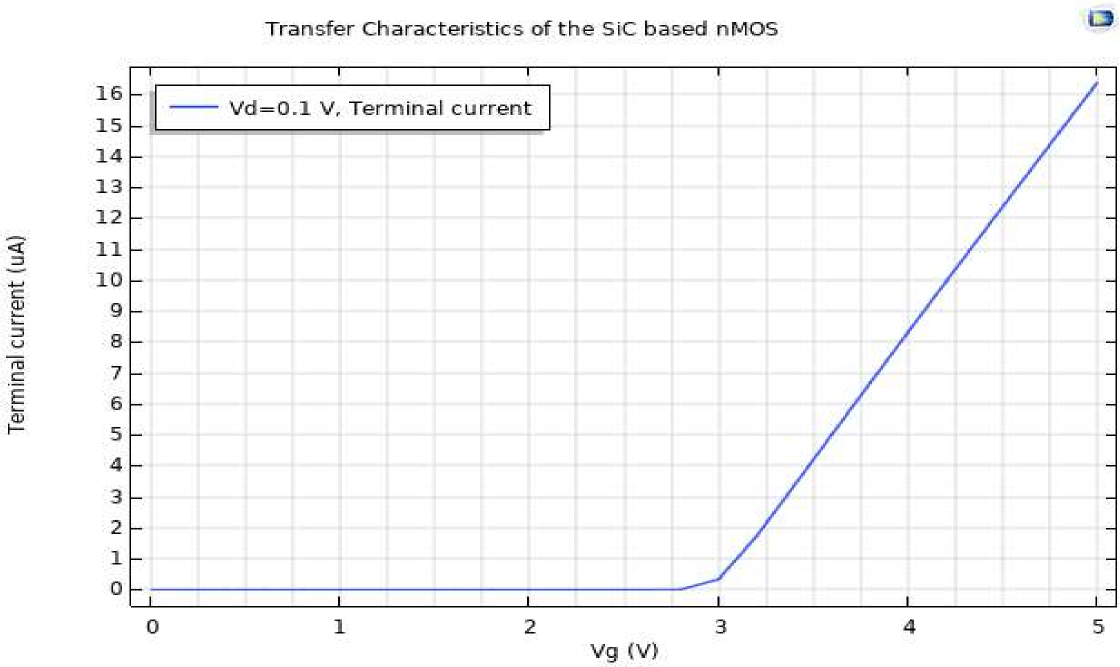

(c) For SiC MOSFET

Fig. 9. Transfer characteristics of Si, Ge and SiC MOSFETs, (a) For Si MOSFET (b) For Ge MOSFET (c) For SiC MOSFET

The transfer characteristics of Si, Ge, and SiC MOSFETs are shown in **Fig. 9(a), 9(b) & 9(c)** respectively. As a switching device, the Ge-MOSFET has an advantage because it only requires a minimum threshold voltage (V_t) of about 1V, whereas the Si-MOSFET requires 1.2V and the SiC-MOSFET requires 2.8V.

Because the SiC-MOSFET requires a higher threshold voltage, it cannot be operated with a drain voltage below 2.8V, and the output characteristics curve for this range cannot be found.

4.1.3 Electron Concentrations

The electron concentrations for Si, Ge and SiC based MOSFETs are shown in **Fig. 10(a), 10(b) & 10(c)** respectively. The results are for V_d = 0V and V_g = 4V range.

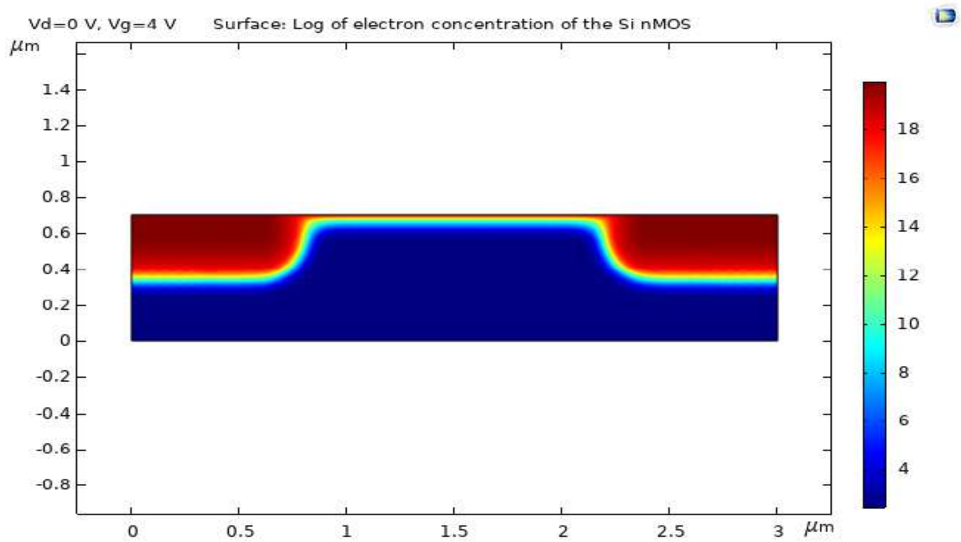

(a) For Si MOSFET

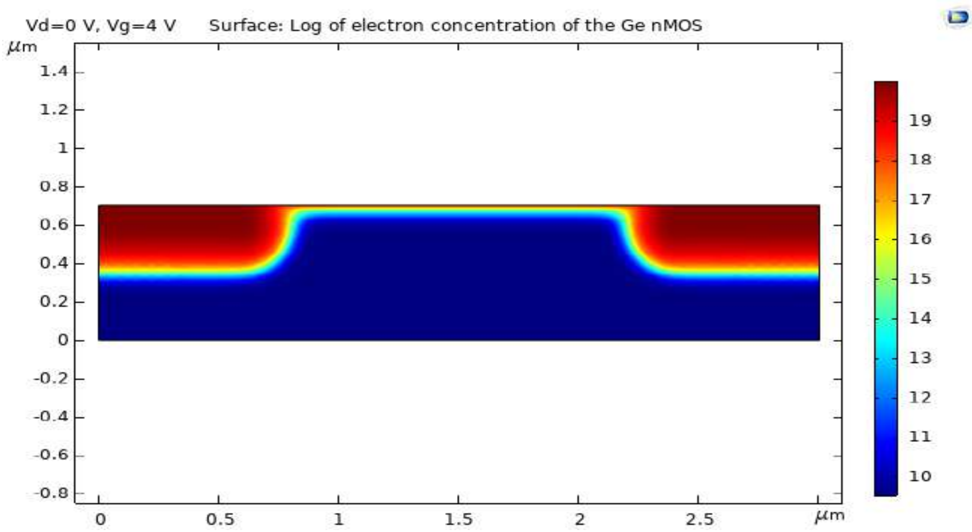

(b) For Ge MOSFET

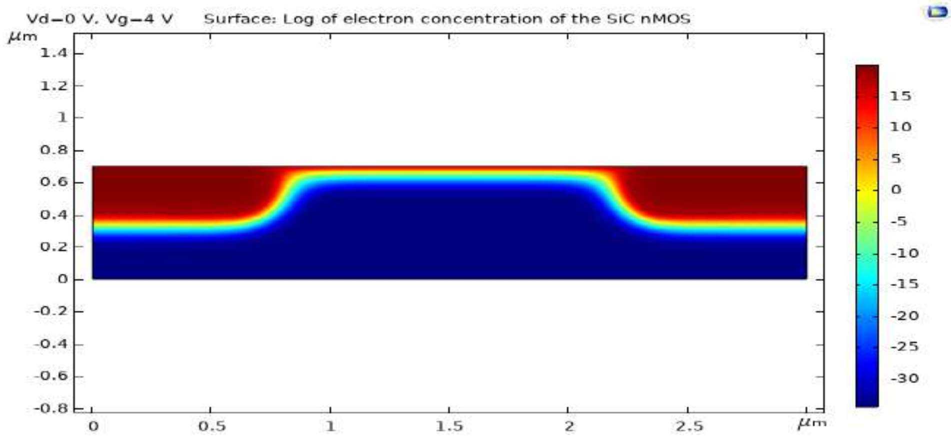

(c) For SiC MOSFET

Fig. 10. Electron Concentration of Si, Ge & SiC MOSFET when V_d=0V & V_g=4V, (a) For Si MOSFET (b) For Ge MOSFET (c) For SiC MOSFET

The electron concentrations for Si, Ge and SiC based MOSFETs are shown in Fig. 11(a), 11(b) & 11(c) respectively. The results are for Vd = 2.5V and Vg = 4V range.

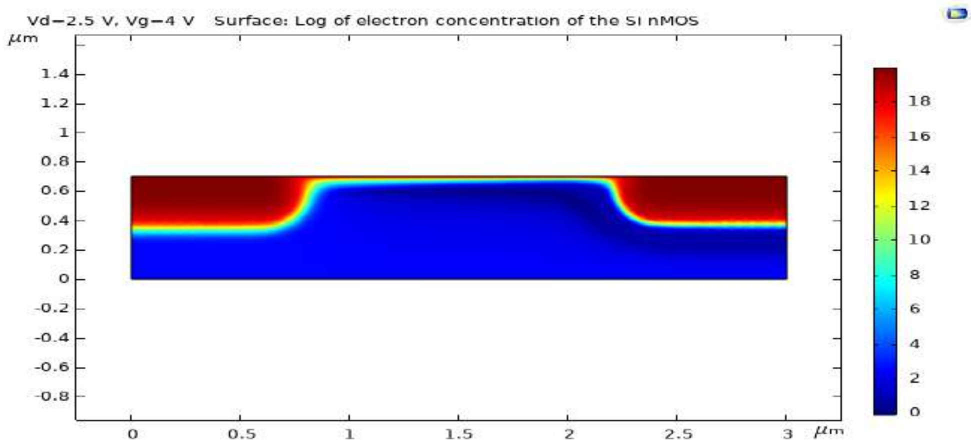

(a) For Si MOSFET

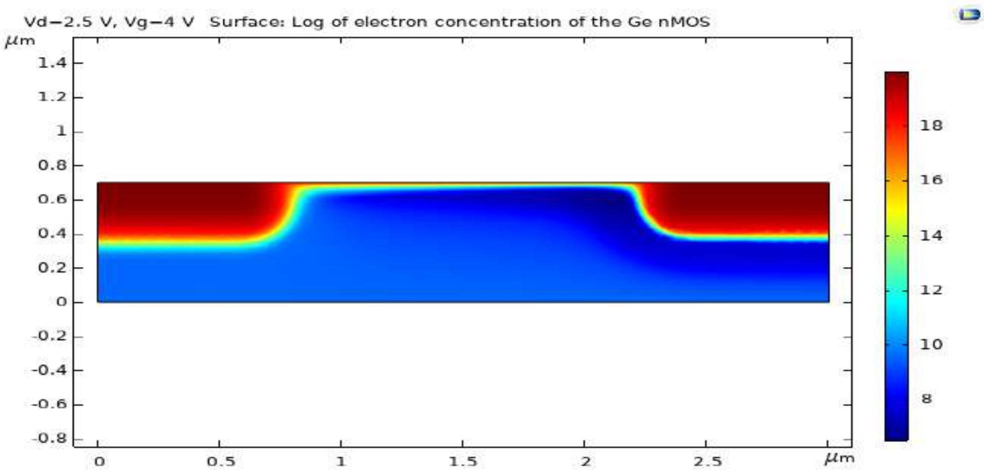

(b) For Ge MOSFET

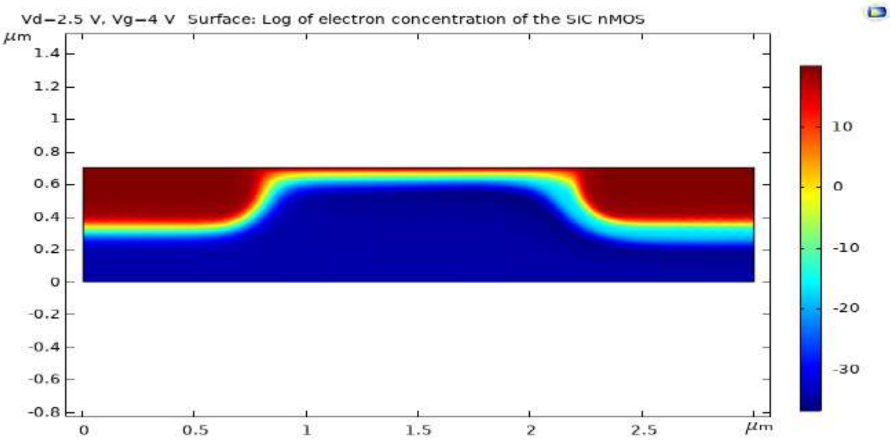

(c) For SiC MOSFET

Fig. 11. Electron Concentration of Si, Ge & SiC MOSFET when V_d=2.5V & V_g=4V, (a) For Si MOSFET (b) For Ge MOSFET (c) For SiC MOSFET

The electron concentrations for Si, Ge and SiC based MOSFETs are shown in **Fig. 12(a), 12(b) & 12(c)** respectively. The results are for V_d = 5V and V_g = 4V range.

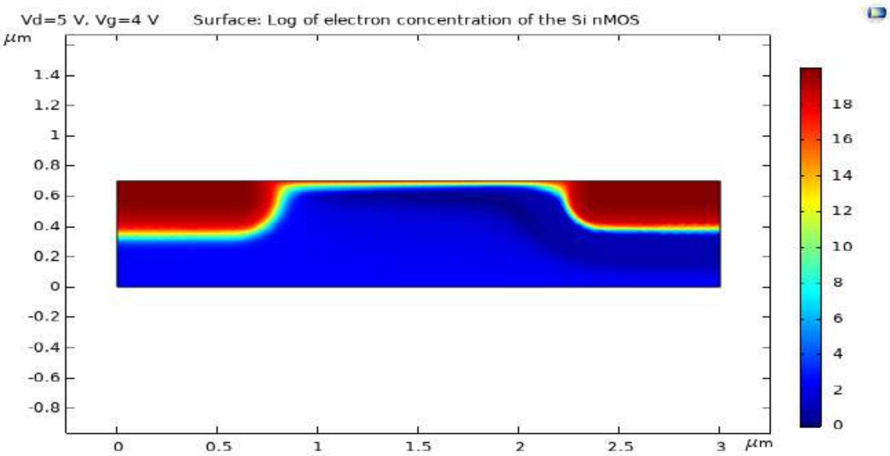

(a) For Si MOSFET

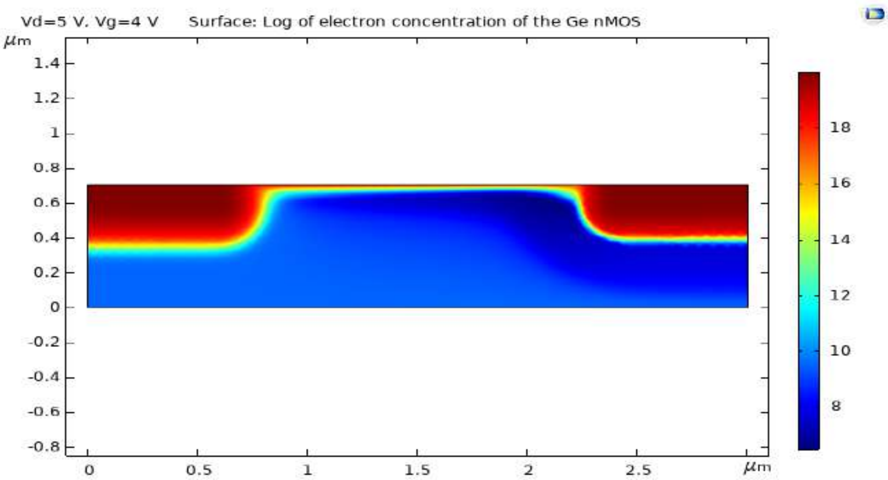

(b) For Ge MOSFET

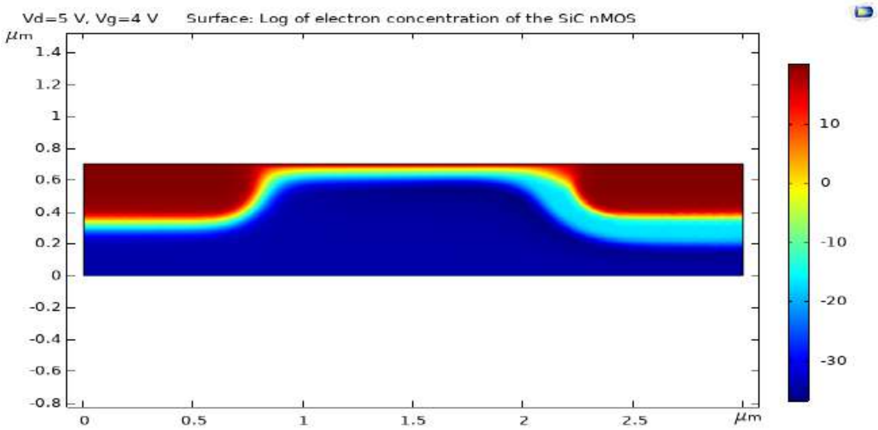

(c) For SiC MOSFET

Fig. 12. Electron Concentration of Si, Ge & SiC MOSFET when V_d=5V & V_g=4V, (a) For Si MOSFET (b) For Ge MOSFET (c) For SiC MOSFET

However, the SiC-MOSFET has a larger depletion region than the other two for the same setup and drain and gate voltages, as shown in both **Fig. 11(c)** and **Fig. 12(c),** which may affect output characteristics. This characteristic could be due to the material properties of SiC. Rest of the output of electron concentration are in **Appendix-I.**

4.1.4 Hole Concentrations:

Fig. 13(a), 13(b), 13(c), 14(a), 14(b), 14(c), 15(a), 15(b) & 15(c) depict the hole concentration in Si, Ge, and SiC MOSFETs, respectively. With the increase of V_g and V_d, we can see how the hole concentrates more around the source, channel, and drain side. The depletion region expands as V_g and V_d increase, as shown in **Fig. 13(a), 13(b), 13(c), 14(a), 14(b), 14(c), 15(a), 15(b) & 15(c)** for all three types of MOSFETs: Si, Ge, and SiC MOSFETs, respectively.

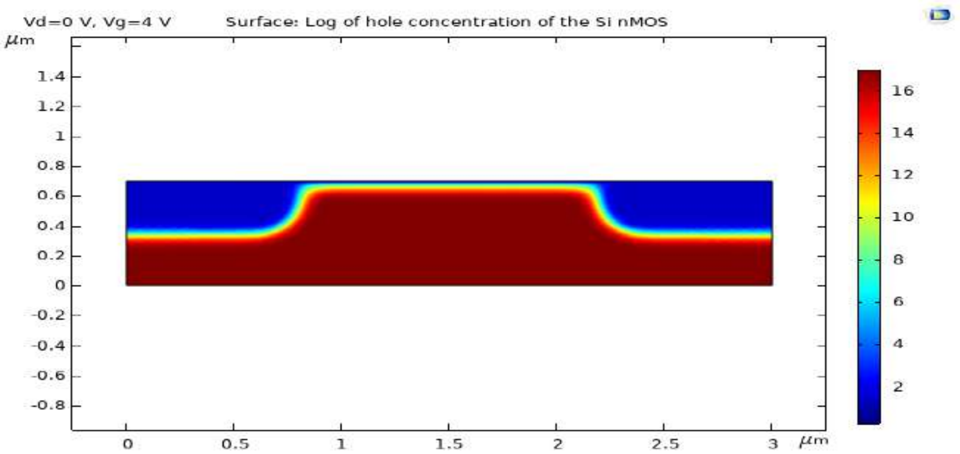

(a) For Si MOSFET

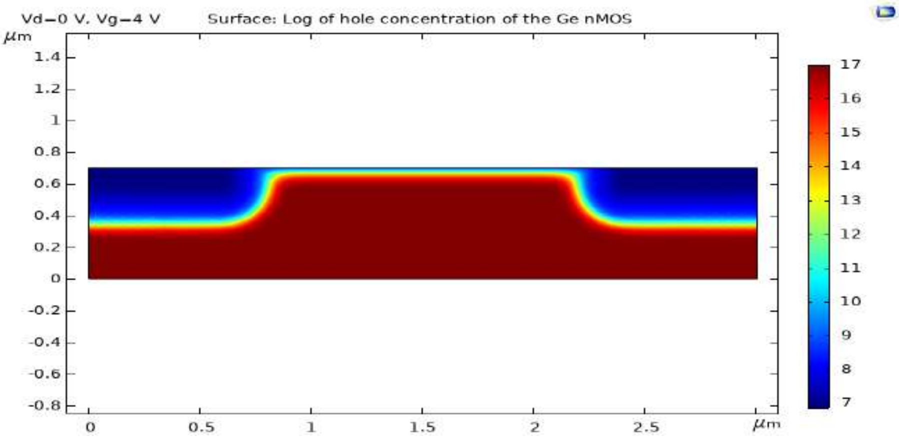

(b) For Ge MOSFET

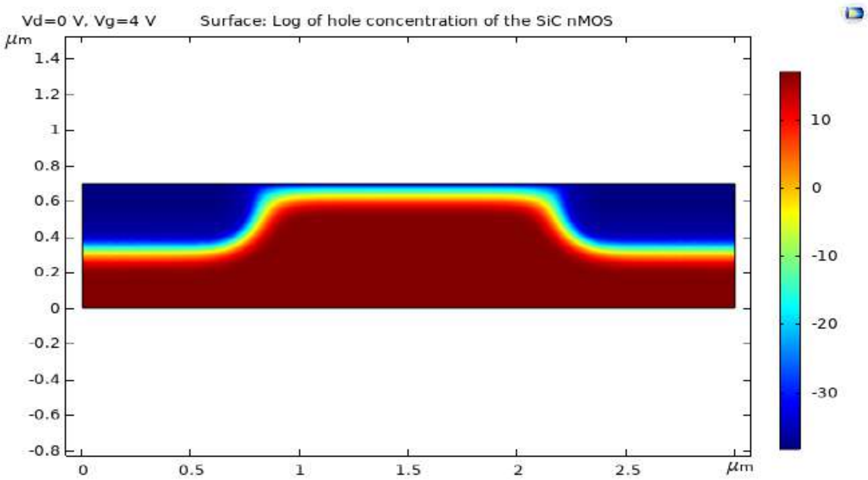

(c) For SiC MOSFET

Fig. 13. Hole Concentrations of Si, Ge & SiC MOSFET when V_d=0V & V_g=4V, (a) For Si MOSFET (b) For Ge MOSFET (c) For SiC MOSFET

The hole concentrations for Si, Ge and SiC based MOSFETs are shown in **Fig. 13(a), 13(b) & 13(c)** respectively. The results are for V_d = 0V and V_g = 4V range.

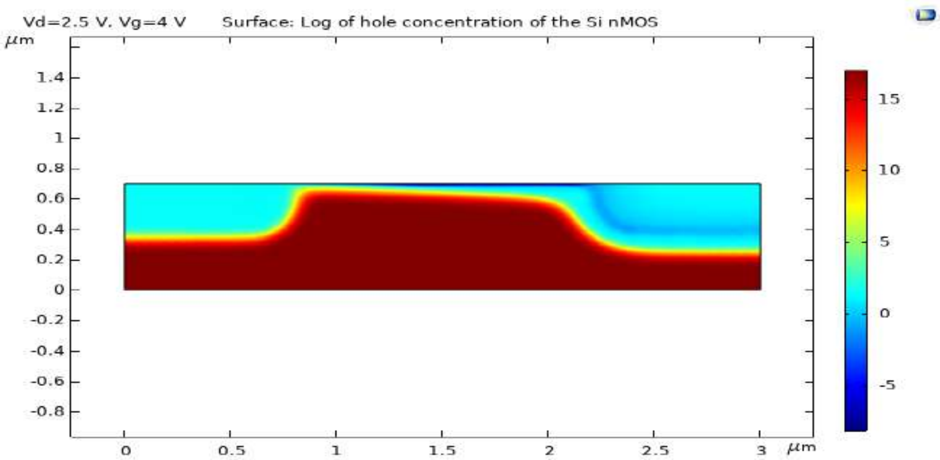

(a) For Si MOSFET

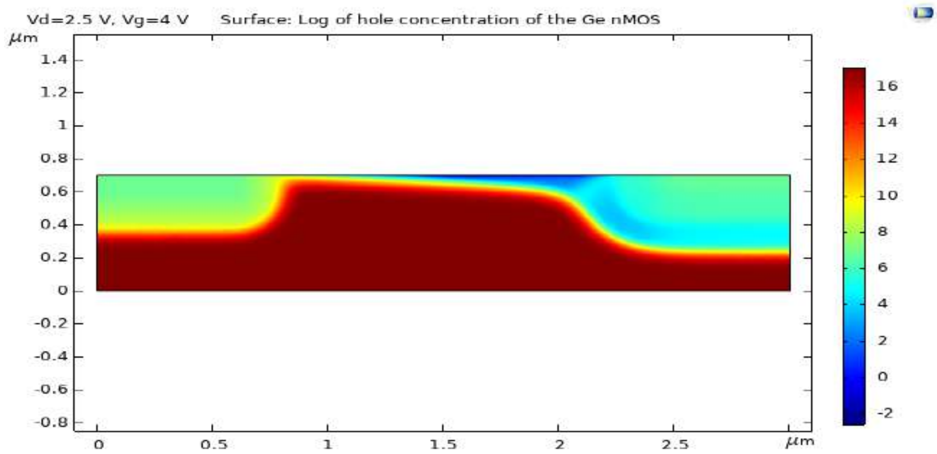

(b) For Ge MOSFET

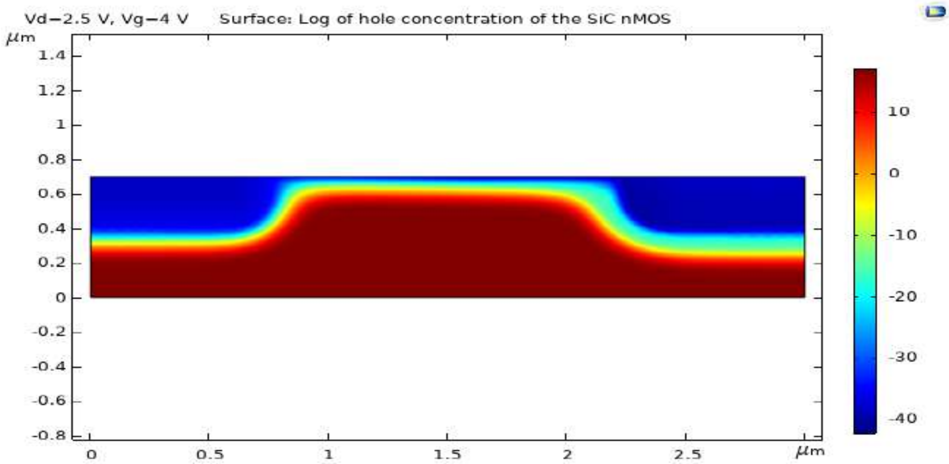

(c) For SiC MOSFET

Fig. 14. Hole Concentrations of Si, Ge & SiC MOSFET when V_d=2.5V & V_g=4V, (a) For Si MOSFET (b) For Ge MOSFET (c) For SiC MOSFET

The hole concentrations for Si, Ge and SiC based MOSFETs are shown in **Fig. 14(a), 14(b) & 14(c)** respectively. The results are for V_d = 2.5V and V_g = 4V range.

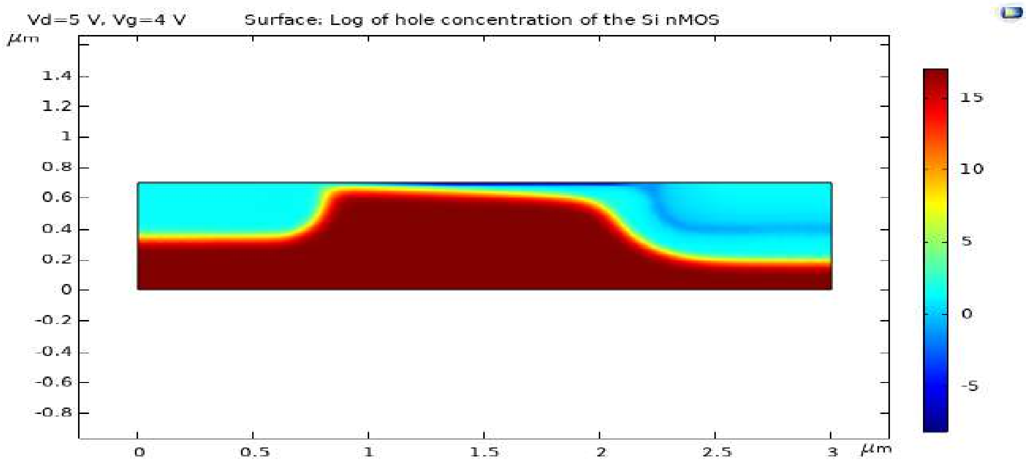

(a) For Si MOSFET

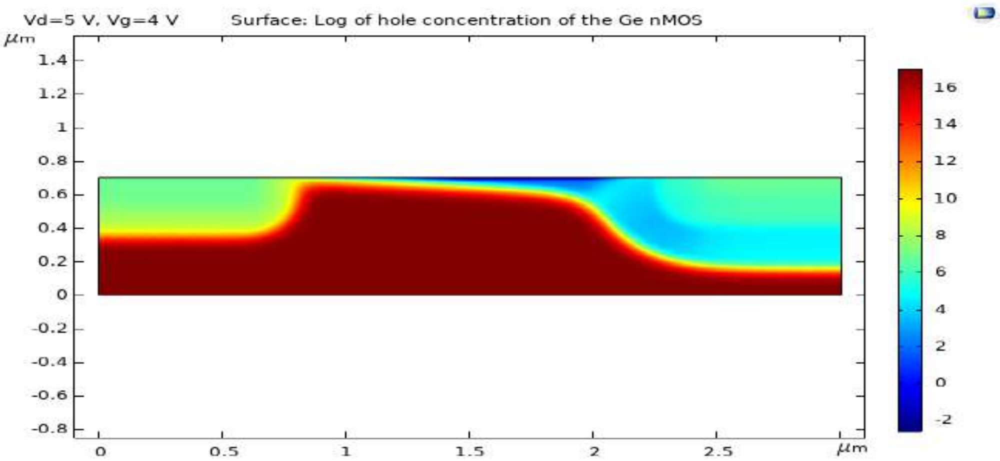

(b) For Ge MOSFET

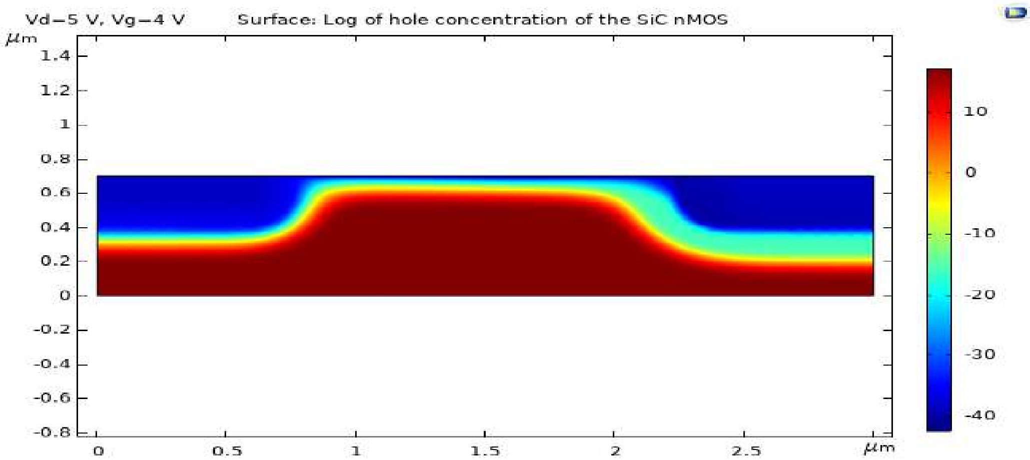

(c) For SiC MOSFET

Fig. 15. Hole Concentrations of Si, Ge & SiC MOSFET when V_d= 5V & V_g=4V, (a) For Si MOSFET (b) For Ge MOSFET (c) For SiC MOSFET

The hole concentrations for Si, Ge and SiC based MOSFETs are shown in **Fig. 15(a), 15(b) & 15(c)** respectively. The results are for V_d = 5V and V_g = 4V range. The depletion region expands as V_g and V_d increase, as shown in **Fig. 13(a), 13(b), 13(c), 14(a), 14(b), 14(c), 15(a), 15(b) & 15(c)** for all three types of MOSFETs: Si, Ge, and SiC MOSFETs, respectively. Here, we can see the SiC-MOSFET has a larger depletion region than the Si-MOSFET and Ge-MOSFET. Rest of the output of hole concentration are in **Appendix-I.**

4.1.5 Electric Potential:

The electric potentials for Si, Ge, and SiC based MOSFETs are shown in **Fig. 16(a), 16(b), 16(c), 17(a), 17(b), 17(c), 18(a), 18(b) & 18(c)**. As the MOSFETs reach saturation, the drain has the highest electric potentials for all three MOSFETs, which is expected due to the given value of $V_d \geq (V_g - V_t)$.

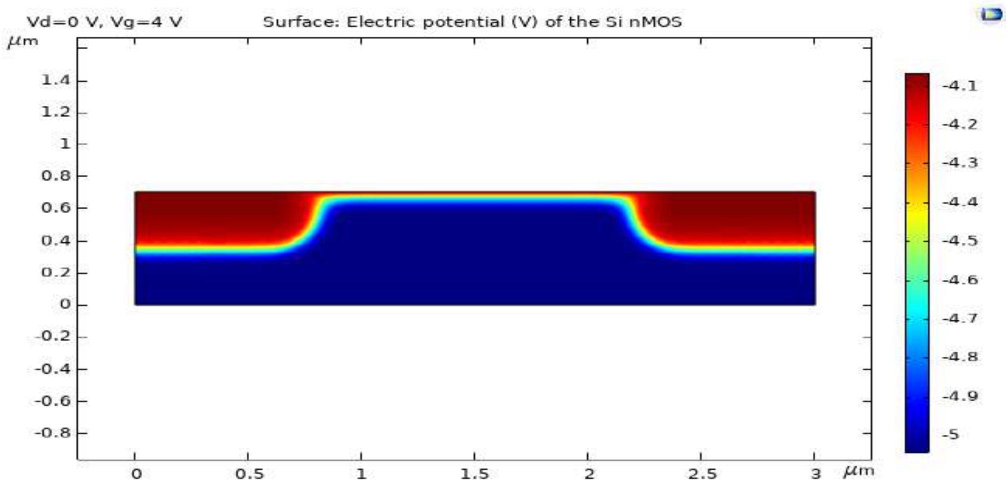

(a) For Si MOSFET

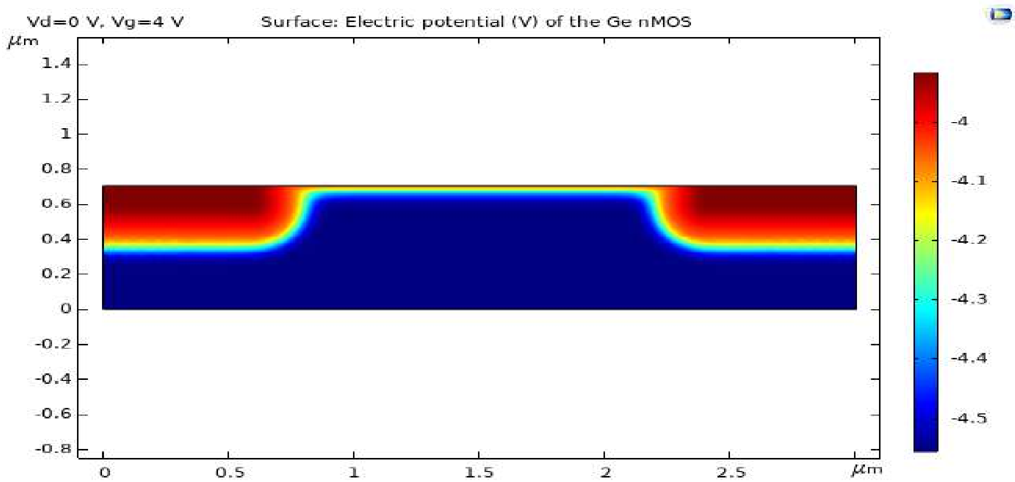

(b) For Ge MOSFET

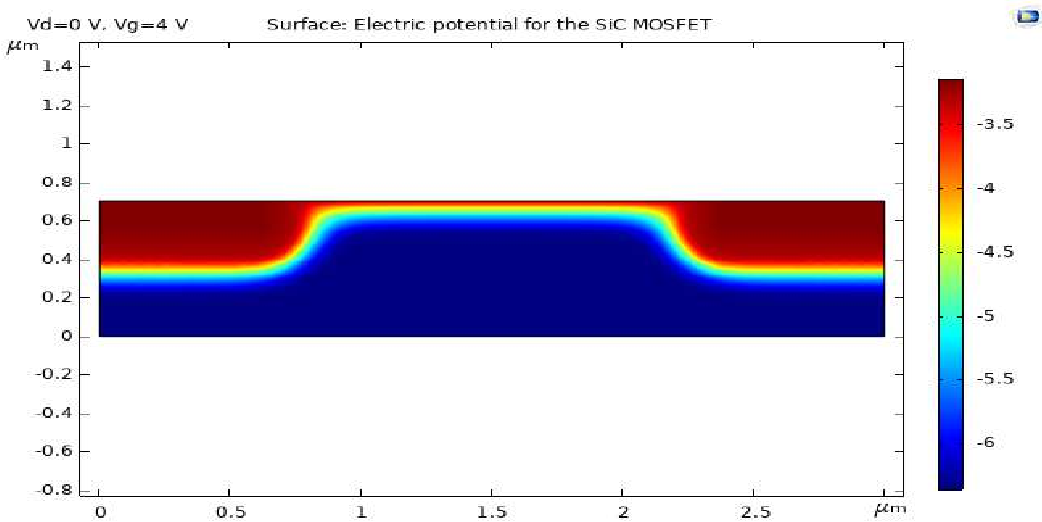

(c) For SiC MOSFET

Fig. 16. Electric Potential of Si, Ge & SiC MOSFET when V_d=0V & Vg=4V, (a) For Si MOSFET (b) For Ge MOSFET (c) For SiC MOSFET

The electric potential for Si, Ge and SiC based MOSFETs are shown in **Fig. 16(a), 16(b) & 16(c)** respectively. The results are for $V_d = 0V$ and $V_g = 4V$ range.

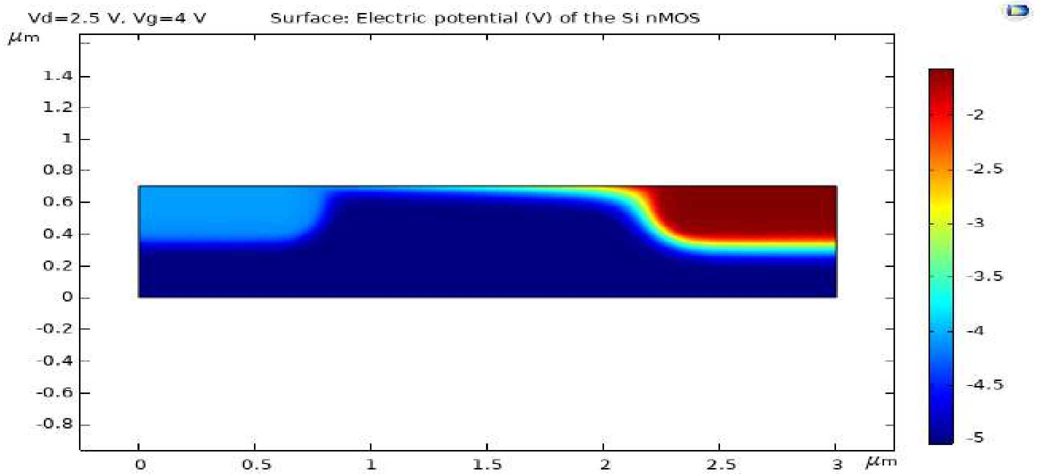

(a) For Si MOSFET

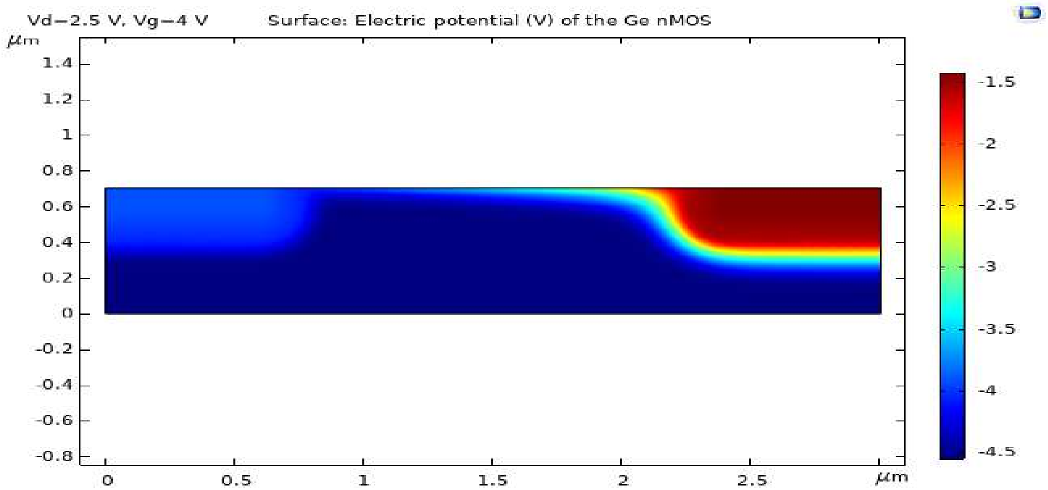

(b) For Ge MOSFET

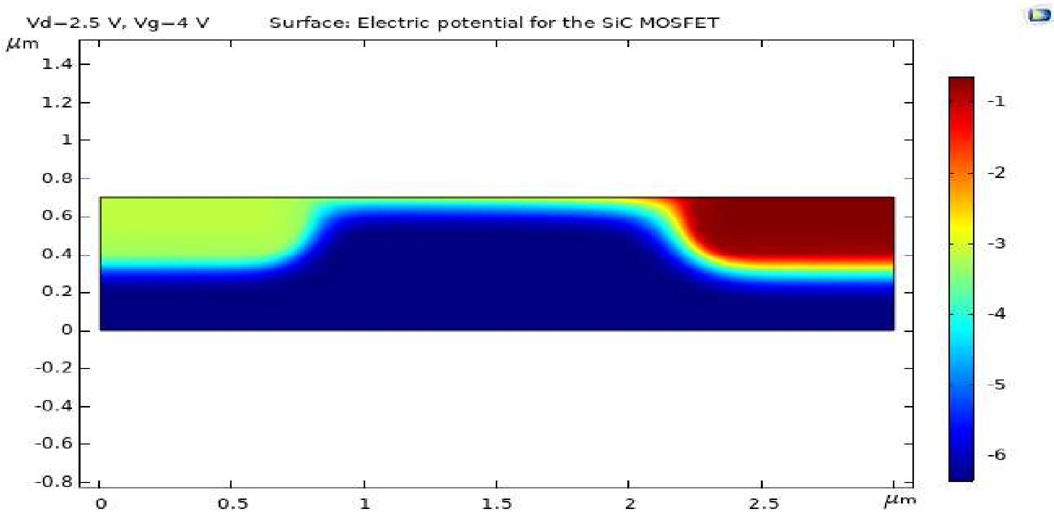

(c) For SiC MOSFET

Fig. 17. Electric Potential of Si, Ge & SiC MOSFET when Vd=2.5 V & Vg=4V, (a) For Si MOSFET (b) For Ge MOSFET (c) For SiC MOSFET

The electric potential for Si, Ge and SiC based MOSFETs are shown in **Fig. 17(a), 17(b) & 17(c)** respectively. The results are for V_d = 2.5V and V_g = 4V range.

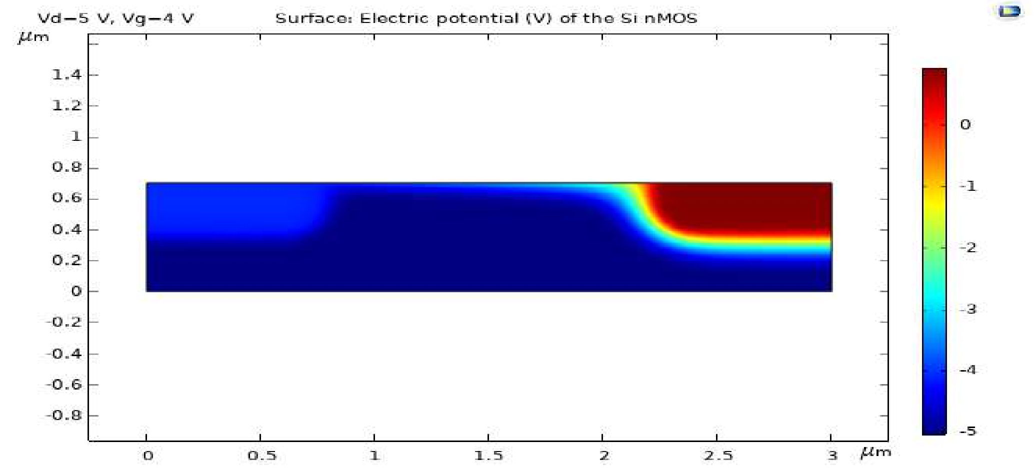

(a) For Si MOSFET

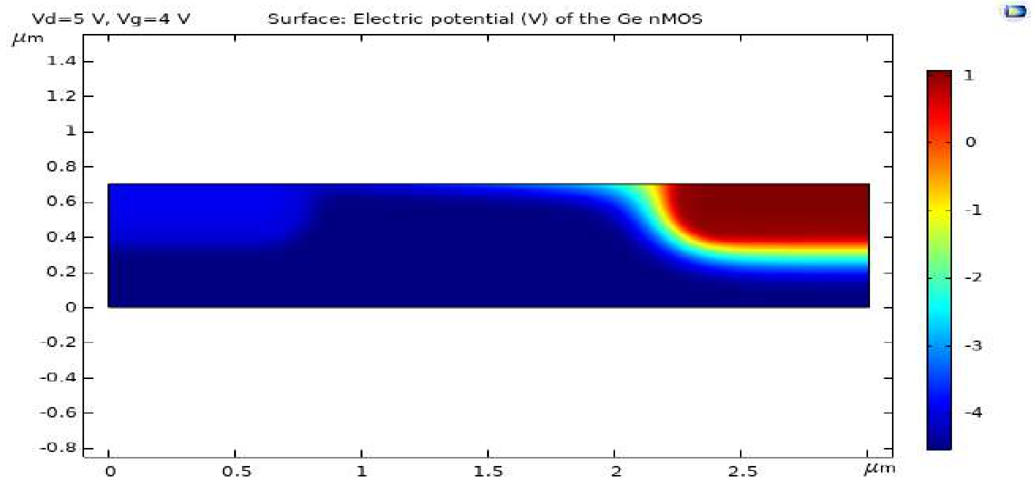

(b) For Ge MOSFET

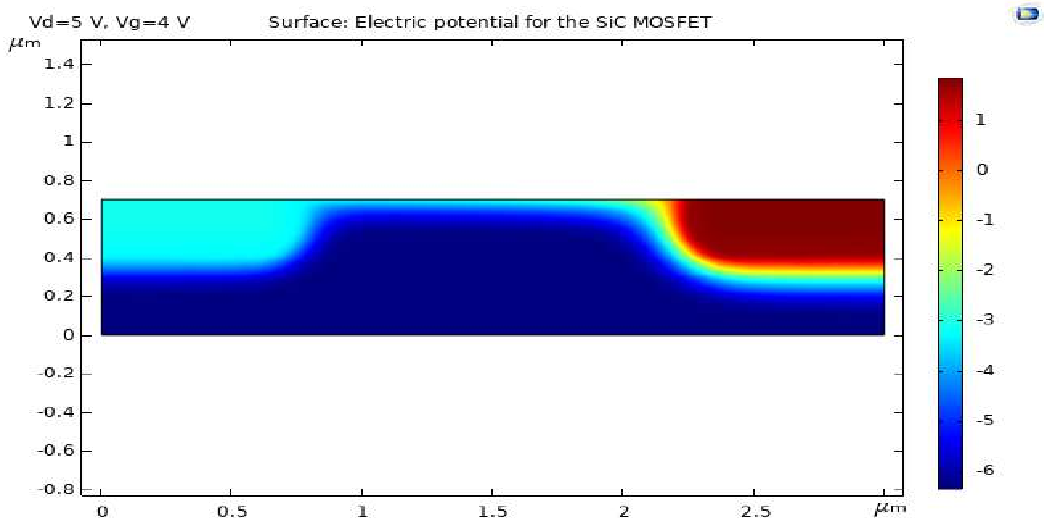

(c) For SiC MOSFET

Fig. 18. Electric Potential of Si, Ge & SiC MOSFET when Vd=5V & Vg=4V, (a) For Si MOSFET (b) For Ge MOSFET (c) For SiC MOSFET

The electric potential for Si, Ge and SiC based MOSFETs are shown in **Fig. 18(a), 18(b) & 18(c)** respectively. The results are for V_d = 5V and V_g = 4V range. From the figures, we can see that, as the MOSFETs reach saturation, the drain has the highest electric potentials for all three MOSFETs, which is expected due to the given value of $V_d \geq (V_g - V_t)$. Rest of the output of electric potential are in **Appendix-I.**

4.1.6 Output Characteristics:

These **Fig. 19(a), 19(b), 19(c), 20(a), 20(b), 20(c), 21(a), 21(b) & 21(c)** shows the output characteristics for the Si, Ge and SiC MOSFETs respectively.

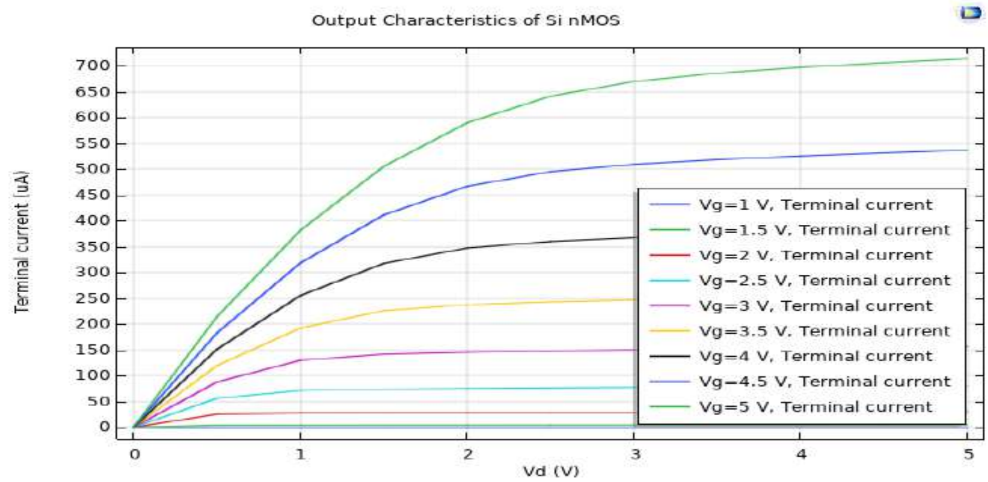

(a) Output Characteristics of Si nMOS

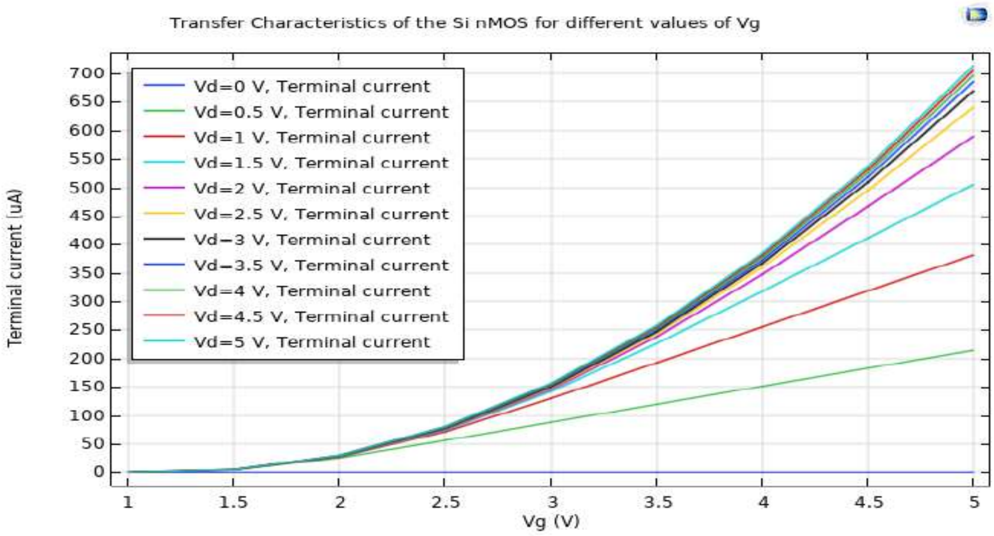

(b) Transfer Characteristics of Si nMOS

Fig. 19. Output and Transfer Characteristics of Si MOSFET, (a) Output Characteristics of Si nMOS (b) Transfer Characteristics of Si nMOS

For Si MOSFET, since V_t=1.2V, is shown in **Fig. 19(a) & 19(b)** we see the output curves for different values of V_g, the terminal currents of the saturation region are different. For example, for V_g=5V, we get the terminal current of saturation is about $700\mu A$, which is shown in **Fig. 19(a) & 19(b)**.

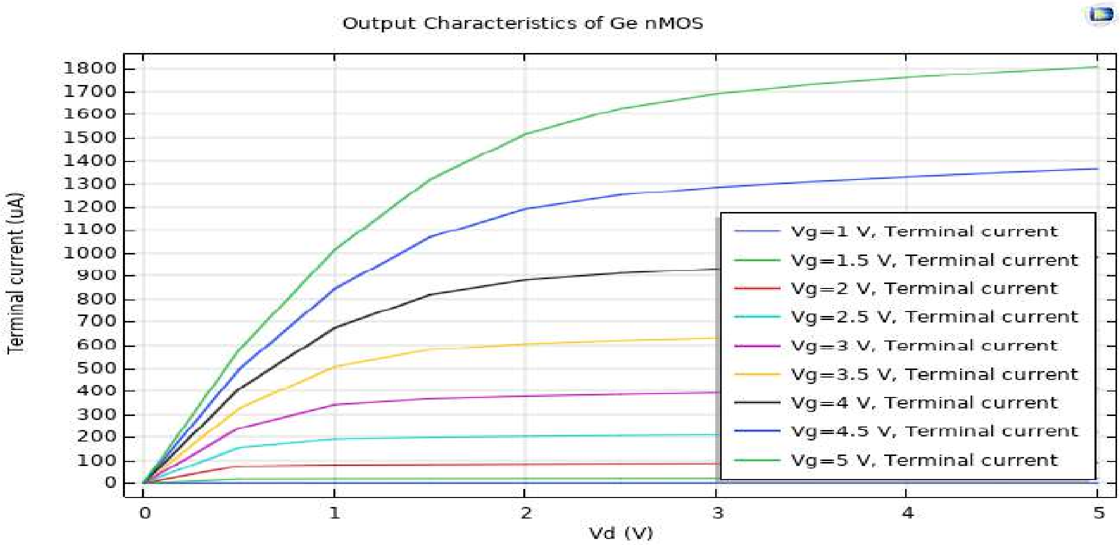

(a) Output Characteristics of Ge nMOS

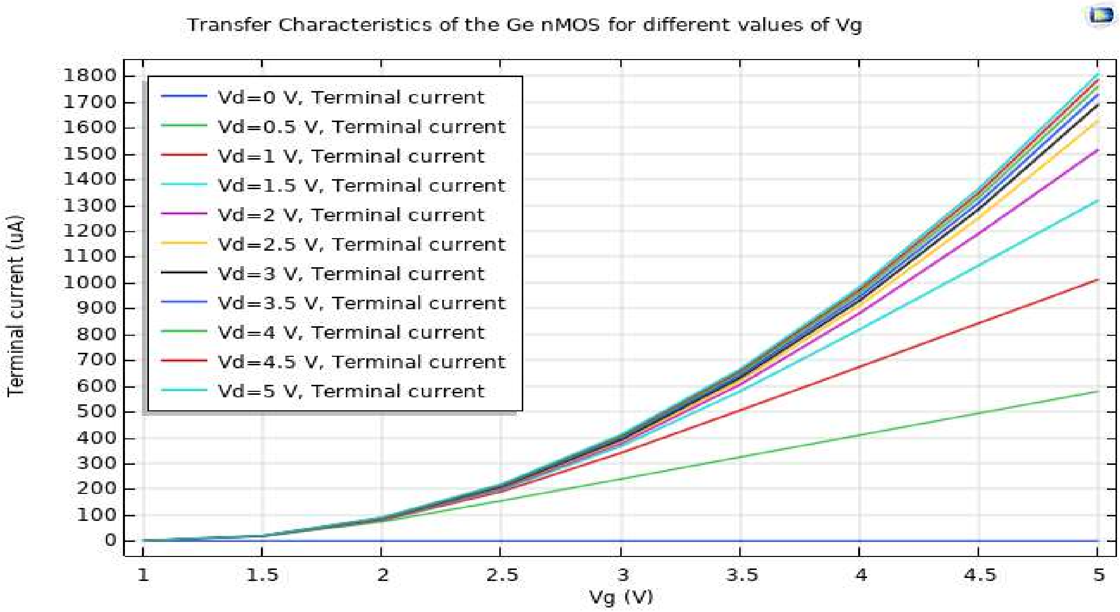

(b) Transfer Characteristics of Ge nMOS

Fig. 20. Output and Transfer Characteristics of Ge MOSFET, (a) Output Characteristics of Ge nMOS (b) Transfer Characteristics of Ge nMOS

After that, for Ge MOSFET, since V_t=1.0V, is shown in **Fig. 20(a) & 20(b),** we see the output curves for different values of V_g, the terminal currents of the saturation region are different. For example, for V_g=5V, we get the terminal current of saturation is higher than the Si and SiC MOSFETs, about 1800µA, which is shown in **Fig. 20(a) & 20(b).**

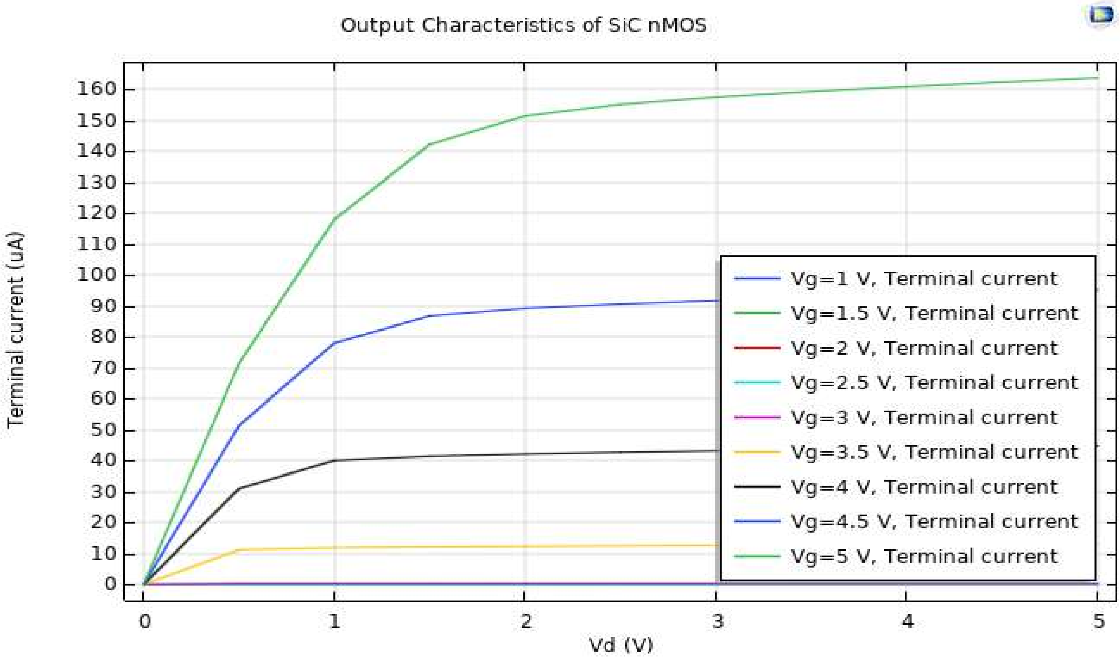

(a) Output Characteristics of SiC nMOS

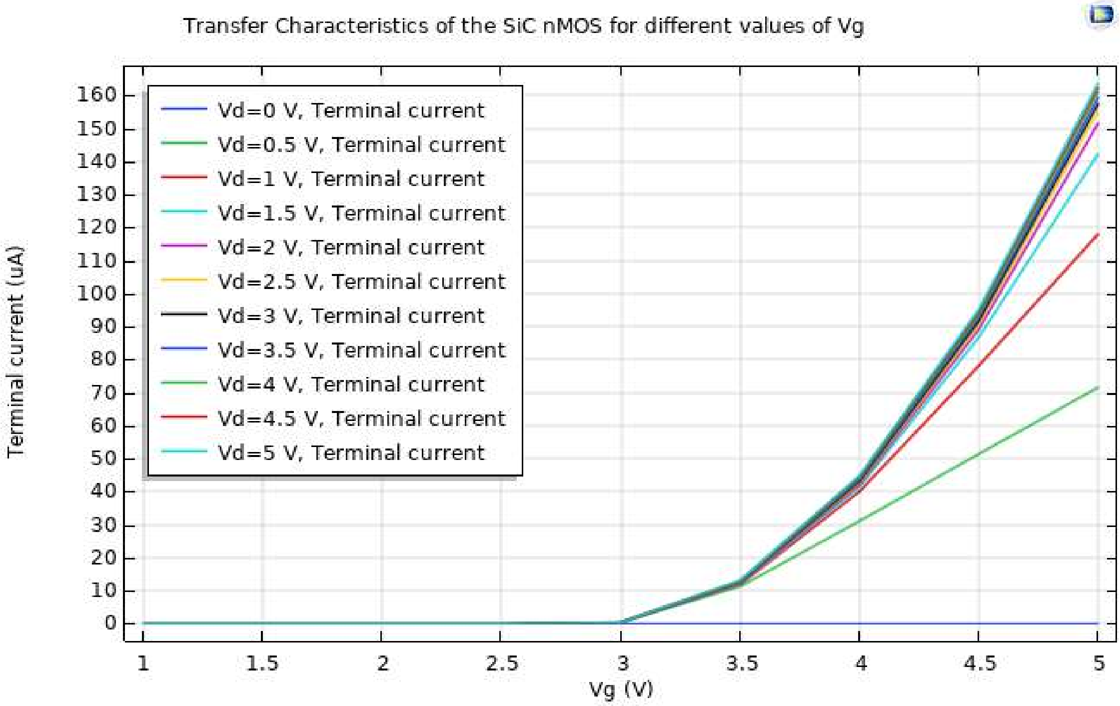

(b) Transfer Characteristics of SiC nMOS

Fig. 21. Transfer and Output Characteristics of SiC MOSFET, (a) Output Characteristics of SiC nMOS (b) Transfer Characteristics of SiC nMOS

Finally, due to the SiC MOSFET's V_t=2.8V, found in **Fig. 21(a) & 21(b),** the output curves couldn't be found for the range of 1V to 2.5V of V_g since the channel can't be created. In **Fig. 21(a) & 21(b)**, after the V_g=2.8V, the output curves are presented, though the terminal current of the saturation is much lower than the Si and Ge based MOSFETs for the same parameters and values. In this study, most of the material properties of SiC are close to the 4H-SiC so that for other types of SiC like 6H-SiC, 3H-SiC, etc. the result may be different.

Another important factor in this study is the simulation is run with the COMSOL Multiphysics 5.5 software which is itself run with pre-assumed and pre-determined values and parameters, which could affect the whole simulation process. However, the geometry of MOSFET used for all three times plays an important role in the characteristics. By changing the oxide layers, doping concentrations, other parameters of the structure or properties of materials, the characteristics would be dramatically changed. But for any study or operational setup like the above scenarios, the Ge-based MOSFET can give better performance, which may show us an alternative, maybe the better scope over today's Si material and devices. Moreover, there are many other research scopes on this particular topic to get faster and efficient semiconductor devices.

4.2 Three Materials based PiN Diode's Forward Recovery Characteristics

Here, some of the PiN diodes forward recovery characteristics such as band energy level diagram, electric potential, electron concentration, forward recovery voltage and switching time have done for Si, Ge & SiC based PiN diodes.

4.2.1 Band Energy Level (Semi) Diagrams of the PiN Diodes:

Fig. 22(a), 22(b) & 22(c), shows the energy conduction band energy level by the blue lines and valance band energy level by green lines for the Si, Ge and SiC PiN diodes respectively, which has an effect on electron concentration, shown in the following figures.

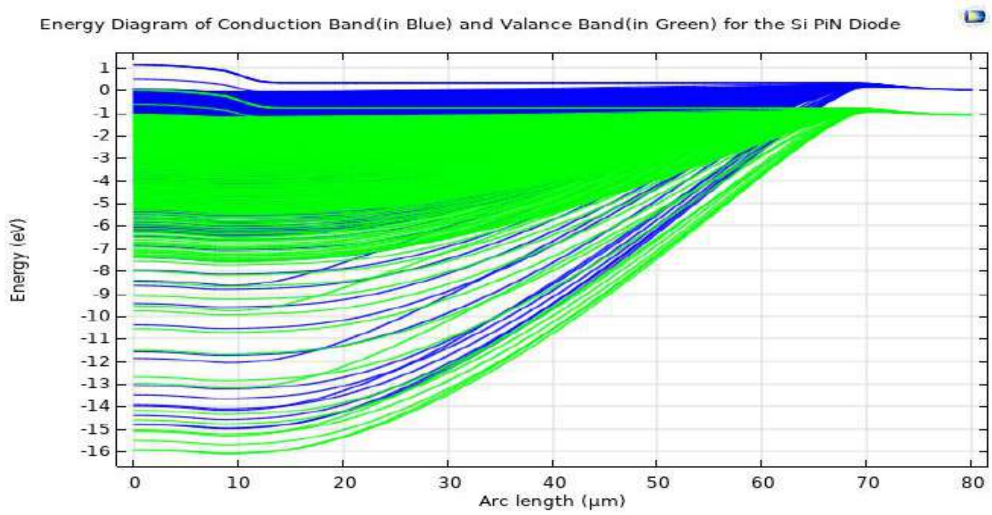

(a) For Si-PiN diode

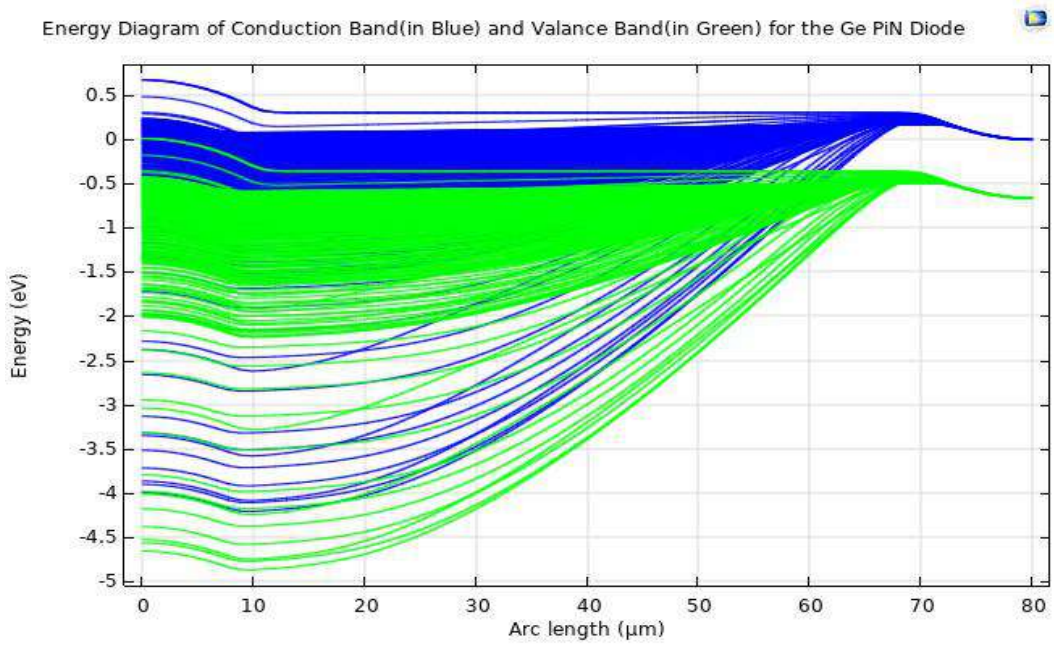

(b) For Ge-PiN diode

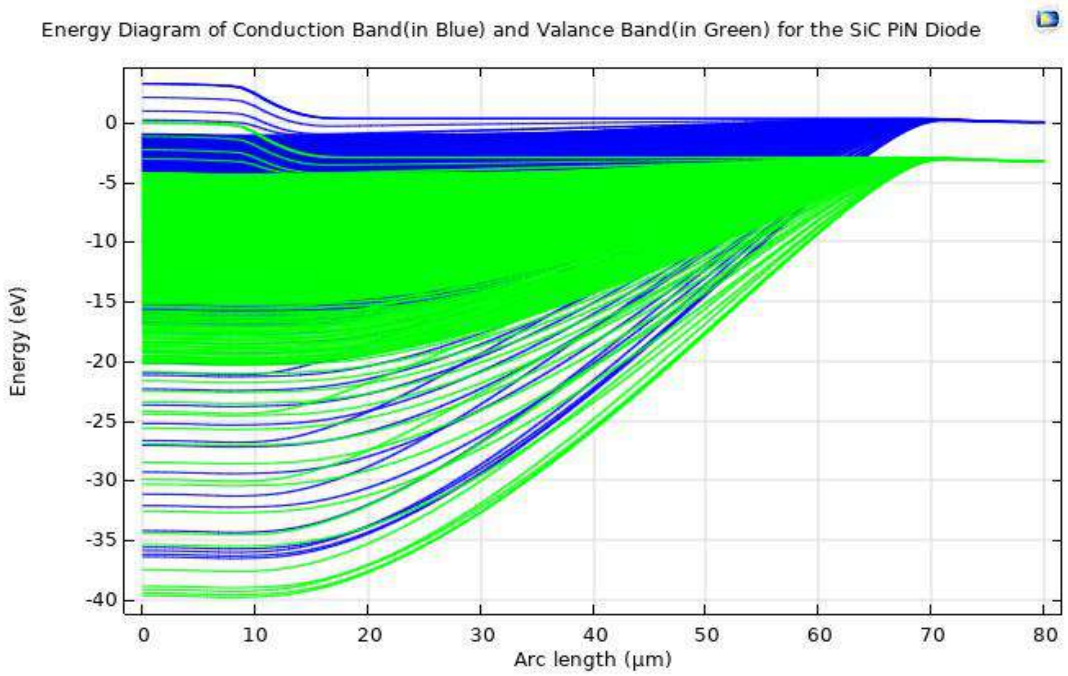

(c) For SiC-PiN diode

Fig. 22. Band energy diagrams of the Si, Ge and SiC PiN diodes for conduction band in Blue lines and for Valance band in Green, (a) For Si-PiN (b) For Ge-PiN (c) For SiC-PiN

From **Fig. 22(a)**, it's shown that the energy of conduction and valance band of the PiN diode overlapped with a large range of -16eV to 1eV. However, in **Fig. 22(b),** the energy of conduction and valance band overlapped with a shorter range of -5eV to 0.5eV than both Si-PiN and SiC-PiN diodes. And finally, in **Fig. 22(c),** band energy for SiC-PiN diode has overlapped each other with a range of -40V to 5V, which is a huge amount of than other two.

4.2.2 Electric Potential of the PiN Diodes:

The electric potential of the Si, Ge and SiC PiN diode is shown in **Fig. 23(a), 23(b) & 23(c),** respectively. In this experimental setup, it's clear that the Si PiN diode showed the higher electric potential of a range -5V to 33V, and the Ge PiN diode showed a negative range of 0V to -4.5V with the arc length of the PiN diode.

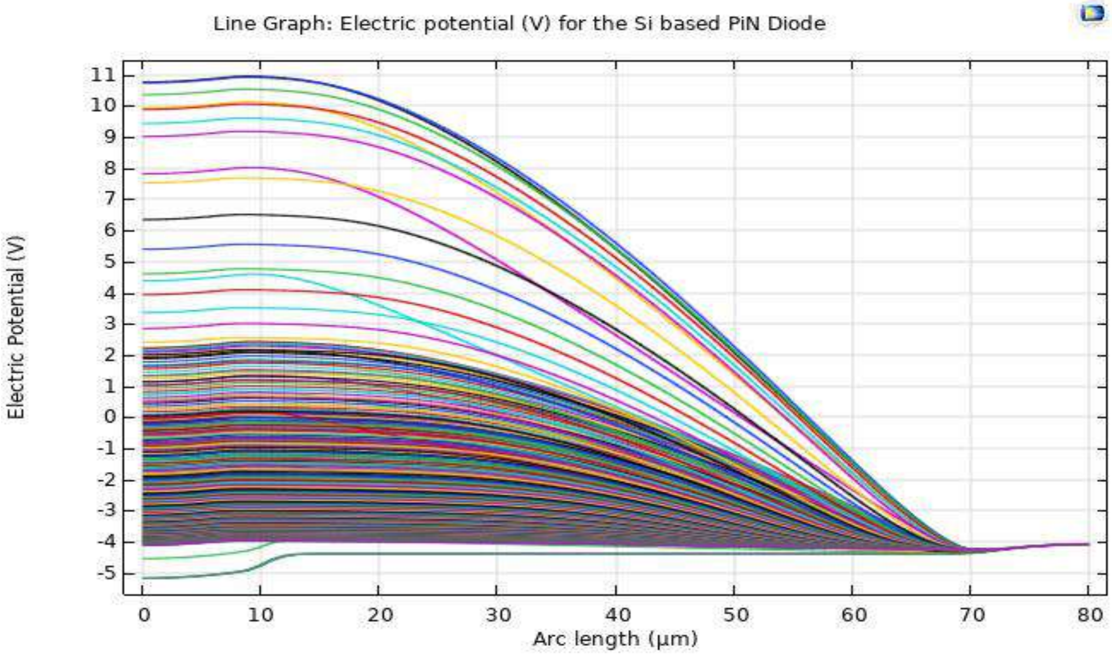

(a) For Si-PiN diode

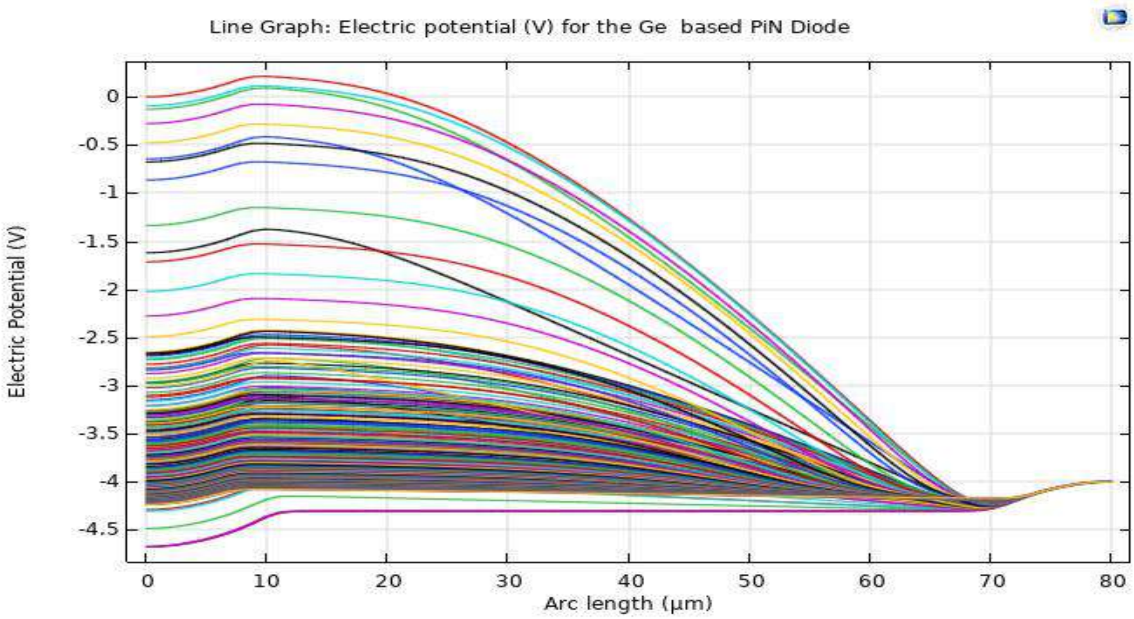

(b) For Ge-PiN diode

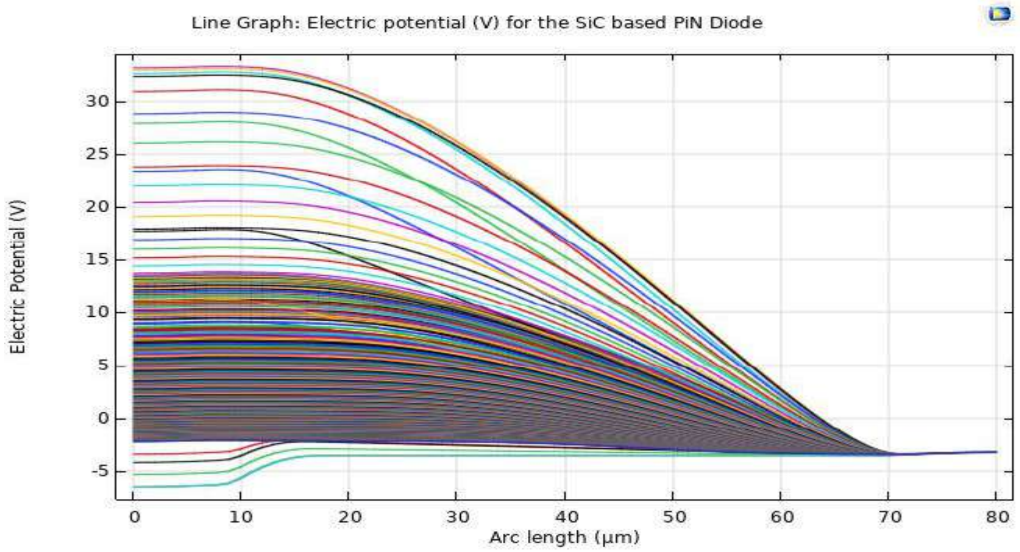

(c) For SiC-PiN diode

Fig. 23. Electric potential (V) of the Si, Ge and SiC PiN diodes, (a) For Si-PiN (b) For Ge-PiN (c) For SiC-PiN

For both materials PiN diodes, the line graph of electric potential is much higher with a large range from 0µm to 10µm arc length of P+ region. After 10µm of arc length, the potential start to be less down because of the intrinsic region from 10µm to 70µm arc length, and finally, the electric potential is fully accumulated and less down because of the N+ region from 70µm to 80µm arc length, which is shown in **Fig. 23(a), 23(b) & 23(c)**.

4.2.3 Electron Concentration of the PiN Diodes:

The electrons are highly concentrated in the arc length of about 9µm for the three PiN diodes of Si, Ge & SiC PiN diodes respectively, shown in **Fig. 24(a), 24(b) & 24(c)**.

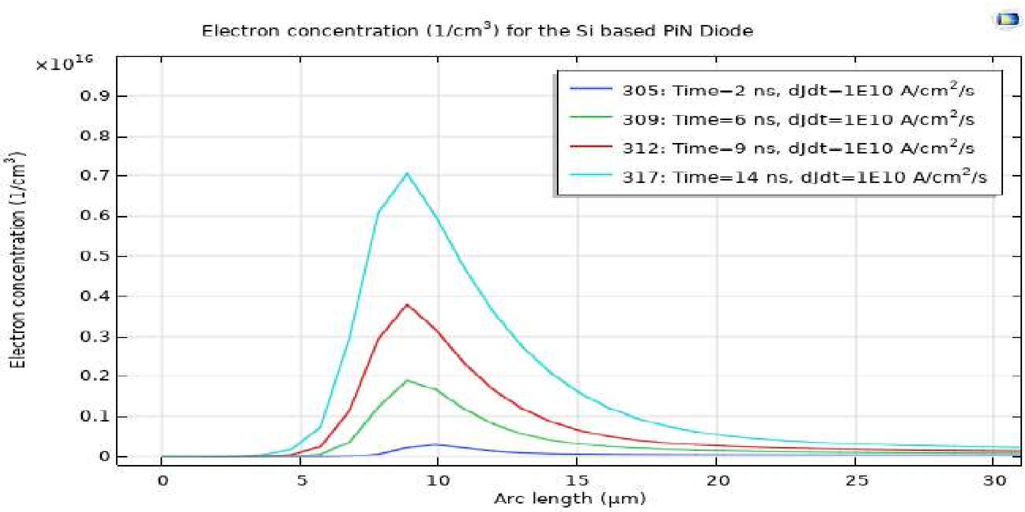

(a) For Si-PiN diode

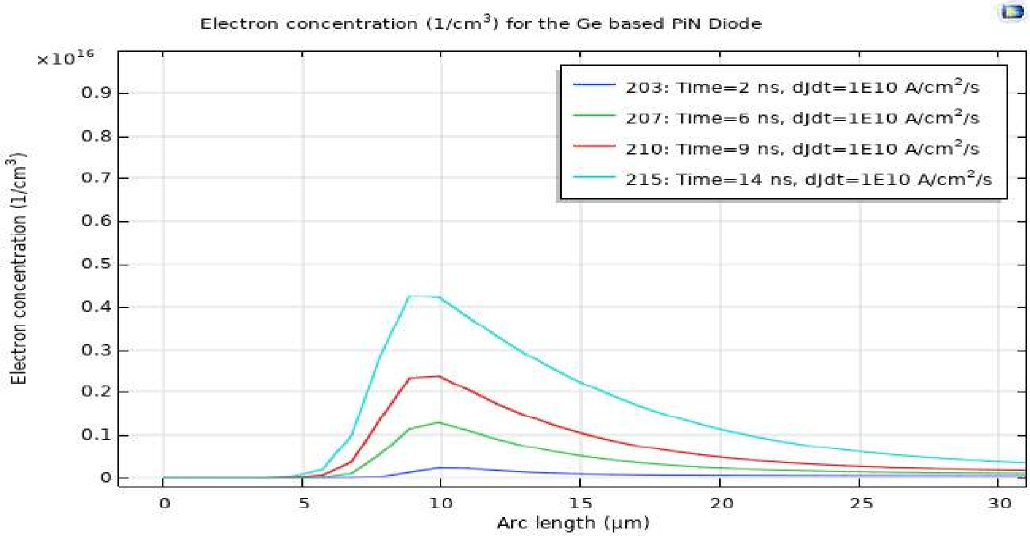

(b) For Ge-PiN diode

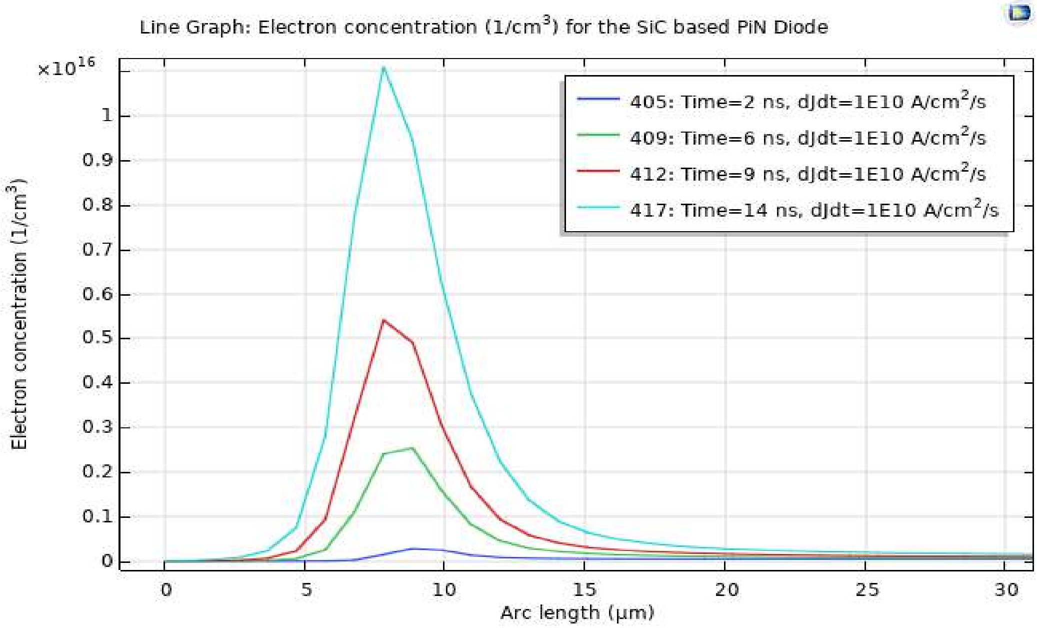

(c) For SiC-PiN diode

Fig. 24. Electron concentration for Si, Ge and SiC PiN diodes, (a) For Si-PiN (b) For Ge-PiN (c) For SiC-PiN

For the current density ramp rate, $\frac{dj}{dt}$ = 1×10^{10} A.cm^{-2}s^{-1} in the time of 14ns, the concentration of electrons in PiN diode for Si is close to $0.7 \times 10^{16}\ 1/cm^3$ shown in **Fig. 24(a),** for Ge is about $0.42 \times 10^{16}\ 1/cm^3$ which is shown in **Fig. 24(b),** and for SiC is about $1.12 \times 10^{16}\ 1/cm^3$ which is shown in **Fig. 24(c).** Due to this response of Si-PiN and SiC-PiN diodes may show the sudden but higher forward voltage drops, V_{Fr}(t) of near 16V and 40V than Ge-PiN diode in time of the forward recovery, which are shown in **Fig. 25(a), 25(b) & 25(c)**.

4.2.4 Forward Recovery Voltage and Time for the PiN diodes:

When a PiN diode is transformed from reverse biased condition to forward conduction mode, the voltage forward drop, $V_{Fr}(t)$ across the diode suddenly rises to a much bigger amount than the actual ON-state voltage drop when operating in steady-state mode and after the forward recovery, t_{fr} time it starts to operate in steady-state level, which are also shown in **Fig. 25(a), 25(b) & 25(c)** for the three- Si, Ge and SiC based PiN diodes respectively and that can be relatable to the forward recovery characteristics [26].

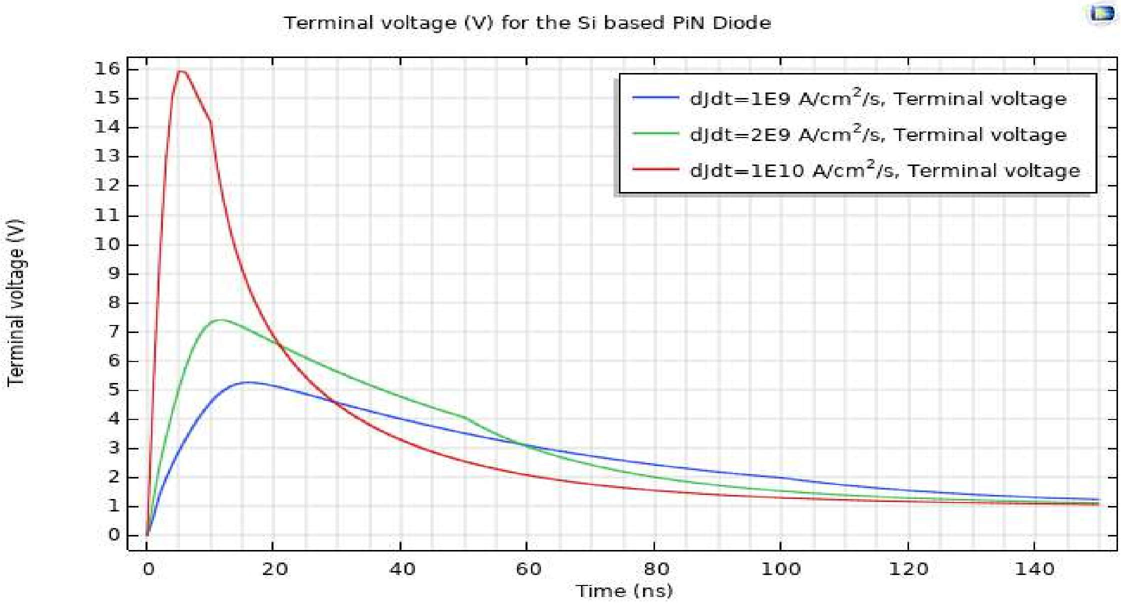

(a) For Si-PiN diode

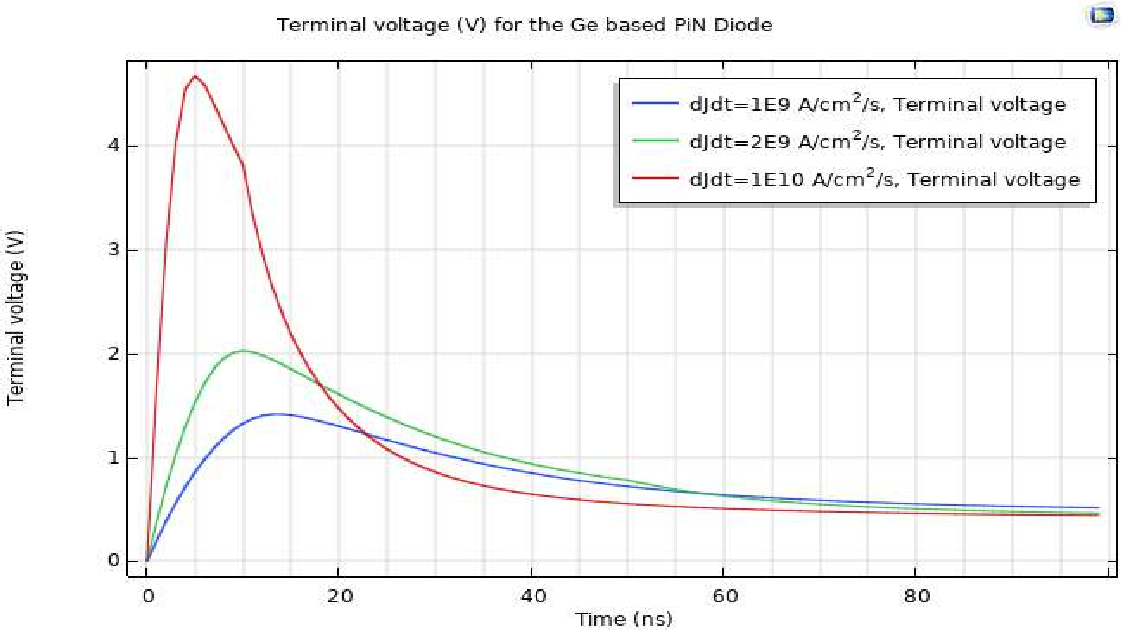

(b) For Ge-PiN diode

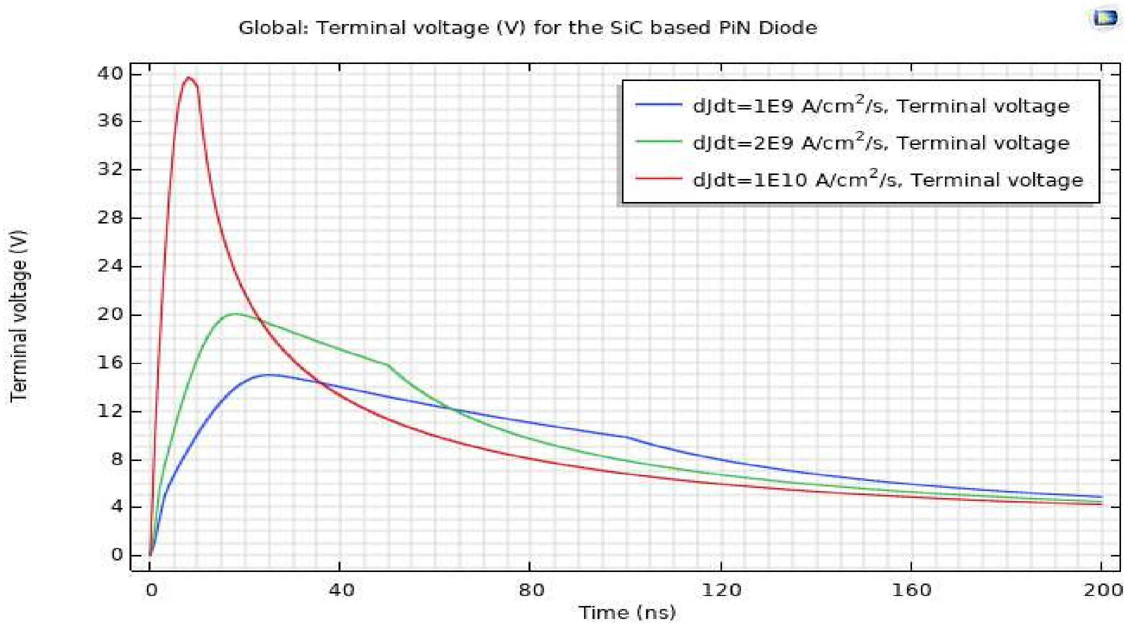

(c) For SiC-PiN diode

Fig. 25. Forward recovery voltage (V_{Fr}) and forward recovery time for Si, Ge and SiC PiN diodes, (a) For Si-PiN (b) For Ge-PiN (c) For SiC-PiN

For the Si-PiN diode in **Fig. 25(a),** the transient rise of $V_{Fr}(t)$ is close to 16V and the forward recovery time is almost 110ns for the current density ramp rate, dj/dt= 1×10^{10} A.cm^{-2}s^{-1}. For the other two dj/dt, the forward recovery times are higher as 120ns and 140ns respectively than the previous one.

In **Fig. 25(b),** for the Ge-PiN diode, the rise of $V_{Fr}(t)$ is less like to 4.7V and the forward recovery time is faster like 50ns for the current density ramp rate, dj/dt= 1×10^{10} A.cm^{-2}s^{-1}. For the other two dj/dt, the forward recovery times are higher than the previous one but lesser than both the Si-PiN and SiC-PiN diode.

For the SiC-PiN diode in **Fig. 25(c),** the transient rise of $V_{Fr}(t)$ is close to 16V and the forward recovery time is almost 110ns for the current density ramp rate, dj/dt= 1×10^{10} A.cm^{-2}s^{-1}, which is much higher from both Si and Ge PiN diode responses for the same current density rate. For the other two dj/dt, the forward recovery times are more than the 200ns.

Here, we represent the changes found among the characteristics of PiN diode after varying the materials by Si, Ge and SiC respectively. From **Fig. 25(a), 25(b), 25(c)** and above studies, we can comment that for this certain study and setup, the PiN diode of Ge material is performing the fastest forward recovery time, t_{fr} as 50ns, which is less than half and one-fourth of the Si-PiN and SiC-PiN diode responses respectively for the current density ramp rate of 1×10^{10} $A.cm^{-2}s^{-1}$ as well as the maximum forward recovery voltage, V_{Fr} is lower than the Si-PiN and SiC-PiN diode, which may give advantages to Ge-PiN diode for less power loss. And with the increment of the current density ramp rate, dj/dt from 1×10^{9} $A.cm^{-2}s^{-1}$ to 1×10^{10} $A.cm^{-2}s^{-1}$, the transients of the maximum forward voltage drops are much higher, and forward recovery time is also slightly higher for both Si, Ge and SiC based PiN diode.

For these certain conditions in material setup as well as study setup, the Ge-based PiN diode performs better than Si-based PiN diodes for the characteristics like the lower terminal voltage, faster forward recovery time along with the electric potential, electron concentration, the energy of valance and conduction band, etc.

The simulation is operated with the COMSOL Multiphysics software with the version of 5.5 so that it runs some algorithm of itself which may have some effects itself on the results.

Furthermore, there are some other factors of parameters in material selection as well as the simulation setups for which the responses may be changed as our expectations, faster and more efficient, which could be explored as a new window of research for the Ge based power devices as Si and SiC based devices by changing individual semiconductors doping, changing the geometry, etc. along with varying other materials in PiN diode studies. But for any study or operational setup like the above scenarios, the Ge-based PiN can give better performance.

CHAPTER 5

CONCLUSIONS AND FUTURE WORKS

5.1 Conclusions

The results for the three different materials MOSFETs, found by the simulations, are surprising as the Ge-MOSFET has shown better switching response than the other Si and SiC MOSFETs on the basis of lower threshold voltage and higher current rating. The Ge-MOSFET needs half the threshold voltage than the SiC-MOSFET for this setup and more than two times more terminal current than Si-MOSFET and more than ten times more terminal current than SiC-MOSFET. Though this study isn't challenging for migrating to other semiconductor devices from Si material, this indicates the possibility and positivity of future research not only on the SiC devices but also on other semiconductors like Ge devices. In case of diode, the potentiality of Ge based devices and others as Si and SiC since the Ge based PiN diode gives the faster forward recovery. For a certain current density, the Ge-PiN diode shows one-third of forward recovery time approximately than the Si based and one-fourth of forward recovery time than the SiC based PiN diode approximately. The Ge-PiN diode also shows much lower transient voltage than the other two. Though there are many challenges for Ge-based devices as SiC-based devices for coming out from the triumph of Si, there are scopes of future research in this topic.

5.2 Limitations

The study is done by COMSOL Multiphysics Software of version 5.5 and 5.6, which has its own algorithm of simulation and computational system, which may have effects on the outcomes. A certain range of study setups has been given for the study.

5.3 Future Works

1. To study the temperature study on these three Si, Ge and SiC based MOSFETs
2. To study the DC characteristics of the same geometrical and setups based MOSFET for other materilas like- GaAs, GaN, etc.
3. To study the reverse recovery characteristics for the above three PiN diodes, which are based on Si, Ge and SiC materials
4. To study the same reverse and forward recovery chractericsts for another materials-based PiN diode
5. To study the recovery reponses for the other types of diodes like- PN junction diode, JBS, Schottky diode, etc.

REFERENCES

[1] J. G. Kassakian and T. M. Jahns, “Evolving and emerging applications of power electronics in systems,” *IEEE J. Emerg. Sel. Top. Power Electron.*, vol. 1, no. 2, pp. 47–58, 2013, doi: 10.1109/JESTPE.2013.2271111.

[2] J. D. Van Wyk and F. C. Lee, “On a future for power electronics,” *IEEE J. Emerg. Sel. Top. Power Electron.*, vol. 1, no. 2, pp. 59–72, 2013, doi: 10.1109/JESTPE.2013.2271499.

[3] J. Millan, P. Godignon, X. Perpina, A. Perez-Tomas, and J. Rebollo, “A survey of wide bandgap power semiconductor devices,” *IEEE Trans. Power Electron.*, vol. 29, no. 5, pp. 2155–2163, 2014, doi: 10.1109/TPEL.2013.2268900.

[4] M. Houssa, A. Satta, E. Simoen, B. D. Jaeger, M. Meuris, M. Caymax and M. Heyns., “Electrical Performance of Ge Devices,” *Ger. Technol.*, pp. 233–265, Dec. 2007, doi: 10.1016/B978-008044953-1/50012-0.

[5] X. She, A. Q. Huang, O. Lucia, and B. Ozpineci, “Review of Silicon Carbide Power Devices and Their Applications,” *IEEE Trans. Ind. Electron.*, vol. 64, no. 10, pp. 8193–8205, 2017, doi: 10.1109/TIE.2017.2652401.

[6] M. L. and Q. K. M Zabeli, N. Caka, “The impact of MOSFET’s physical parameters on its threshold voltage,” *MINO’07 Proc. 6th Conf. Microelectron. Nanoelectron. Optoelectron.*, pp. 54–58, 2007, [Online]. Available: http://www.researchgate.net/profile/Nebi_Caka/publication/235955639_The_impact_of_MOSFET’s_physical_parameters_on_its_threshold_voltage/file/72e7e514b8eec1764c.pdf.

[7] J. Wang, “A Comparison between Si and SiC MOSFETs,” *IOP Conf. Ser. Mater. Sci. Eng.*, vol. 729, no. 1, 2020, doi: 10.1088/1757-899X/729/1/012005.

[8] R. Kibushi, T. Hatakeyama, K. Yuki, N. Unno and M. Ishizuka, "Comparison of thermal properties between Si and SiC power MOSFET using electro-thermal analysis," *2017 International Conference on Electronics Packaging (ICEP)*, 19-22 April 2017, Yamagata, Japan, pp. 188-192, doi: 10.23919/ICEP.2017.7939354.

[9] M. Nawaz and K. Ilves, “Replacing Si to SiC: Opportunities and challenges,” *Eur. Solid-State Device Res. Conf.*, vol. 2016-Octob, pp. 472–475, 2016, doi: 10.1109/ESSDERC.2016.7599688.

[10] X. Gu, Q. Shui, C. W. Myles, and M. A. Gundersen, “Comparison of Si, GaAs, SiC and GaN FET-type switches for pulsed power applications,” *Dig. Tech. Pap. Int. Pulsed Power Conf.*, pp. 362–365, 2003, doi: 10.1109/ppc.2003.1277729.

[11] R. Kannan, H. Khalid, V. Indragandhi, and S. Albert Alexander, “Threshold voltage and drain current investigation of power MOSFET ZVN3320FTA by 2D simulations,” *Int. J. Simul. Syst. Sci. Technol.*, vol. 19, no. 6, pp. 39.1-39.6, 2018, doi: 10.5013/IJSSST.a.19.06.39.

[12] P. Jain and B. K. Mishra, “An Investigation of DC Characteristics in Multifinger Optically Illuminated MOSFET,” *Int. J. Comput. Appl.*, vol. 61, no. 2, pp. 12–17, 2013, doi: 10.5120/9899-4479.

[13] K. K. Ng, “p-i-n Diode,” *Complet. Guid. to Semicond. Devices*, pp. 24–30, 2010, doi: 10.1002/9781118014769.ch2.

[14] P. A. Ivanov, I. V. Grekhov, A. S. Potapov, N. D. Il’inskaya, T. P. Samsonova, and O. I. Kon’kov, “Experimental 4H-SiC junction-barrier Schottky (JBS) diodes,” *Semiconductors*, vol. 43, no. 9, pp. 1209–1212, 2009, doi: 10.1134/s106378260909019x.

[15] M. Berthou, P. Godignon, J. Calvo, A. Mihaila, E. Bianda, and I. Nistor, “Comparison of 5kV SiC JBS and pin diodes,” *Mater. Sci. Forum*, vol. 778–780, pp. 867–870, 2014, doi: 10.4028/www.scientific.net/MSF.778-780.867.

[16] J. Lutz, H. Schlangenotto, U. Scheuermann, and R. De Doncker, *pin Diodes*. 2018.

[17] C. D. Root, J. Melillo, and S. Ammon, “Computer Modeling of Diode Forward Recovery Characteristics,” *IEEE Trans. Electron Devices*, vol. 29, no. 3, pp. 461–463, 1982, doi: 10.1109/T-ED.1982.20724.

[18] A. G. M. Strollo and E. Napoli, “Improved PIN diode circuit model with automatic parameter extraction technique,” *IEE Proc. Circuits, Devices Syst.*, vol. 144, no. 6, pp. 329–334, 1997, doi: 10.1049/ip-cds:19971487.

[19] Y. Wang, Q. Zhang, J. Ying, and C. Sun, “Prediction of PIN diode reverse recovery,” *PESC Rec. - IEEE Annu. Power Electron. Spec. Conf.*, vol. 4, pp. 2956–2959, 2004, doi: 10.1109/PESC.2004.1355304.

[20] Y. C. Liang and V. J. Gosbell, “Diode Forward and Reverse Recovery Model for Power Electronic SPICE Simulations,” *IEEE Trans. Power Electron.*, vol. 5, no. 3, pp. 346–356, 1990, doi: 10.1109/63.56526.

[21] “Chapter 5 – Field-Effect Transistors (FETs) - ppt video online download.”

https://slideplayer.com/slide/5122876/ (accessed Nov. 27, 2021).
[22] "Analysis of MOSFET as a Switch with Circuit Diagram, Example." https://www.electronicshub.org/mosfet-as-a-switch/ (accessed Nov. 27, 2021).
[23] W. Dorothy and R. Joos, "the Pin Diode Circuit Designers' Handbook," *Watertown*, no. 617, 1998, [Online]. Available: https://www.ieee.li/pdf/essay/pin_diode_handbook.pdf.
[24] P. Bhushan, "Module 1," *Dermatology a Week*, pp. 1–1, 2006, doi: 10.5005/jp/books/10200_1.
[25] B. J. Baliga, *Fundamentals of power semiconductor devices, Second edition*. 2018.
[26] D. a. Neamen, *Semiconductor Physics and Devices: Basics Aplications*. 2012.
[27] A. Elasser, M. Ghezzo, N. Krishnamurthy, J. Kretchmer, A. W. Clock, D. M. Brown and T. P. Chow, "Switching characteristics of silicon carbide power PiN diodes," *Solid. State. Electron.*, vol. 44, no. 2, pp. 317–323, 2000, doi: 10.1016/S0038-1101(99)00238-5.
[28] A. Pérez-Tomás, P. Brosselard, J. Hassan, X. Jordà, P. Godignon, M. Placidi, A. Constant, J. Millán and J. P. Bergman, "Schottky versus bipolar 3.3 kV SiC diodes," *Semicond. Sci. Technol.*, vol. 23, p. 125004, Sep. 2008, doi: 10.1088/0268-1242/23/12/125004.
[29] C. Multiphysics, C. Software, and L. Agreement, "Reverse Recovery of a PIN Diode." https://www.comsol.com/model/reverse-recovery-of-a-pin-diode-57971 (accessed Nov. 27, 2021).
[30] L. Zhang, J. Zhu, M. Zhao, D. Ding, J. Chen, and W. Sun, "Fast recovery SOI PiN diode with multiple trenches," *Superlattices Microstruct.*, vol. 111, pp. 405–413, 2017, doi: 10.1016/j.spmi.2017.06.056.
[31] T. J. Flack, B. N. Pushpakaran, and S. B. Bayne, "GaN Technology for Power Electronic Applications: A Review," *J. Electron. Mater.*, vol. 45, no. 6, pp. 2673–2682, 2016, doi: 10.1007/s11664-016-4435-3.
[32] C. H. Lee, T. Nishimura, T. Tabata, S. K. Wang, K. Nagashio, K. Kita and A. Toriumi, "Ge MOSFETs performance: Impact of Ge interface passivation," *Tech. Dig. - Int. Electron Devices Meet. IEDM*, vol. 2, pp. 416–419, 2010, doi: 10.1109/IEDM.2010.5703384.

APPENDIX - I

1. Si Based nMOS's characteristics

1.1. Si based nMOS's Signed Dopent Concentrations

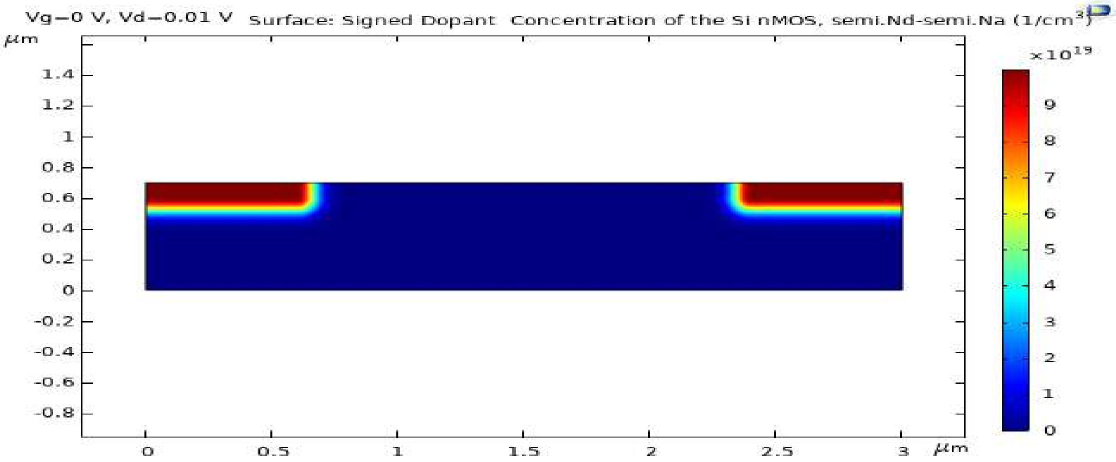

(a) For the V_g= 0V with a fixed V_d= 0.01V

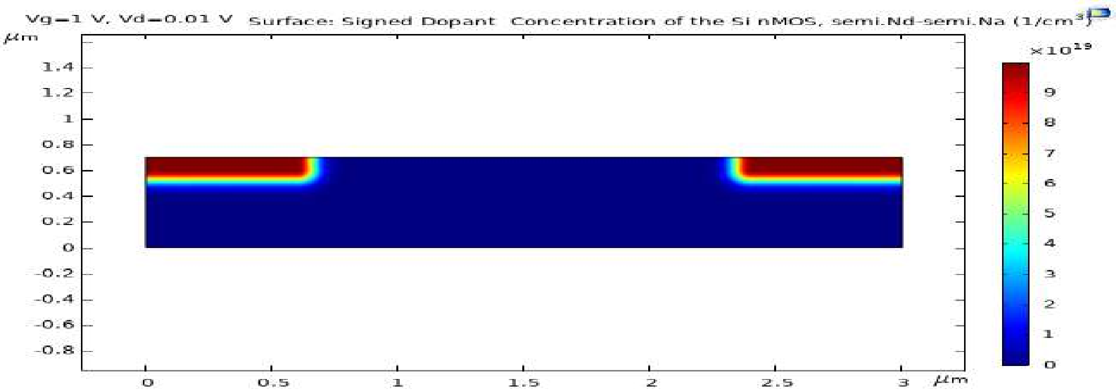

(b) For the V_g= 1V with a fixed V_d= 0.01V

Fig. 26. Signed Dopant Concentration of the Si based n-type MOSFET for different values of V_g

1.2 Si based nMOS's Electron Concentrations

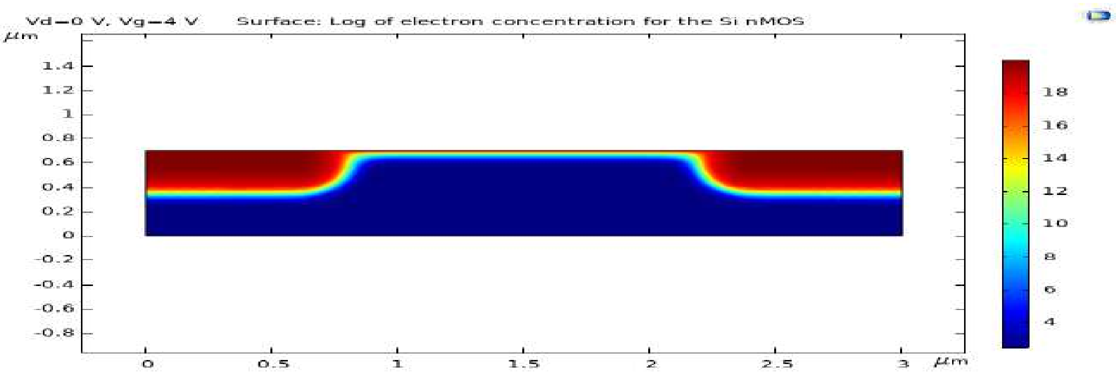

(a) For the V_d= 0V with a fixed V_g= 4V

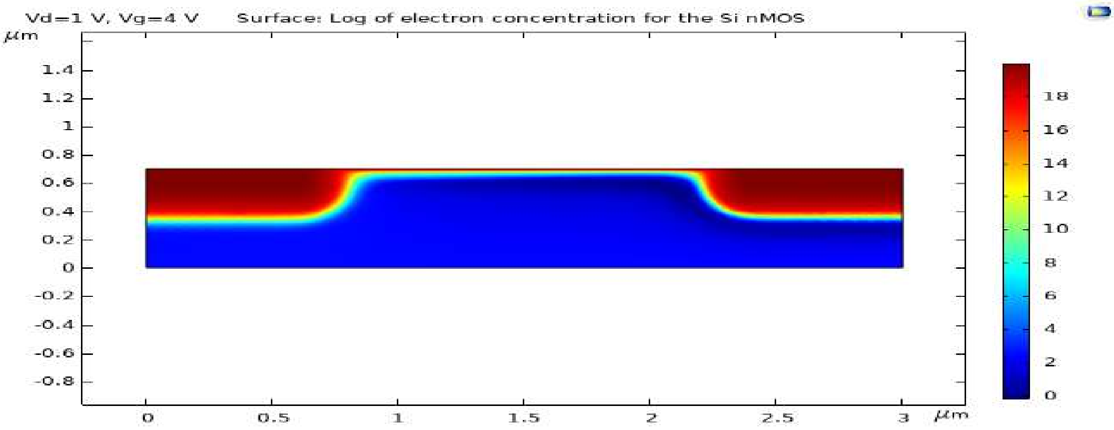

(b) For the V_d= 1V with a fixed V_g= 4V

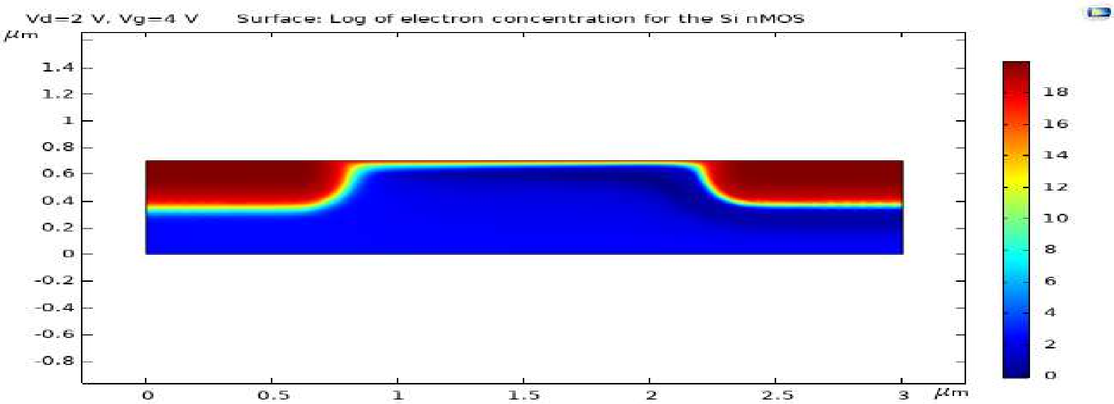

(c) For the V_d= 2V with a fixed V_g= 4V

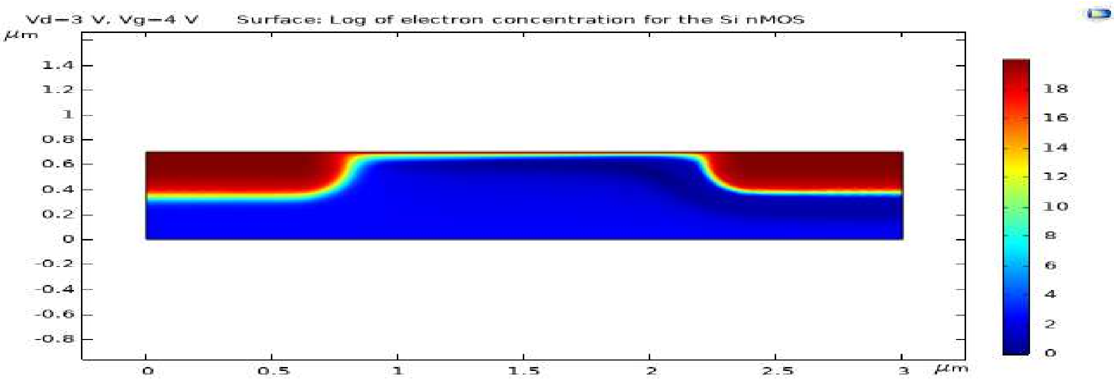

(d) For the V_d= 3V with a fixed V_g= 4V

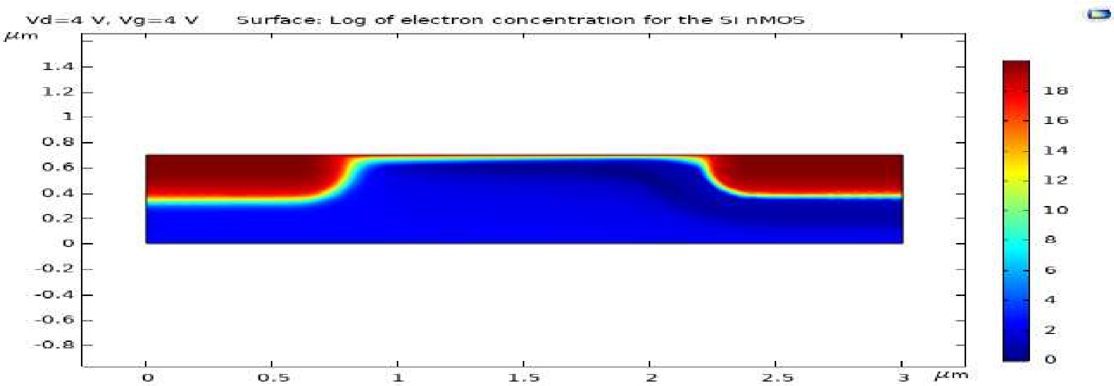

(e) For the V_d= 4V with a fixed V_g= 4V

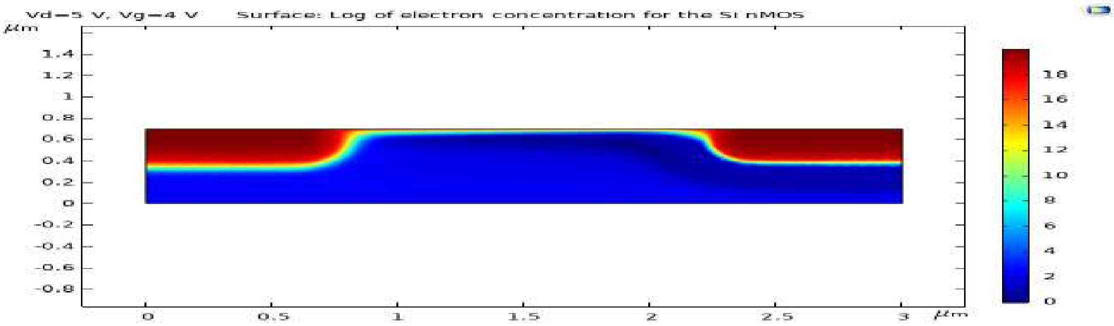

(f) For the V_d= 5V with a fixed V_g= 4V

Fig. 27. Electron Concentration of the Si based n-type MOSFET with a range of 0V to 5V of V_d with a fixed V_g = 4V

1.3 Si based nMOS's Hole Concentrations

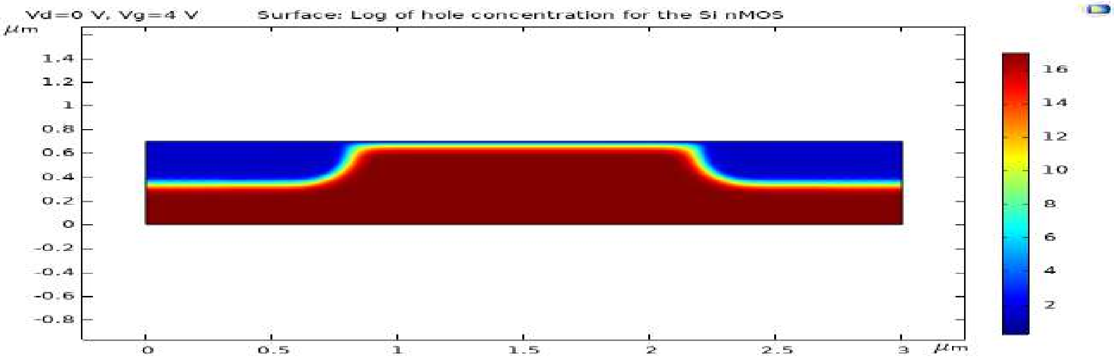

(a) For the V_d= 0V with a fixed V_g= 4V

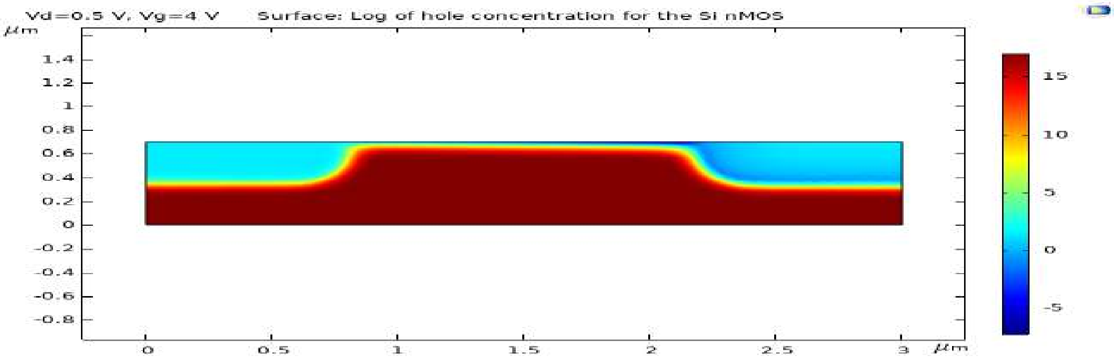

(b) For the V_d= 0.5V with a fixed V_g= 4V

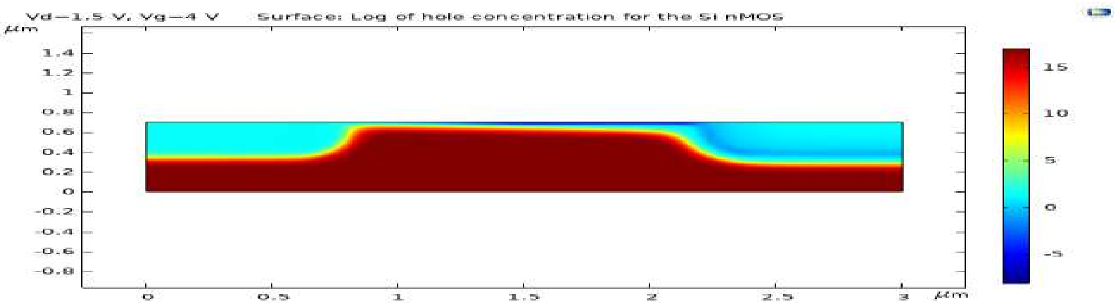

(c) For the Vd= 1.5V with a fixed Vg= 4V

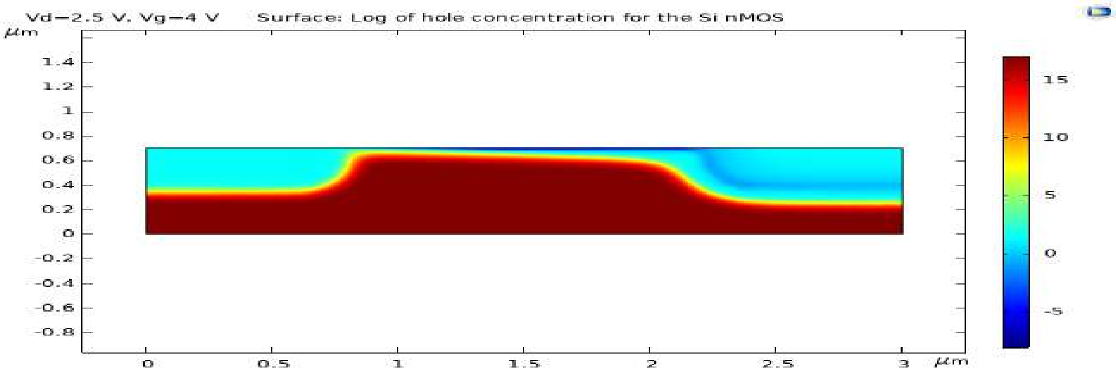

(d) For the V_d= 2.5V with a fixed V_g= 4V

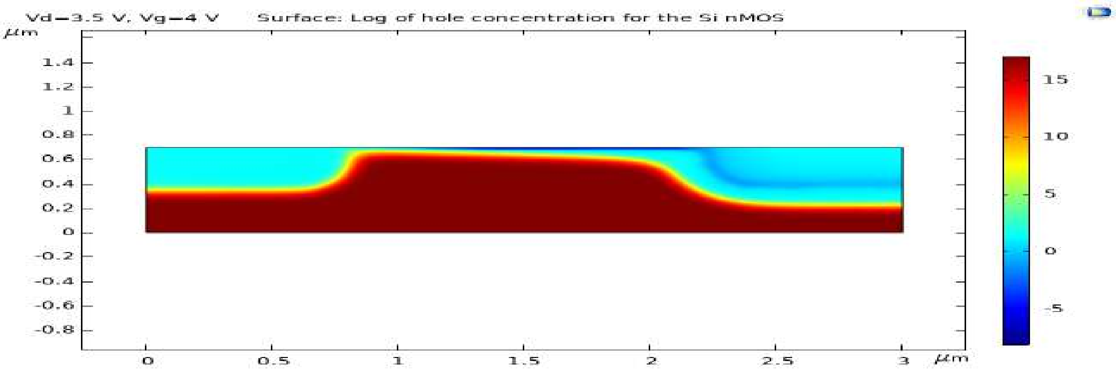

(e) For the V_d= 3.5V with a fixed V_g= 4V

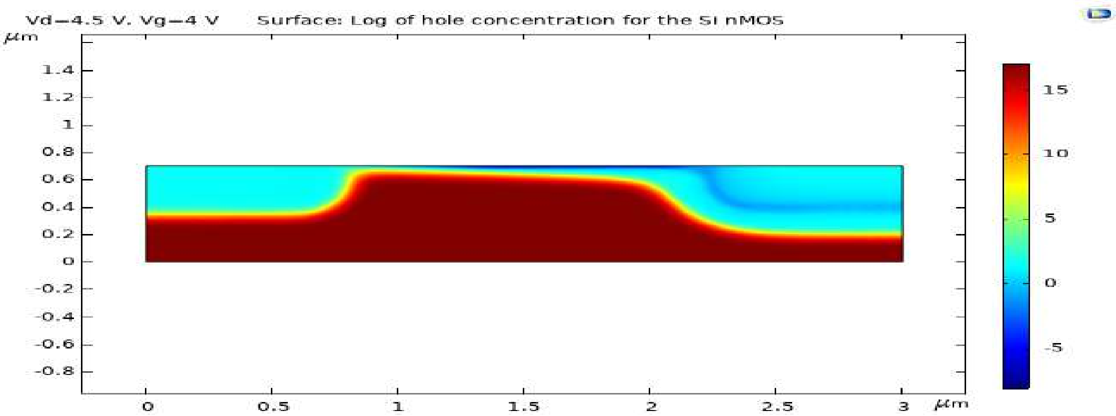

(f) For the V_d= 4.5V with a fixed V_g= 4V

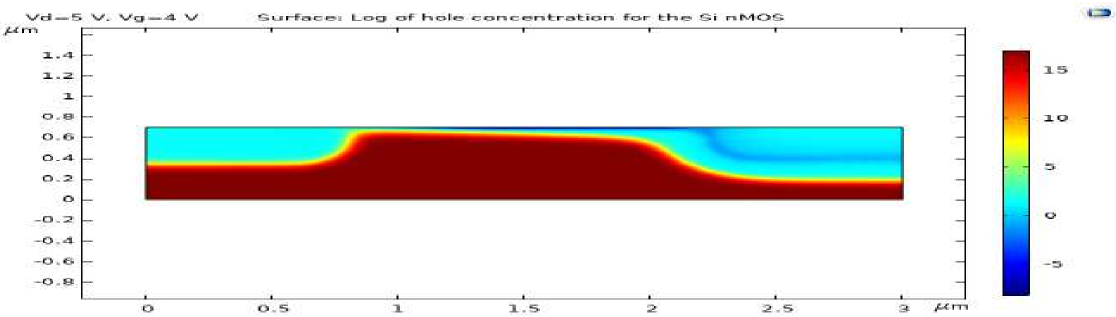

(g) For the V_d= 5V with a fixed V_g= 4V

Fig. 28. Hole Concentration of the Si based n-type MOSFET with a range of 0V to 5V of V_d with a fixed V_g = 4V

1.4 Si based nMOS's Electric potentials

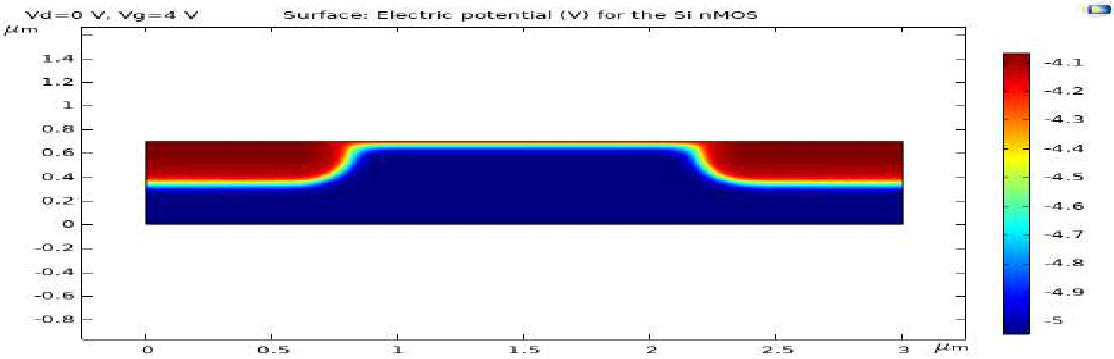

(a) For the V_d= 0V with a fixed V_g= 4V

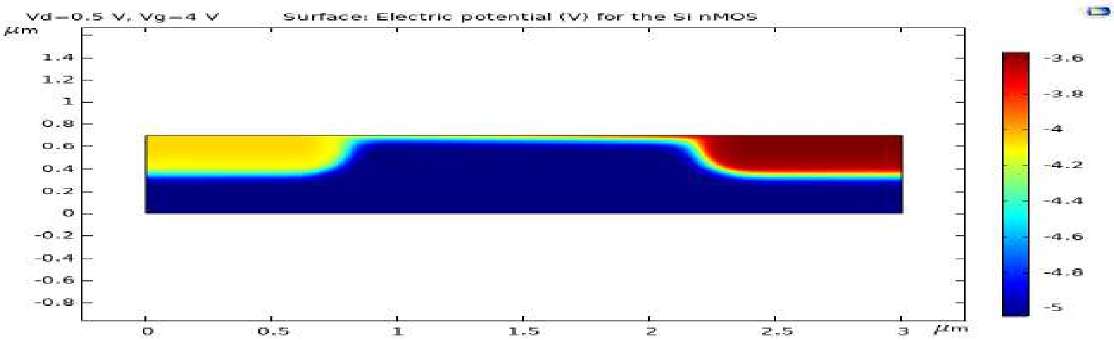

(b) For the V_d= 0.5V with a fixed V_g= 4V

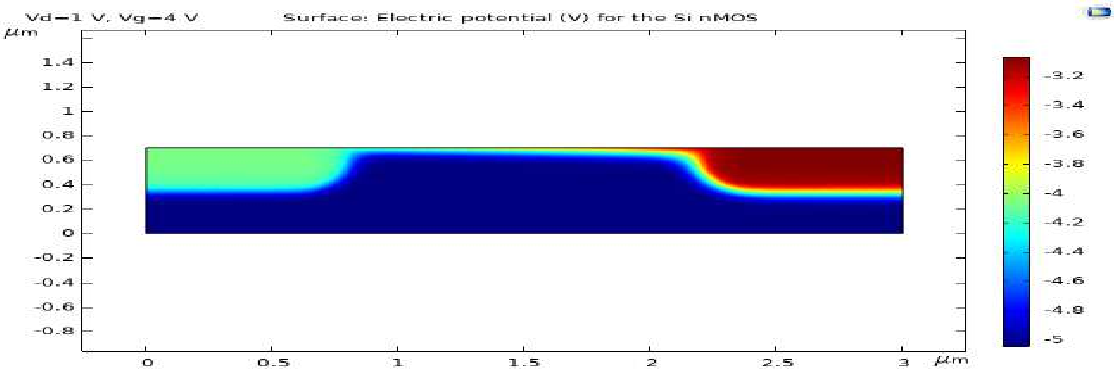

(c) For the V_d= 1V with a fixed V_g= 4V

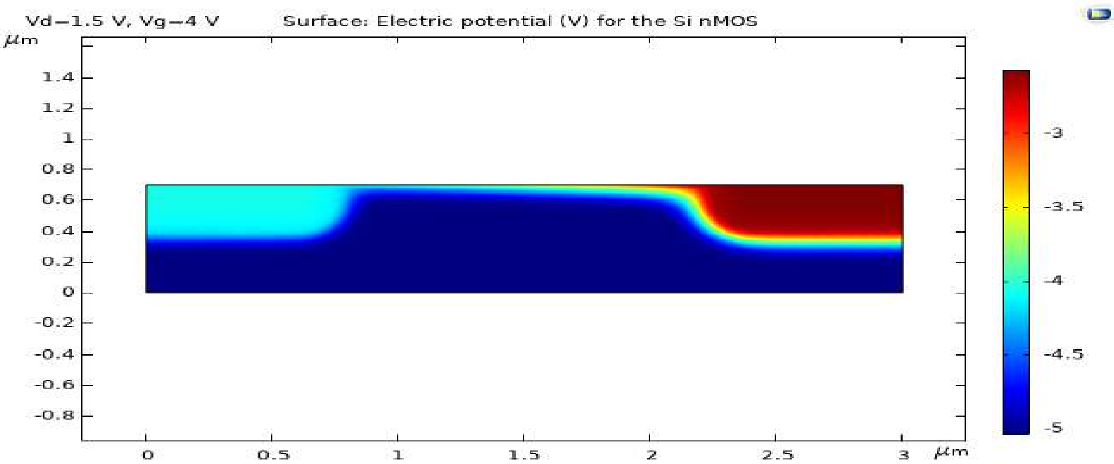

(d) For the V_d= 1.5V with a fixed V_g= 4V

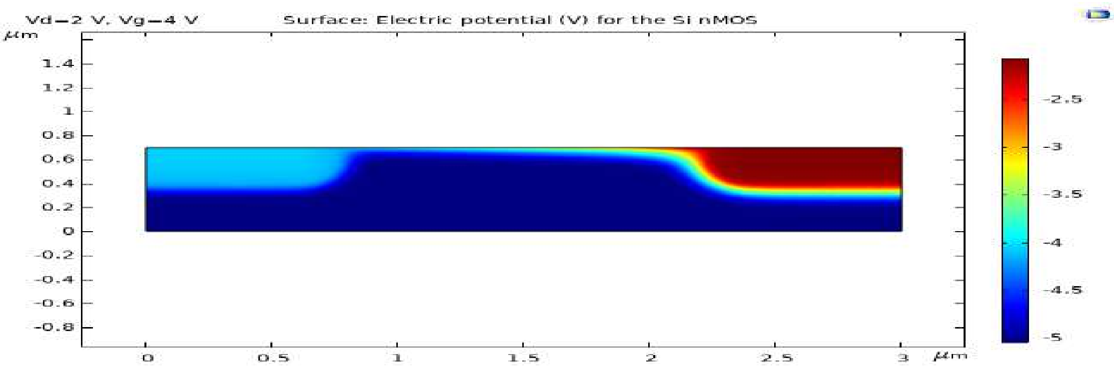

(e) For the V_d= 2V with a fixed V_g= 4V

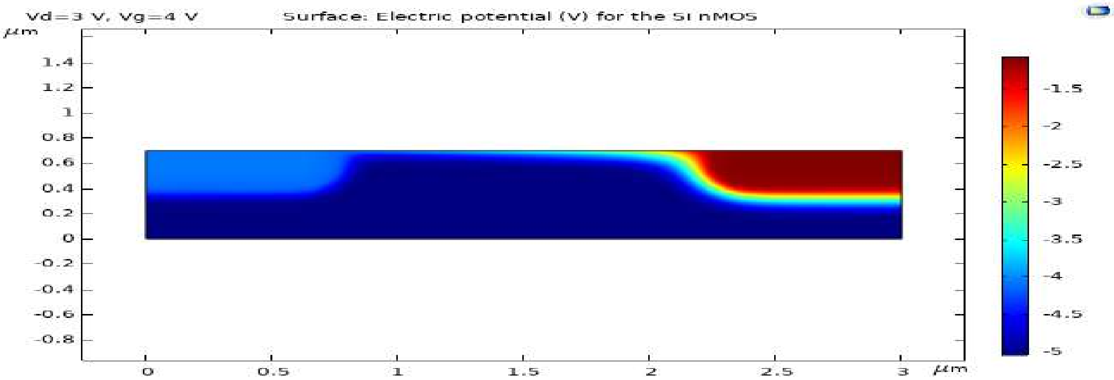

(f) For the V_d= 3V with a fixed V_g= 4V

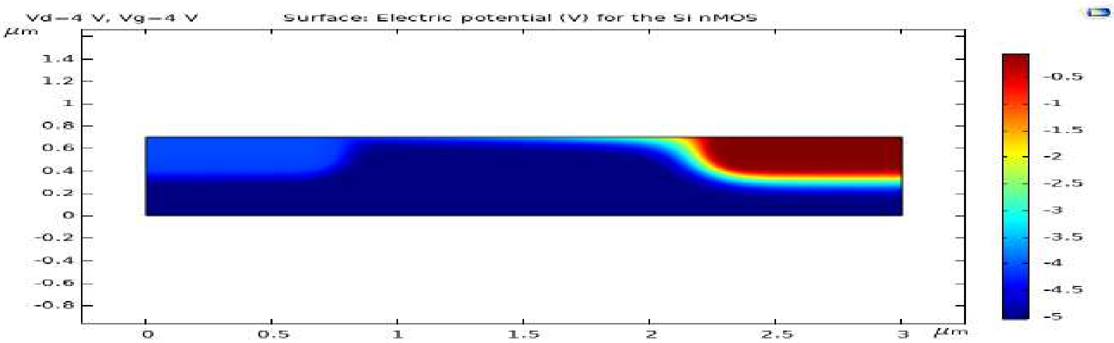

(g) For the V_d= 4V with a fixed V_g= 4V

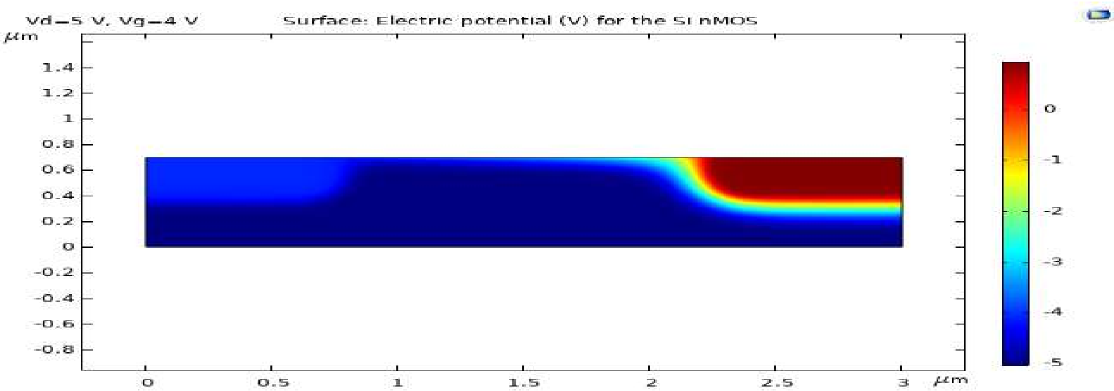

(h) For the V_d= 5V with a fixed V_g= 4V

Fig. 29. **Electric Potential (V) of the Si based n-type MOSFET with a range of 0V to 5V of V_d with a fixed V_g = 4V**

2. Ge Based nMOS's Characteristics

2.1 Ge based nMOS's Signed Dopent Concentrations

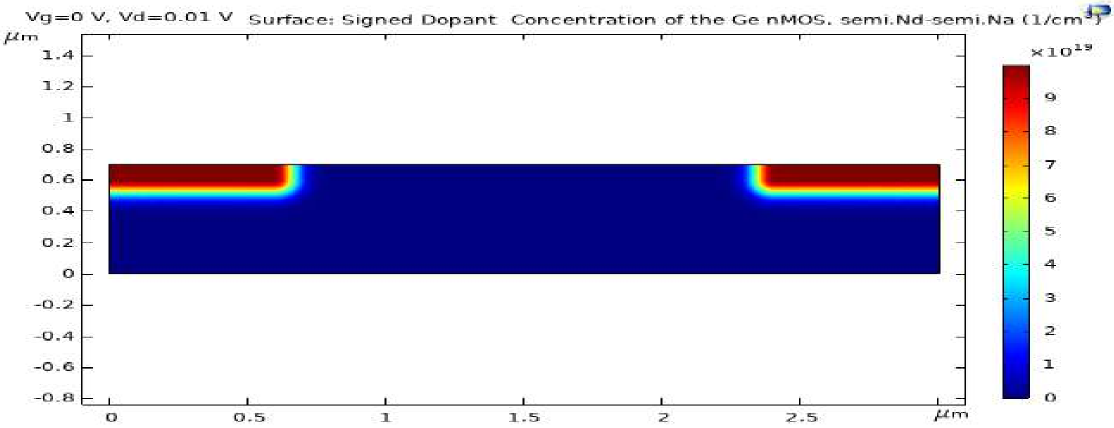

(a) For the V_g= 0V with a fixed V_d= 0.01V

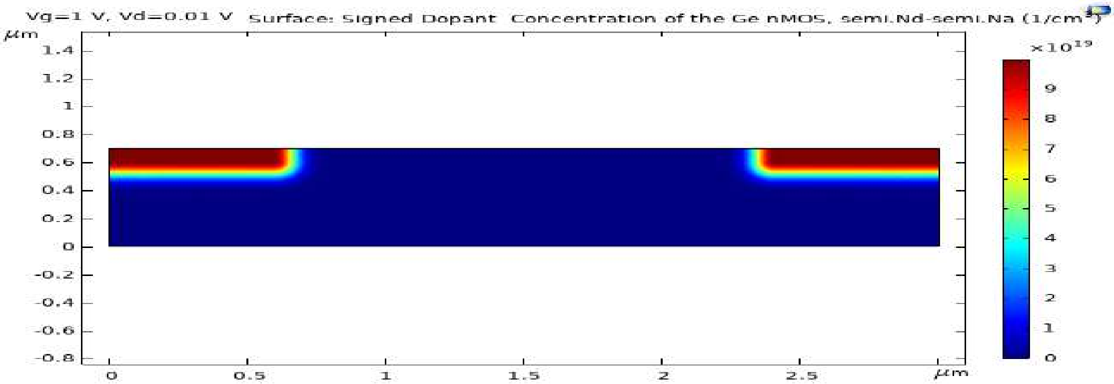

(a) For the V_g= 1V with a fixed V_d= 0.01V

Fig. 30. Signed Dopant Concentration of the Ge based n-type MOSFET for different values of V_g

2.2 Ge based nMOS's Electron Concentrations

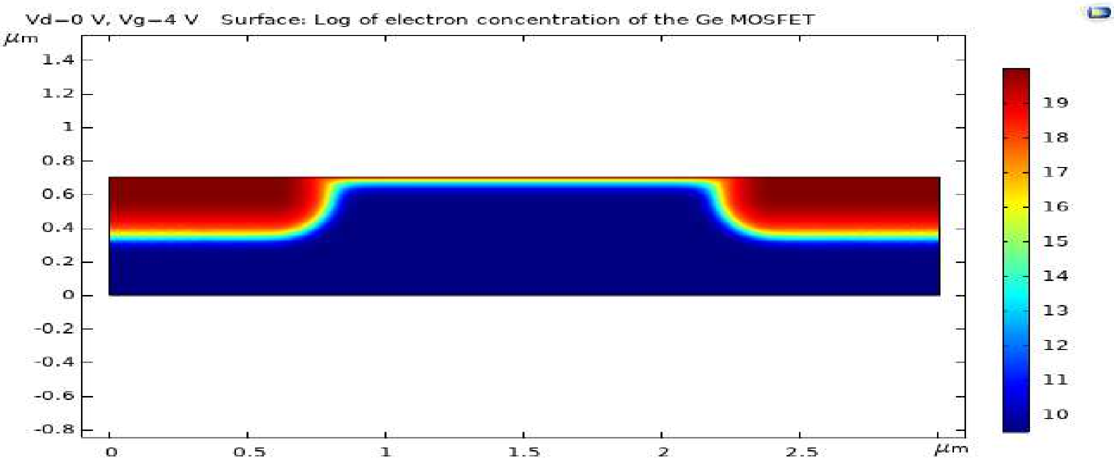

(a) For the V_d= 0V with a fixed V_g= 4V

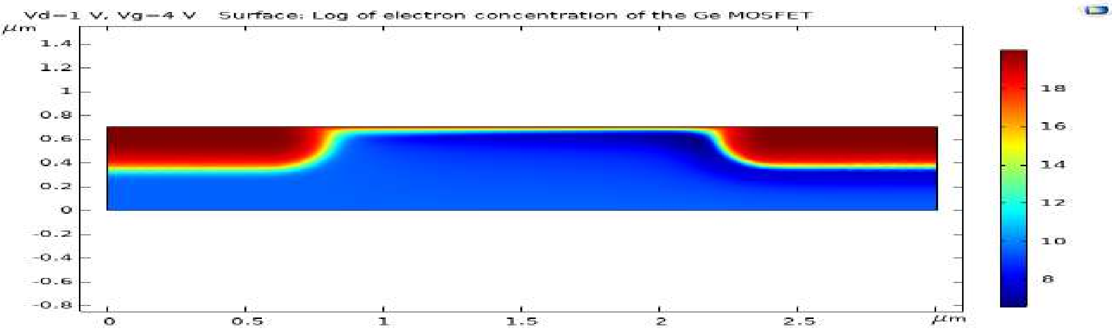

(C) For the V_d= 1V with a fixed V_g= 4V

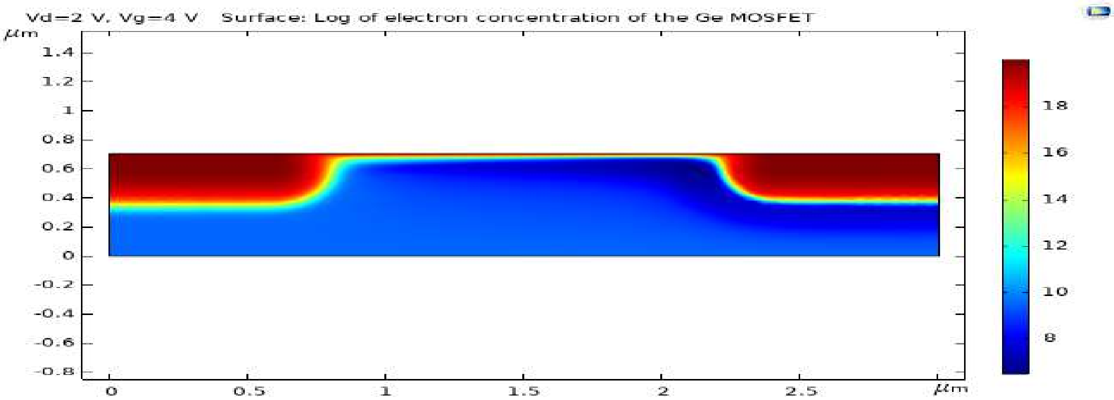

(e) For the V_d= 2V with a fixed V_g= 4V

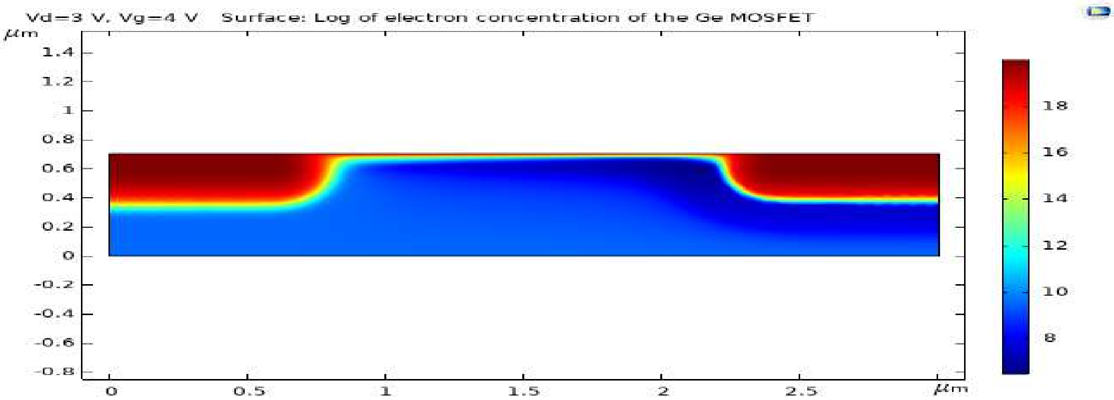

(g) For the V_d= 3V with a fixed V_g= 4V

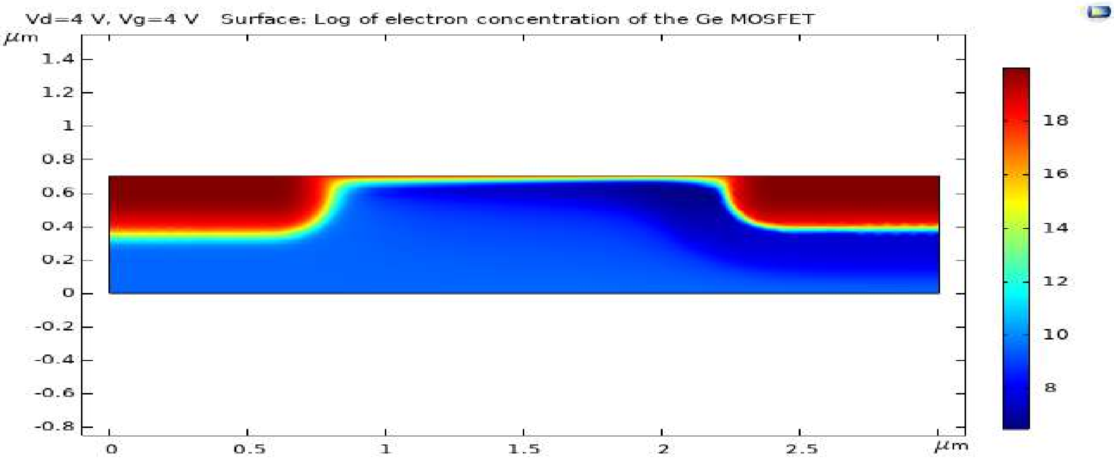

(i) For the V_d= 4V with a fixed V_g= 4V

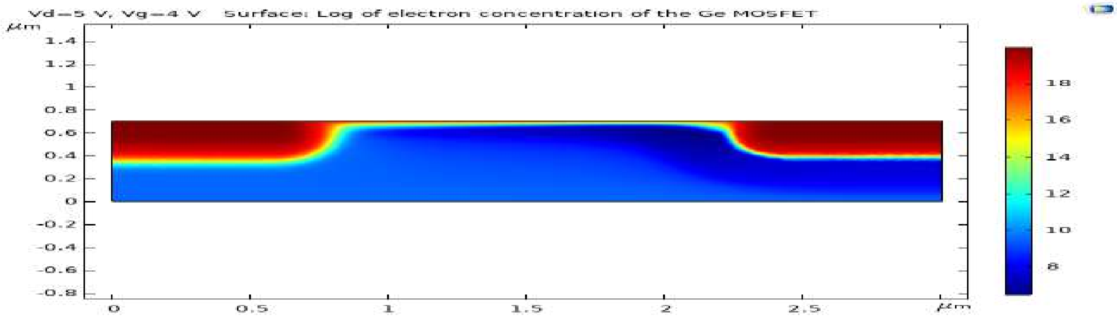

(k) For the V_d= 5V with a fixed V_g= 4V

Fig. 31. Electron Concentration of the Ge based n-type MOSFET with a range of 0V to 5V of V_d with a fixed V_g = 4V

2.3 Ge based nMOS's Hole Concentrations

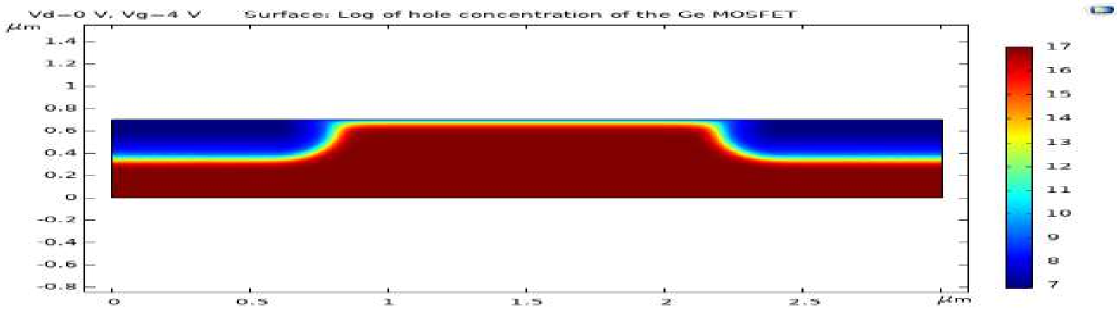

(a) For the V_d= 0V with a fixed V_g= 4V

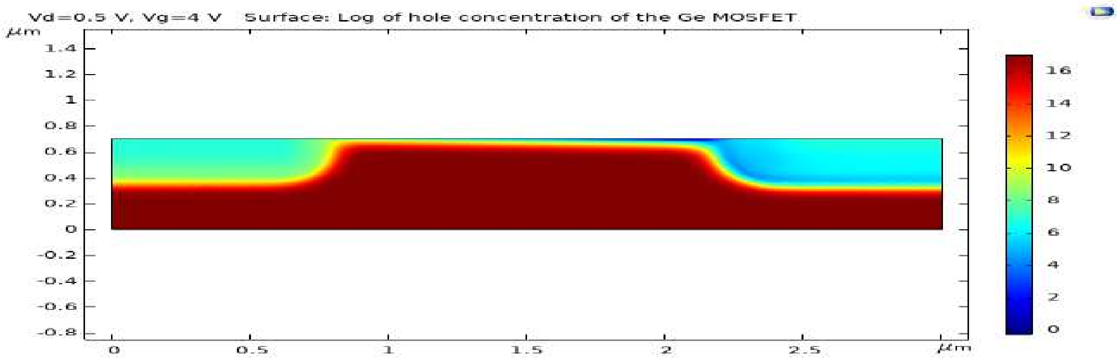

(b) For the V_d= 0.5V with a fixed V_g= 4V

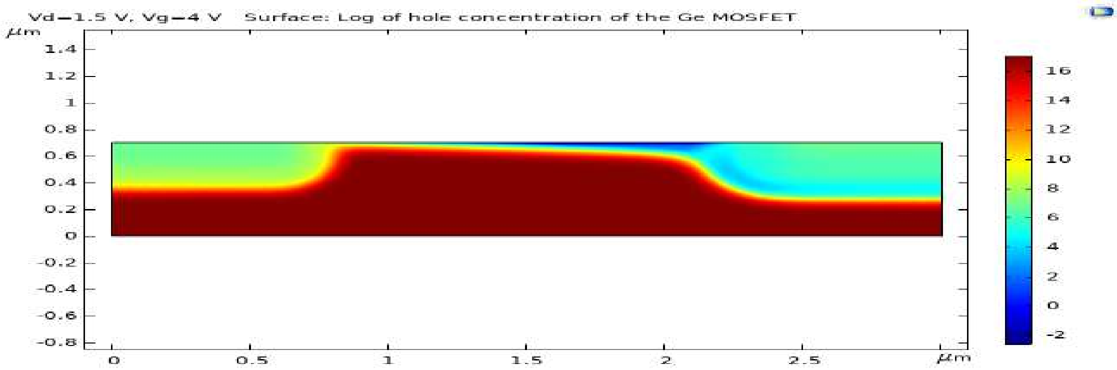

(d) For the V_d= 1.5V with a fixed V_g= 4V

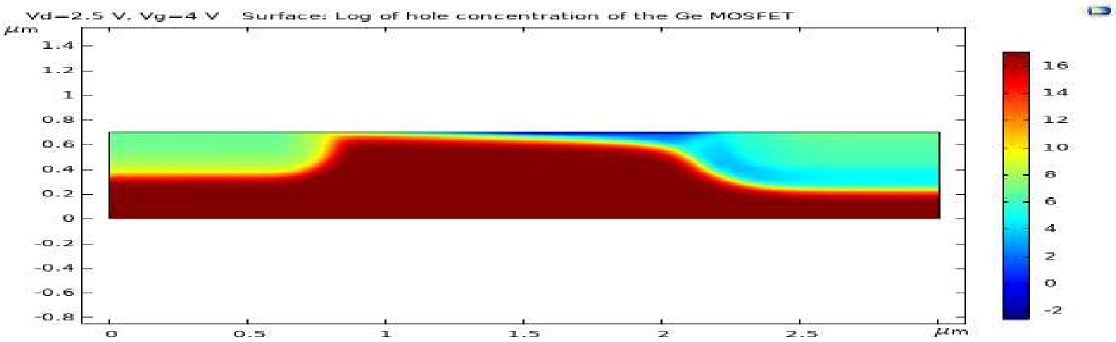

(f) For the V_d= 2.5V with a fixed V_g= 4V

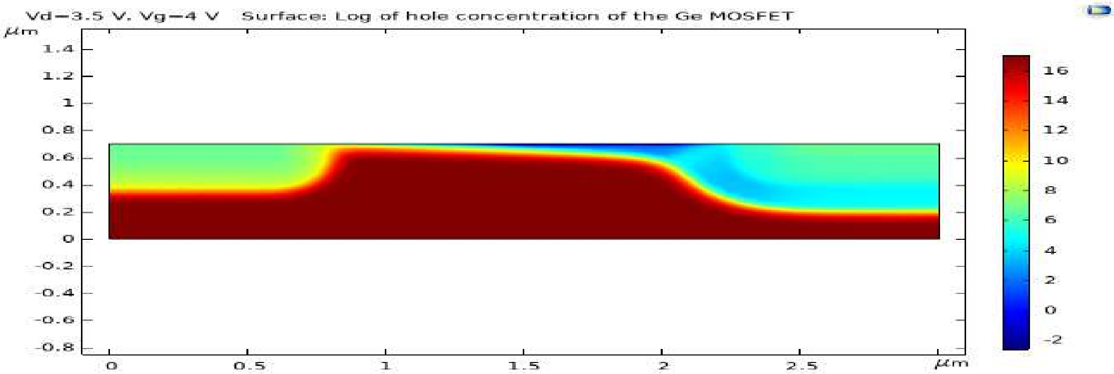

(h) For the V_d= 3.5V with a fixed V_g= 4V

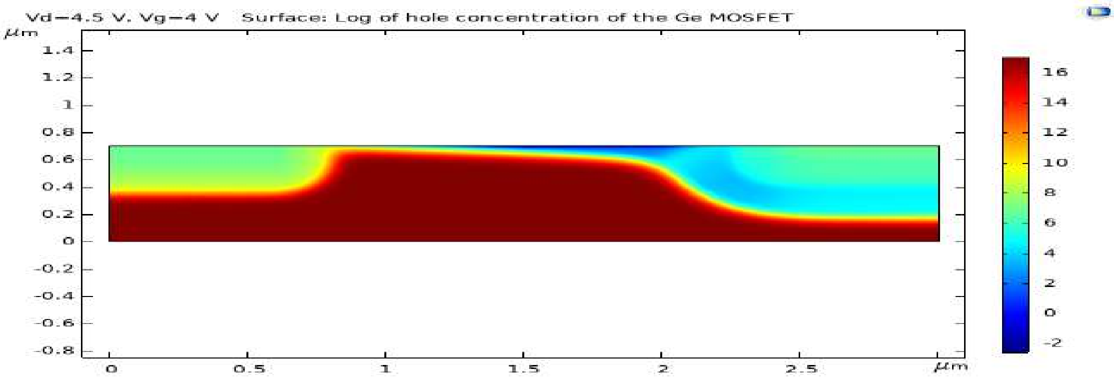

(j) For the V_d= 4.5V with a fixed V_g= 4V

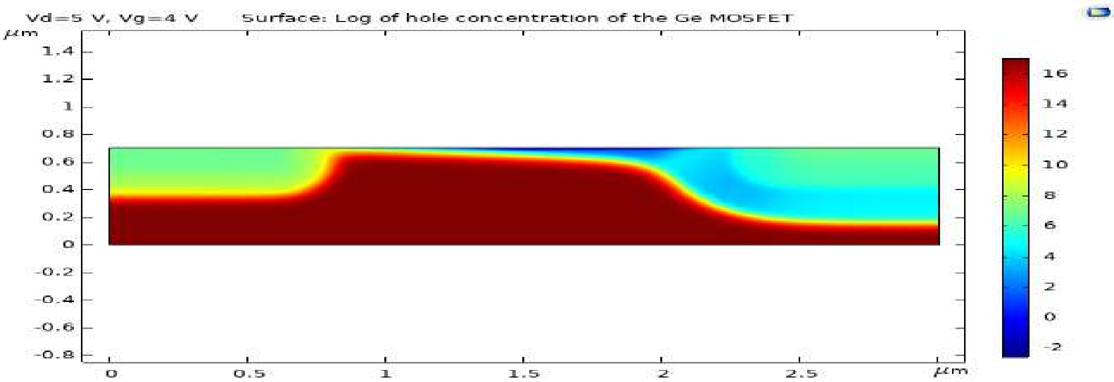

(k) For the V_d= 5V with a fixed V_g= 4V

Fig. 32. Hole Concentration of the Ge based n-type MOSFET with a range of 0V to 5V of V_d with a fixed V_g = 4V

2.4 Ge based nMOS's Electric potentials

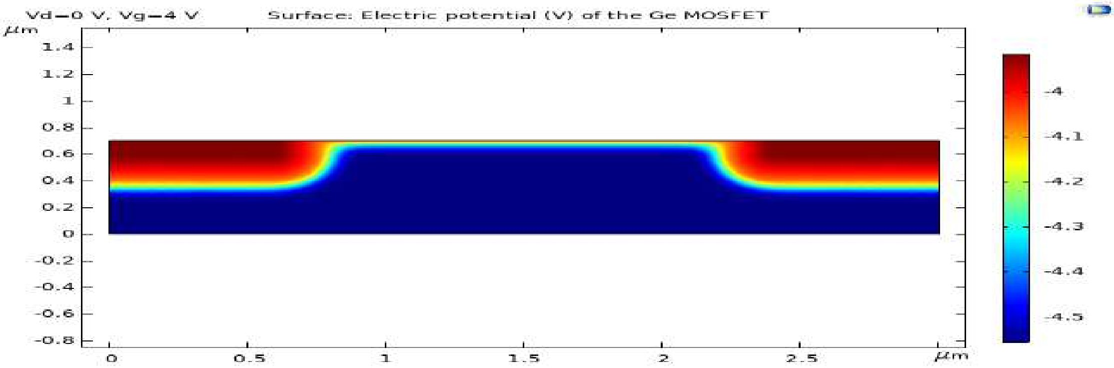

(a) For the V_d= 0V with a fixed V_g= 4V

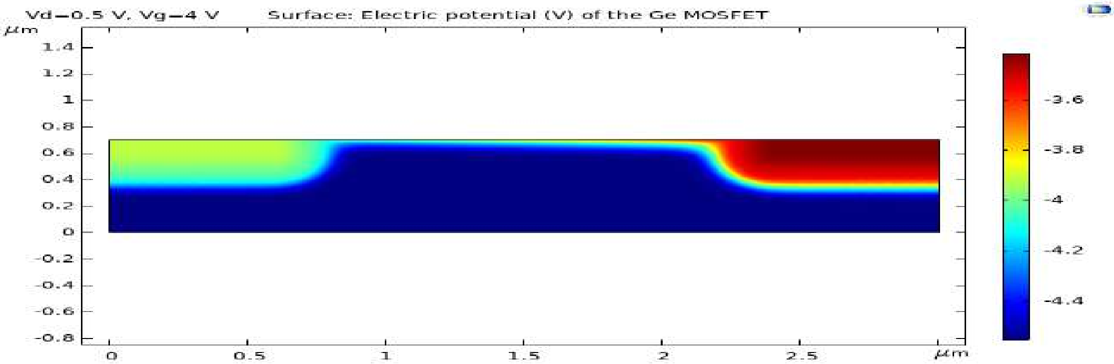

(b) For the V_d= 0.5V with a fixed V_g= 4V

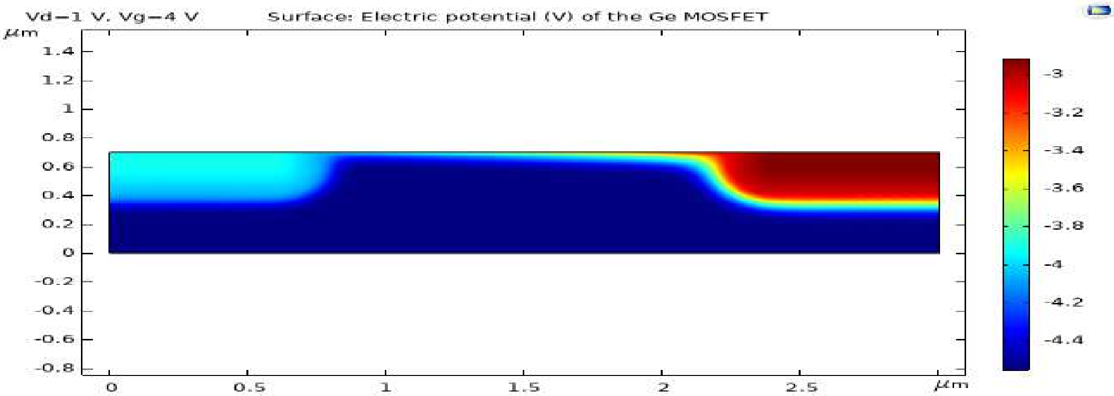

(C) For the V_d= 1V with a fixed V_g= 4V

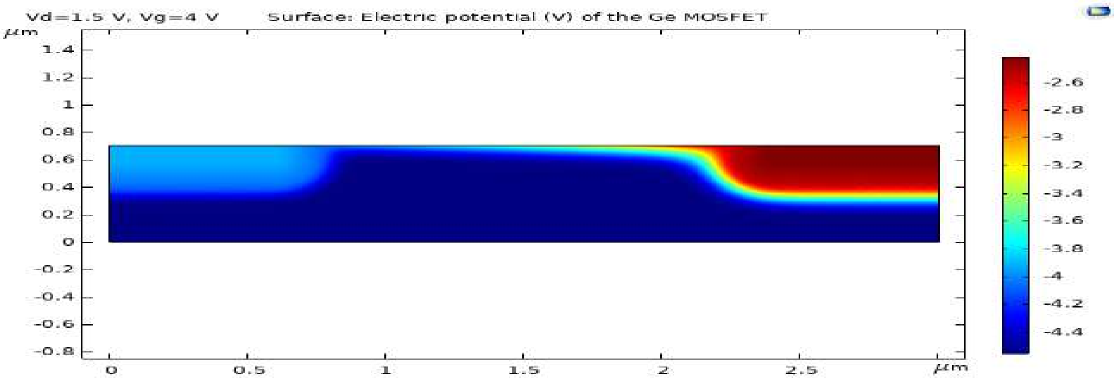

(d) For the V_d= 1.5V with a fixed V_g= 4V

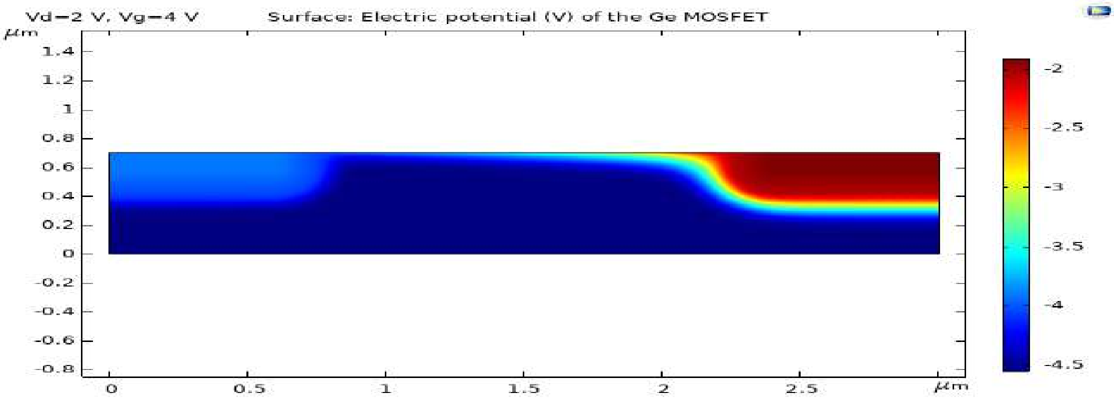

(e) For the V_d= 2V with a fixed V_g= 4V

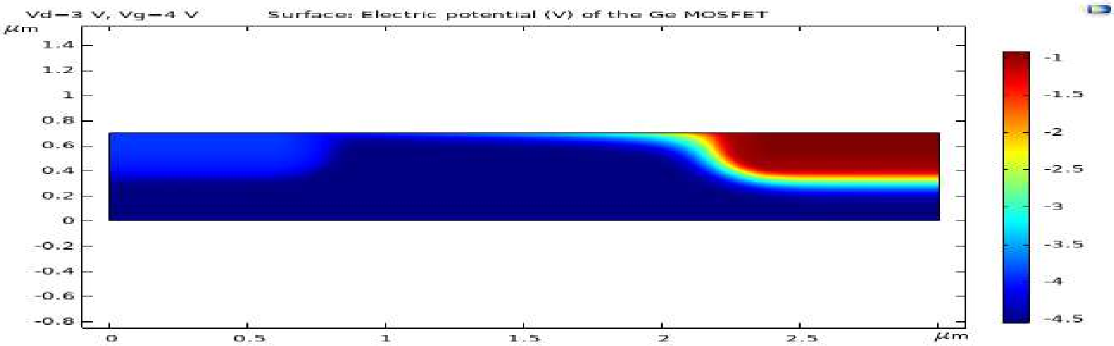

(g) For the V_d= 3V with a fixed V_g= 4V

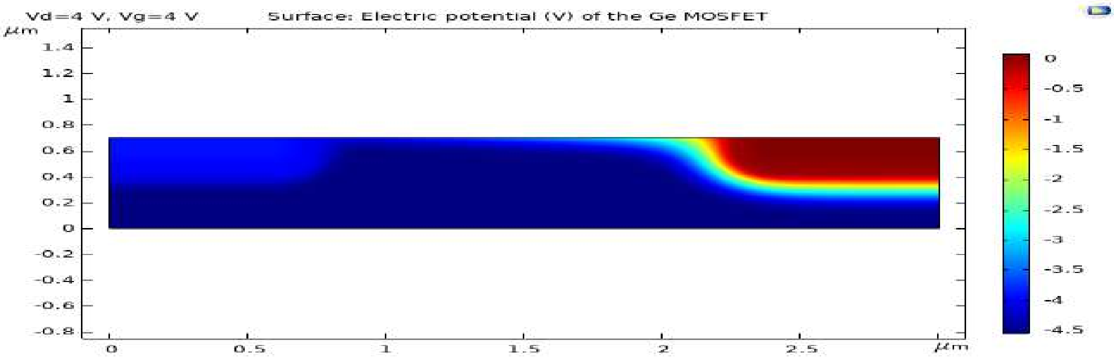

(i) For the V_d= 4V with a fixed V_g= 4V

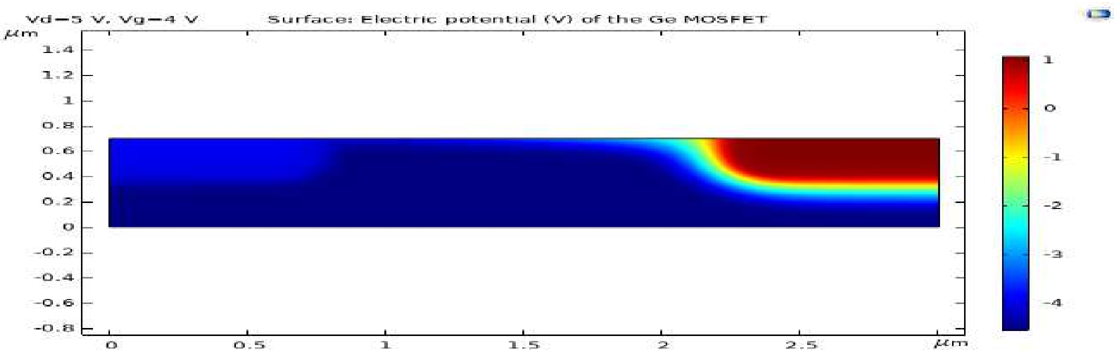

(k) For the V_d= 5V with a fixed V_g= 4V

Fig. 33. Electric Potential (V) of the Ge based n-type MOSFET with a range of 0V to 5V of V_d with a fixed V_g = 4V

3. SiC Based nMOS's Characteristics

3.1 SiC based nMOS's Signed Dopent Concentrations

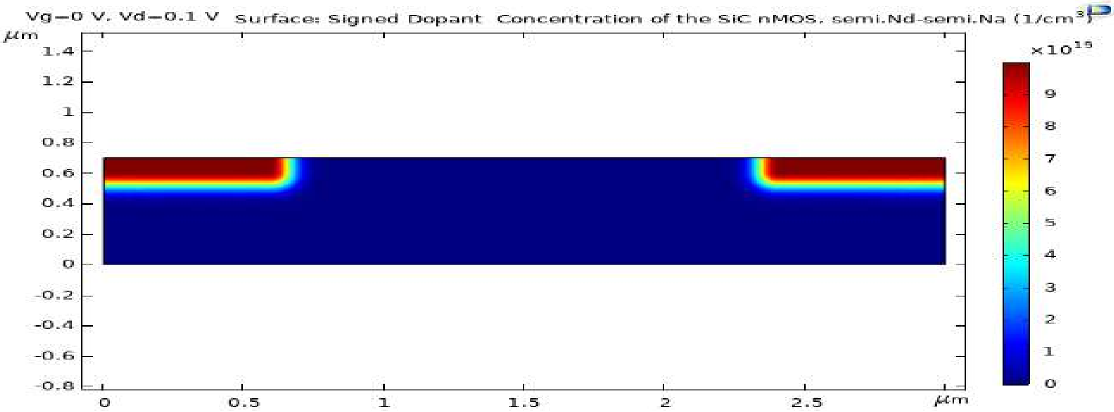

(a) For the V_g= 0V with a fixed V_d= 0.01V

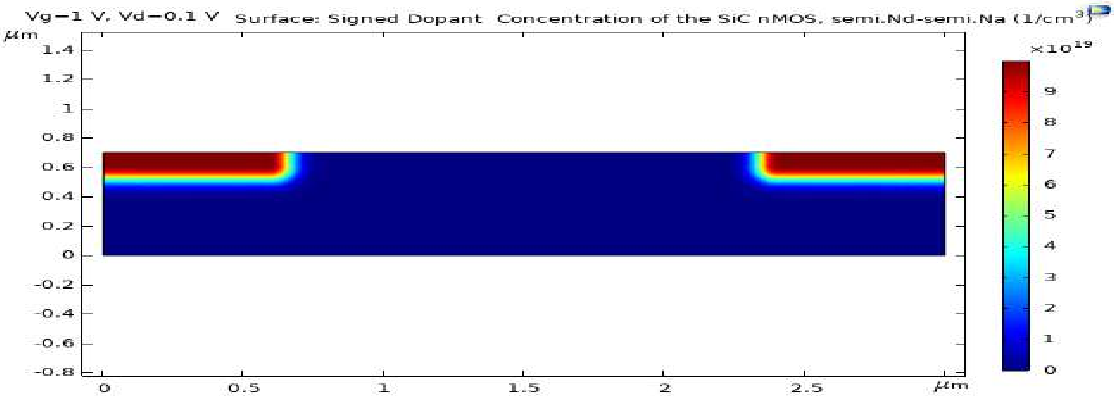

(a) For the V_g= 1V with a fixed V_d= 0.01V

Fig. 34. Signed Dopant Concentration of the SiC based n-type MOSFET for different values of V_g

3.2 SiC based nMOS's Electron Concentrations

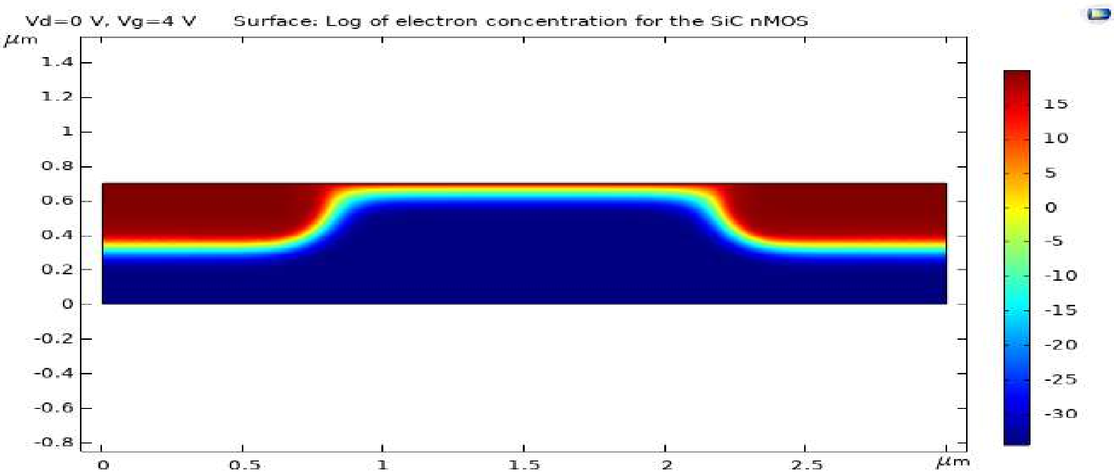

(a) For the V_d= 0V with a fixed V_g= 4V

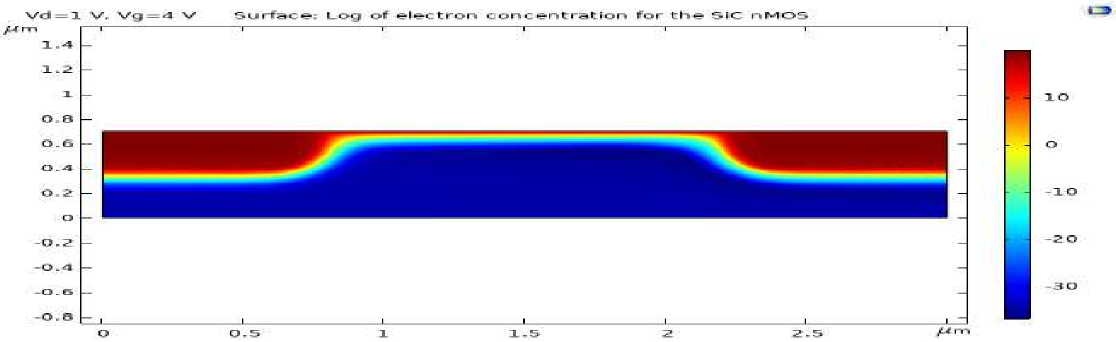

(C) For the V_d= 1V with a fixed V_g= 4V

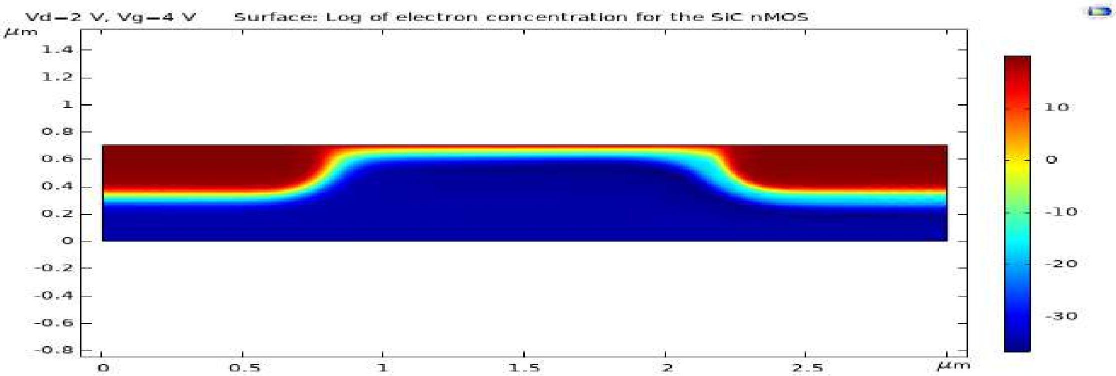

(e) For the V_d= 2V with a fixed V_g= 4V

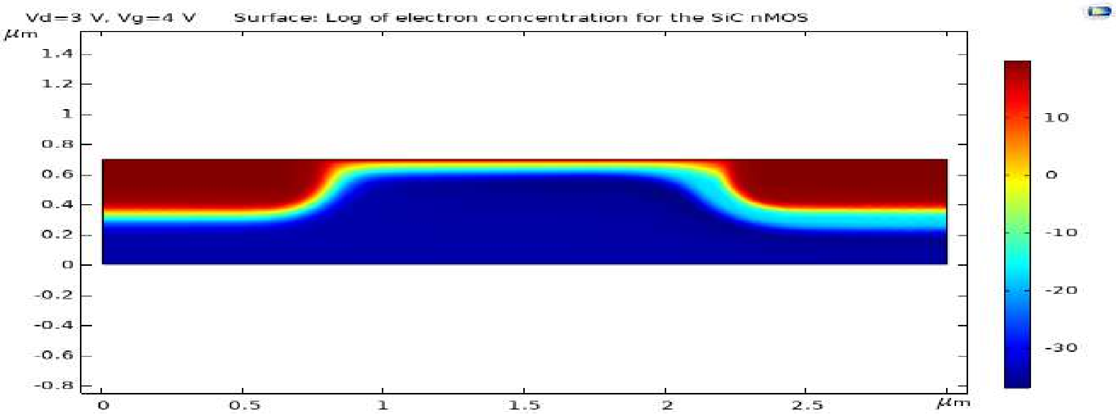

(g) For the V_d= 3V with a fixed V_g= 4V

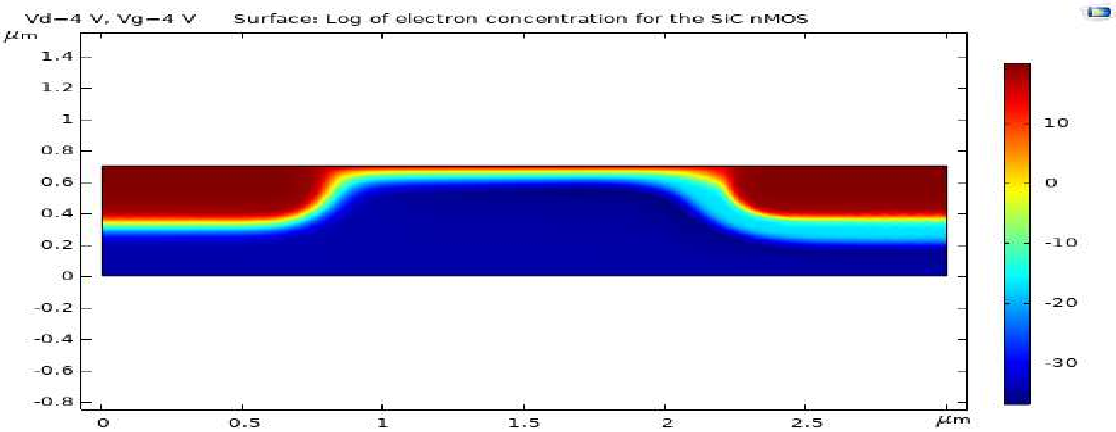

(i) For the V_d= 4V with a fixed V_g= 4V

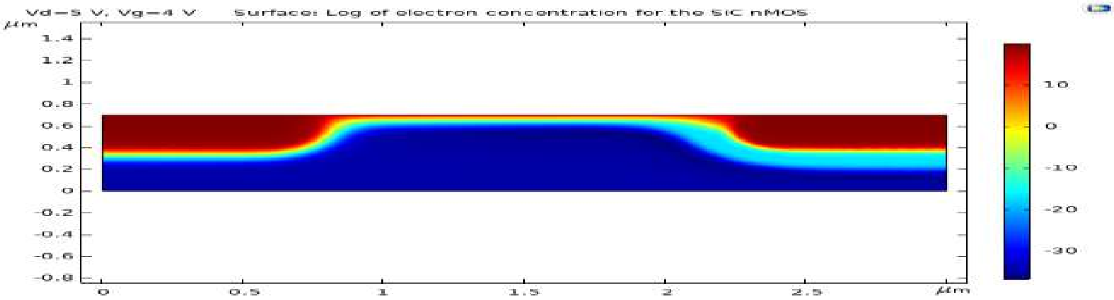

(k) For the V_d= 5V with a fixed V_g= 4V

Fig. 35. Electron Concentration of the SiC based n-type MOSFET with a range of 0V to 5V of V_d with a fixed V_g = 4V

3.3 SiC based nMOS's Hole Concentrations

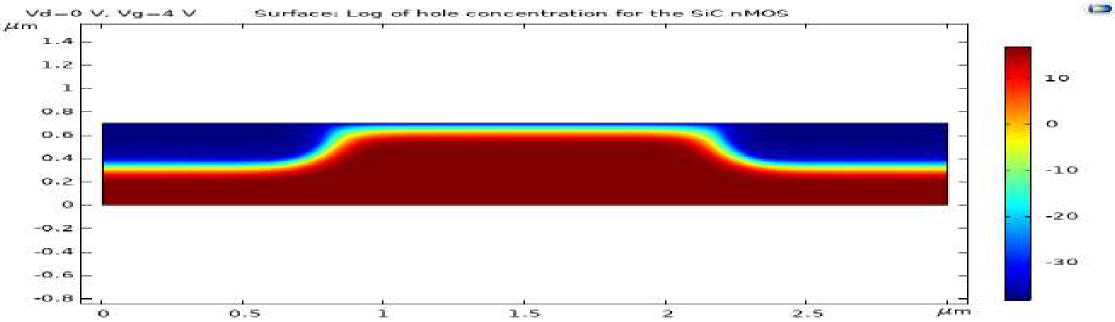

(a) For the V_d= 0V with a fixed V_g= 4V

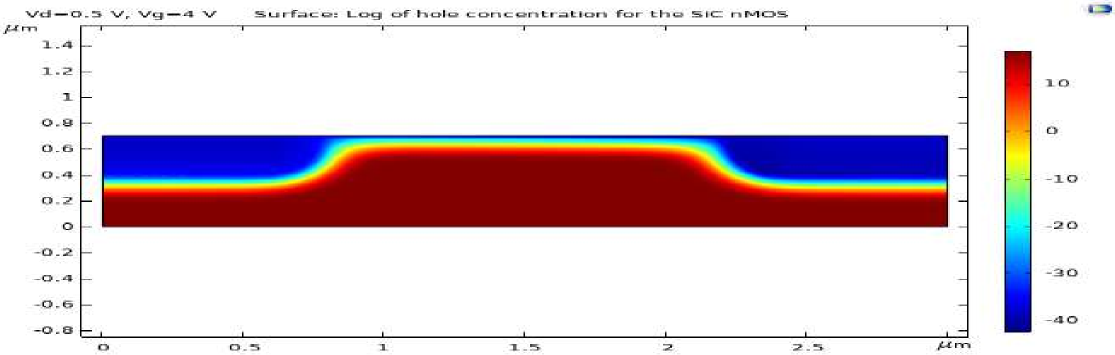

(b) For the V_d= 0.5V with a fixed V_g= 4V

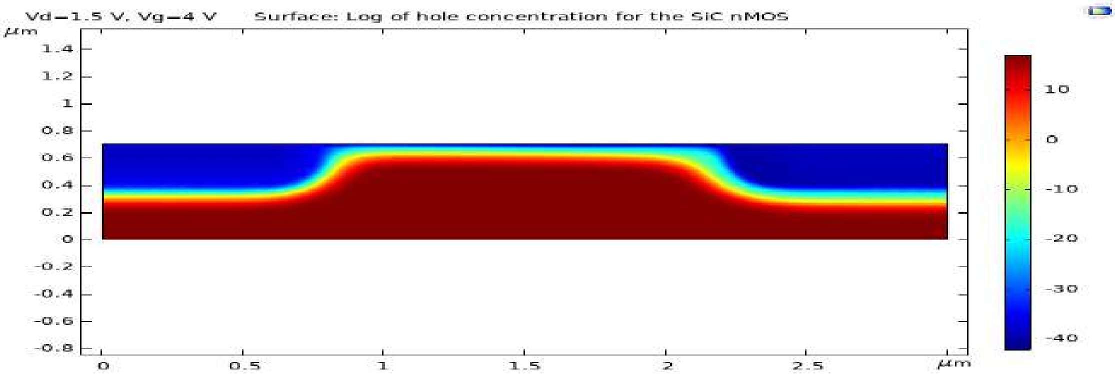

(d) For the V_d= 1.5V with a fixed V_g= 4V

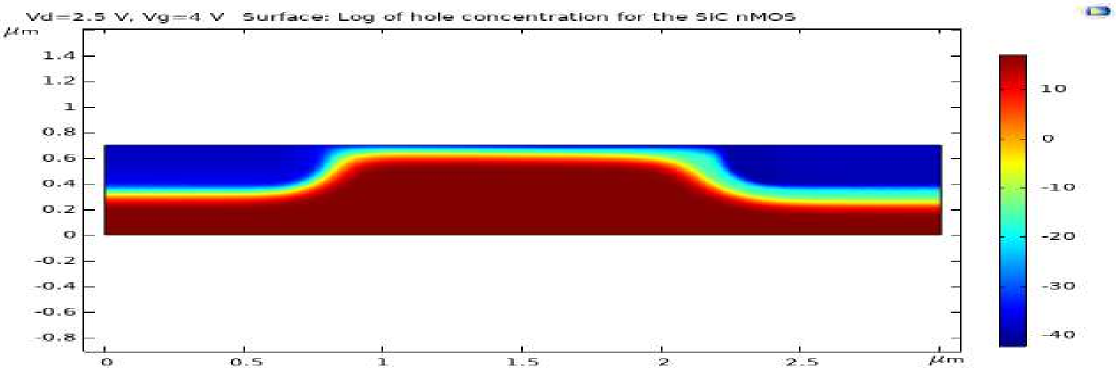

(f) For the V_d= 2.5V with a fixed V_g= 4V

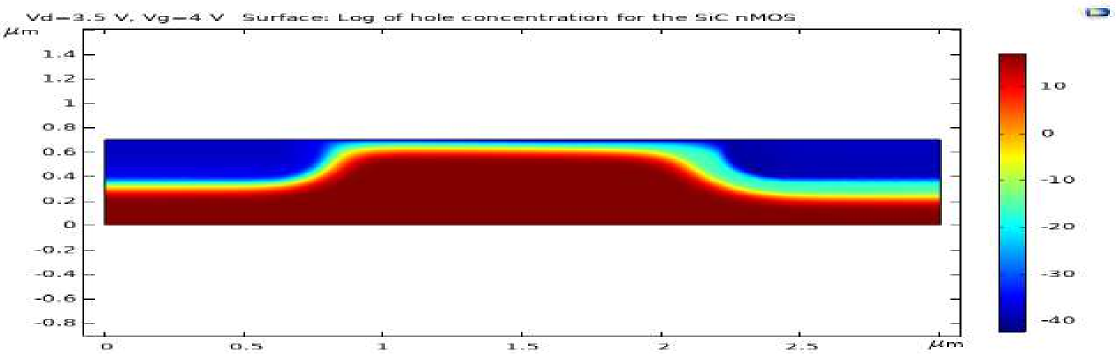

(h) For the V_d= 3.5V with a fixed V_g= 4V

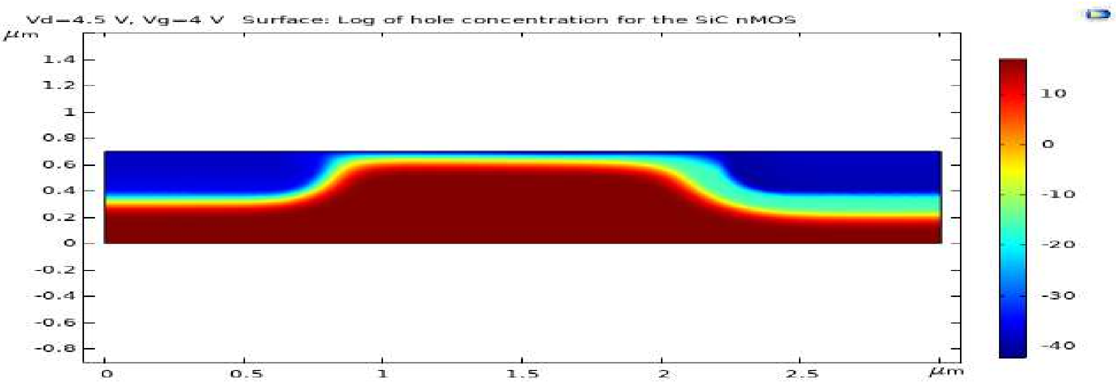

(j) For the V_d= 4.5V with a fixed V_g= 4V

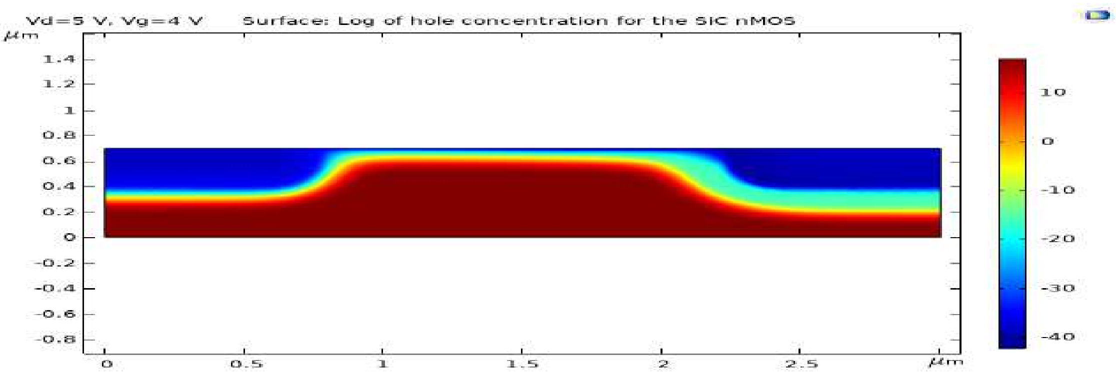

(k) For the V_d= 5V with a fixed V_g= 4V

Fig. 36. Hole Concentration of the SiC based n-type MOSFET with a range of 0V to 5V of V_d with a fixed V_g = 4V

3.4 SiC based nMOS's Electric potentials (V)

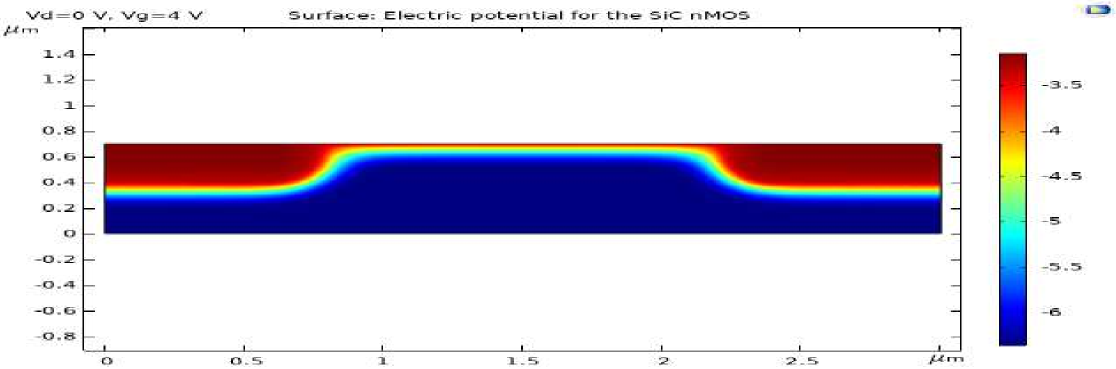

(a) For the V_d= 0V with a fixed V_g= 4V

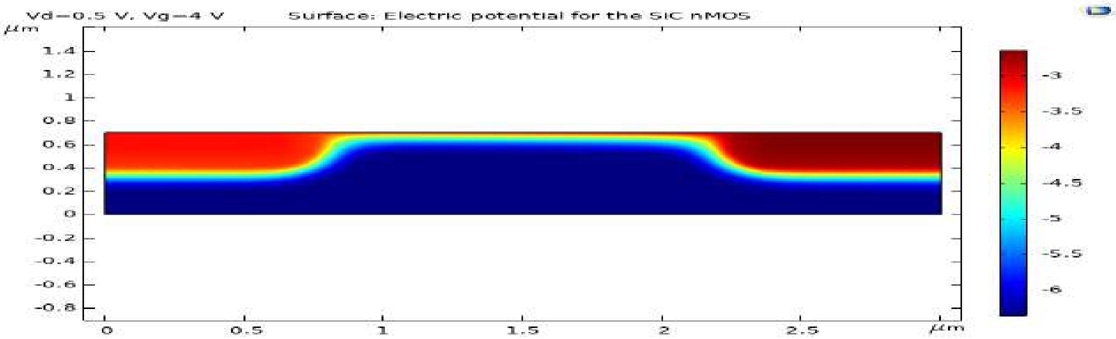

(b) For the V_d= 0.5V with a fixed V_g= 4V

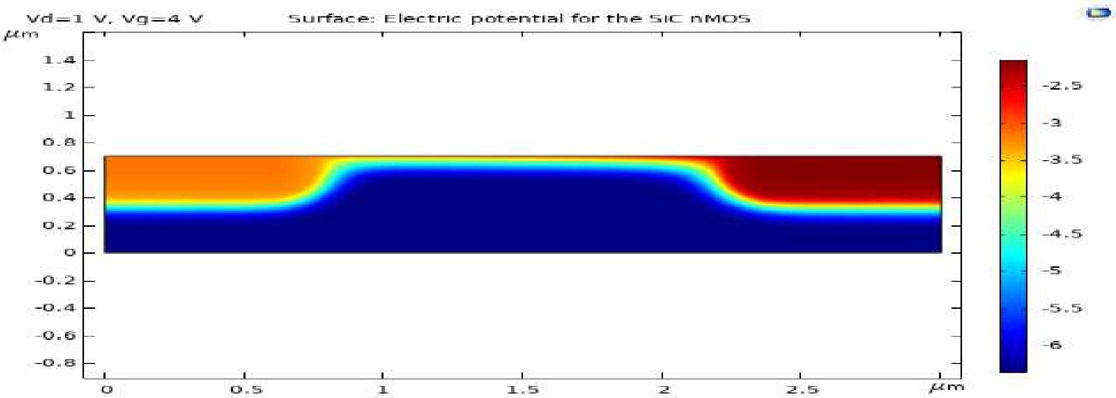

(C) For the V_d= 1V with a fixed V_g= 4V

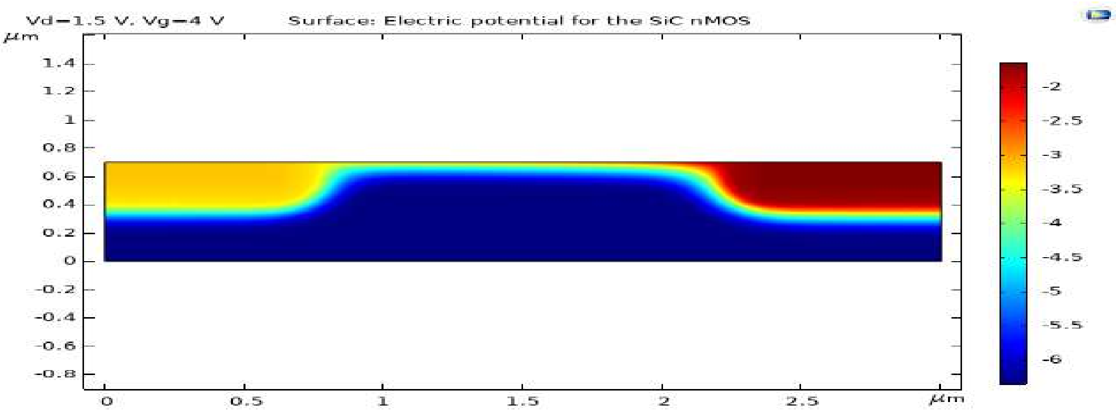

(d) For the V_d= 1.5V with a fixed V_g= 4V

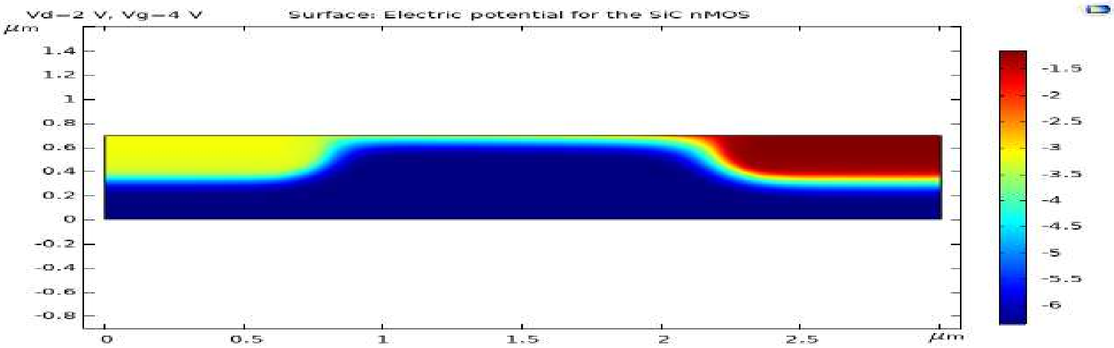

(e) For the V_d= 2V with a fixed V_g= 4V

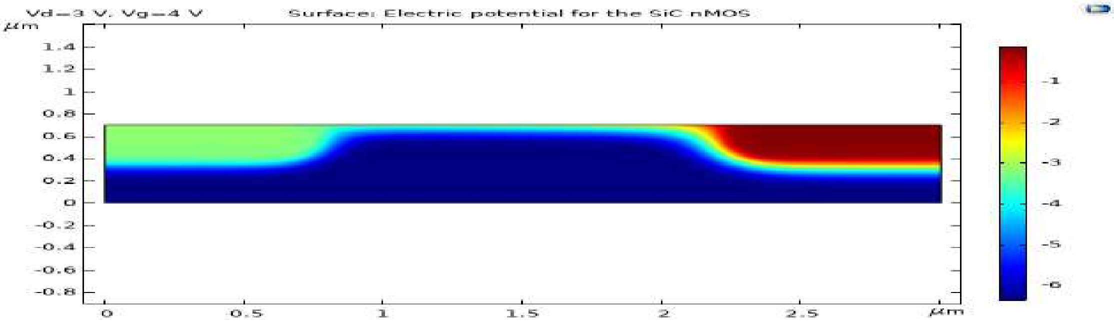

(g) For the V_d= 3V with a fixed V_g= 4V

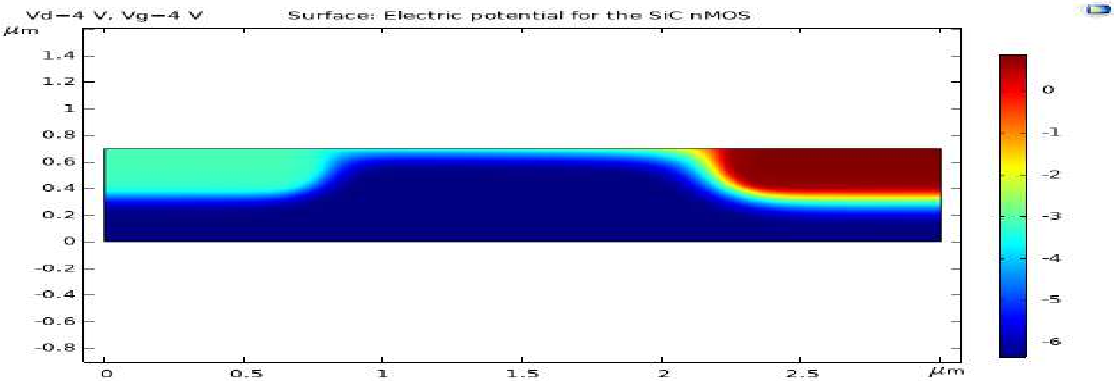

(i) For the V_d= 4V with a fixed V_g= 4V

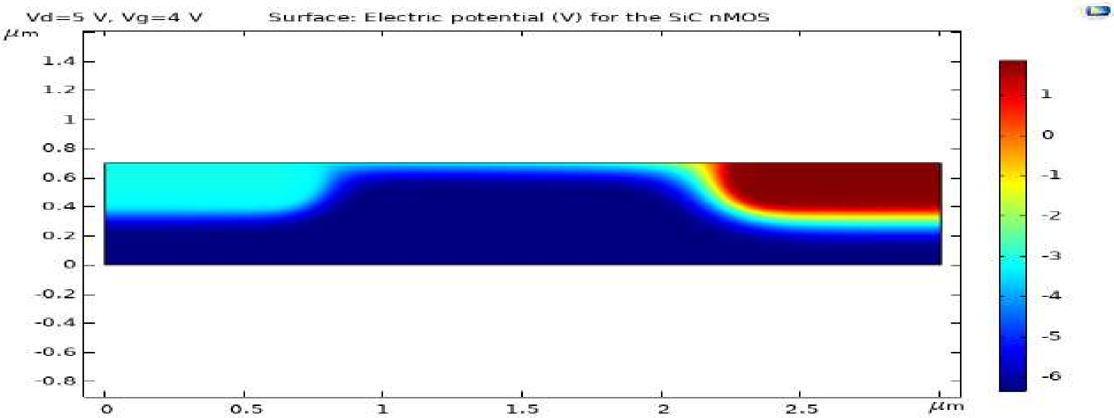

(k) For the V_d= 5V with a fixed V_g= 4V

Fig. 37. Electric Potential (V) of the SiC based n-type MOSFET with a range of 0V to 5V of V_d with a fixed V_g = 4V

APPENDIX-II

1. All Properties of given Material

(a) For MOSFET

Table 3. The properties of Si, Ge and SiC given in COMSOL Multiphysics 5.5

Property	Si	Ge	SiC	unit	Model Name
Relative permittivity	11.7	16.2	9.7	1	Basic
Thermal conductivity	131	60	450	W/(m·K)	Basic
Density	2329	5323	3200	kg/m³	Basic
Heat capacity at constant pressure	700	310	1200	J/(kg·K)	Basic
Band gap	1.12	0.664	3.26	V	Semiconductor material
Electron affinity	4.05	4	3.24	V	Semiconductor material
Effective density of states, valence band	1.04e19	5.0e18	2.5e19	1/cm³	Semiconductor material
Effective density of states, conduction band	2.8e19	1.0e19	1.7e19	1/cm³	Semiconductor material
Electron mobility	1450	3900	900	cm²/(V·s)	Semiconductor material
Hole mobility	500	1900	120	cm²/(V·s)	Semiconductor material
Electron lifetime, SRH	10e-6	10^-3	2.50E-06	s	Shockley-Read-Hall recombination
Hole lifetime, SRH	10e-6	10^-4	5.00E-07	s	Shockley-Read-Hall recombination
Jain-Roulston coefficient (n-type), A	3.5e-8	8.67e-9	1.00E-08	V	Jain-Roulston model
Jain-Roulston coefficient (n-type), B	0	2.57e-7	3.00E-07	V	Jain-Roulston model
Jain-Roulston coefficient (n-type), C	0[V]	4.31e-12	1.00E-11	V	Jain-Roulston model
Jain-Roulston coefficient (p-type), A	3.5e-8	8.21e-9	1.00E-08	V	Jain-Roulston model
Jain-Roulston coefficient (p-type), B	0	2.90e-7	3.00E-07	V	Jain-Roulston model
Jain-Roulston coefficient (p-type), C	0	5.77e-12	1.00E-11	V	Jain-Roulston model
Band-gap narrowing reference concentration	1	1	1.3*10^23	1/cm³	Jain-Roulston model
Conduction band fraction	0.5	0.5	0.5	1	Jain-Roulston model
Electron mobility reference	1252			cm²/(V·s)	Arora mobility model
Hole mobility reference	407			cm²/(V·s)	Arora mobility model
Electron mobility reference minimum	88			cm²/(V·s)	Arora mobility model
Hole mobility reference minimum	54.3			cm²/(V·s)	Arora mobility model

Property	Si	Ge	SiC	unit	Model Name
Electron reference impurity concentration	1.26e17			1/cm³	Arora mobility model
Hole reference impurity concentration	2.35e17			1/cm³	Arora mobility model
Alpha coefficient	0.88			1	Arora mobility model
Mobility reference minimum exponent	-0.57			1	Arora mobility model
Mobility reference exponent	-2.33			1	Arora mobility model
Impurity concentration reference exponent	-2.33			1	Arora mobility model
Alpha coefficient exponent	-0.146			1	Arora mobility model
Reference temperature	300			K	Arora mobility model
Auger recombination factor, electrons	2.8e-31			cm⁶/s	Auger recombination
Auger recombination factor, holes	9.9e-32			cm⁶/s	Auger recombination
Electrical Conductivity			1e3	S/m	Basic
Surface emissivity			0.5	1	Basic
Relative permeability			1	1	Basic
Electron alpha coefficient	1.11			1	Caughey-Thomas mobility model
Hole alpha coefficient	1.21			1	Caughey-Thomas mobility model
Electron saturation velocity	1e7			cm/s	Caughey-Thomas mobility model
Hole saturation velocity	8.37e6			cm/s	Caughey-Thomas mobility model
Electron alpha exponent	0.66			1	Caughey-Thomas mobility model
Hole alpha exponent	0.17			1	Caughey-Thomas mobility model
Electron velocity saturation exponent	-0.87			1	Caughey-Thomas mobility model
Hole velocity saturation exponent	-0.52			1	Caughey-Thomas mobility model
Reference temperature	300			K	Caughey-Thomas mobility model
Direct recombination factor	0			cm³/s	Direct recombination
Fletcher mobility coefficient 1	1.04e21			1/(V·cm·s)	Fletcher mobility model
Fletcher mobility coefficient 2	7.45e13			1/cm²	Fletcher mobility model
Reference temperature	300			K	Fletcher mobility model
a factor, electrons, impact ionization	0.426			1/V	Impact ionization

Property	Si	Ge	SiC	unit	Model Name
a factor, holes, impact ionization	0.243			1/V	Impact ionization
b factor, electrons, impact ionization	4.81E5			V/cm	Impact ionization
b factor, holes, impact ionization	6.53E5			V/cm	Impact ionization
c factor, electrons, impact ionization	3.05E-04			1/K	Impact ionization
c factor, holes, impact ionization	5.35E-04			1/K	Impact ionization
d factor, electrons, impact ionization	6.86E-04			1/K	Impact ionization
d factor, holes, impact ionization	5.67E-04			1/K	Impact ionization
Electron delta coefficient	5.82e14			V/s	Lombardi surface mobility model
Hole delta coefficient	2.05e14			V/s	Lombardi surface mobility model
Electron mobility reference 1	4.75e7			$cm^2/(V \cdot s)$	Lombardi surface mobility model
Hole mobility reference 1	9.93e7			$cm^2/(V \cdot s)$	Lombardi surface mobility model
Electron mobility reference 2	1.74e5			$cm^2/(V \cdot s)$	Lombardi surface mobility model
Hole mobility reference 2	8.84e5			$cm^2/(V \cdot s)$	Lombardi surface mobility model
Electron alpha coefficient	0.125			1	Lombardi surface mobility model
Hole alpha coefficient	0.0317			1	Lombardi surface mobility model
Reference temperature	1[K]			K	Lombardi surface mobility model
Electric field reference	1			V/cm	Lombardi surface mobility model
Doping concentration reference	1			$1/cm^3$	Lombardi surface mobility model
Electron mobility reference	1448			$cm^2/(V \cdot s)$	Power law mobility model
Hole mobility reference	473			$cm^2/(V \cdot s)$	Power law mobility model
Electron exponent	2.33			1	Power law mobility model
Hole exponent	2.23			1	Power law mobility model
Reference temperature	300			K	Power law mobility model
Band-gap narrowing reference energy	0.00692			V	Slotboom model
Band-gap narrowing reference concentration	1.3e17			$1/cm^3$	Slotboom model
Conduction band fraction	0.5			1	Slotboom model

(b) For PiN Diode

Table 4. The properties of Si, Ge and SiC given in COMSOL Multiphysics 5.5

Property	Si	Ge	SiC	unit	Model Name
Relative permittivity	11.7	16.2	10	1	Basic
Band gap	1.12	0.664	3.26	V	Semiconductor material
Electron affinity	4.05	4	3.24	V	Semiconductor material
Effective density of states, valence band	1.04e19	6.0e18	2.5E+25	1/cm³	Semiconductor material
Effective density of states, conduction band	2.8e19	1.04e19	1.7E+25	1/cm³	Semiconductor material
Electron mobility	1450	3900	0.09	cm²/(V·s)	Semiconductor material
Hole mobility	500	1900	0.012	cm²/(V·s)	Semiconductor material
Heat capacity at constant pressure	700	310	1200	J/(kg·K)	Basic
Thermal conductivity	131	60	450	W/(m·K)	Basic
Density	2329	5323	3200	kg/m³	Basic
Electrical conductivity			1e3	S/m	Basic
Relative permeability			1.00E+00	1	Basic
Surface emissivity			5.00E-01	1	Basic
Electron mobility reference	1252			cm²/(V·s)	Arora mobility model
Hole mobility reference	407			cm²/(V·s)	Arora mobility model
Electron mobility reference minimum	88			cm²/(V·s)	Arora mobility model
Hole mobility reference minimum	54.3			cm²/(V·s)	Arora mobility model
Electron reference impurity concentration	1.26e17			1/cm³	Arora mobility model
Hole reference impurity concentration	2.35e17			1/cm³	Arora mobility model
Alpha coefficient	0.88			1	Arora mobility model
Mobility reference minimum exponent	-0.57			1	Arora mobility model
Mobility reference exponent	-2.33			1	Arora mobility model
Impurity concentration reference exponent	-2.33			1	Arora mobility model
Alpha coefficient exponent	-0.146			1	Arora mobility model
Reference temperature	300			K	Arora mobility model
Electron mobility reference	1448			cm²/(V·s)	Power law mobility model
Hole mobility reference	473			cm²/(V·s)	Power law mobility model

Property	Si	Ge	SiC	unit	Model Name
Electron exponent	2.33			1	Power law mobility model
Hole exponent	2.23			1	Power law mobility model
Reference temperature	300			K	Power law mobility model
Auger recombination factor, electrons	2.8e-31			cm^6/s	Auger recombination
Auger recombination factor, holes	9.9e-32			cm^6/s	Auger recombination
Direct recombination factor	0			cm^3/s	Direct recombination
Electron lifetime, SRH	10e-6			s	Shockley-Read-Hall recombination
Hole lifetime, SRH	10e-6			S	Shockley-Read-Hall recombination
Fletcher mobility coefficient 1	1.04e21			1/(V·cm·s)	Fletcher mobility model
Fletcher mobility coefficient 2	7.45e13			$1/cm^2$	Fletcher mobility model
Reference temperature	300			K	Fletcher mobility model
Electron alpha coefficient	1.11			1	Caughey-Thomas mobility model
Hole alpha coefficient	1.21			1	Caughey-Thomas mobility model
Electron saturation velocity	1e7			cm/s	Caughey-Thomas mobility model
Hole saturation velocity	8.37e6			cm/s	Caughey-Thomas mobility model
Electron alpha exponent	0.66			1	Caughey-Thomas mobility model
Hole alpha exponent	0.17			1	Caughey-Thomas mobility model
Electron velocity saturation exponent	-0.87			1	Caughey-Thomas mobility model
Hole velocity saturation exponent	-0.52			1	Caughey-Thomas mobility model
Reference temperature	300			K	Caughey-Thomas mobility model
Electron delta coefficient	5.82e14			V/s	Lombardi surface mobility model
Hole delta coefficient	2.05e14			V/s	Lombardi surface mobility model
Electron mobility reference 1	4.75e7			$cm^2/(V·s)$	Lombardi surface mobility model
Hole mobility reference 1	9.93e7			$cm^2/(V·s)$	Lombardi surface mobility model
Electron mobility reference 2	1.74e5			$cm^2/(V·s)$	Lombardi surface mobility model
Hole mobility reference 2	8.84e5			$cm^2/(V·s)$	Lombardi surface mobility model

Property	Si	Ge	SiC	unit	Model Name
Electron alpha coefficient	0.125			1	Lombardi surface mobility model
Hole alpha coefficient	0.0317			1	Lombardi surface mobility model
Reference temperature	1			K	Lombardi surface mobility model
Electric field reference	1			V/cm	Lombardi surface mobility model
Doping concentration reference	1			$1/cm^3$	Lombardi surface mobility model
a factor, electrons, impact ionization	0.426			1/V	Impact ionization
a factor, holes, impact ionization	0.243			1/V	Impact ionization
b factor, electrons, impact ionization	4.81E5			V/cm	Impact ionization
b factor, holes, impact ionization	6.53E5			V/cm	Impact ionization
c factor, electrons, impact ionization	0.000305			1/K	Impact ionization
c factor, holes, impact ionization	0.000535			1/K	Impact ionization
d factor, electrons, impact ionization	0.000686			1/K	Impact ionization
d factor, holes, impact ionization	0.000567			1/K	Impact ionization
Band-gap narrowing reference energy	0.00692			V	Slotboom model
Band-gap narrowing reference concentration	1.3e17			$1/cm^3$	Slotboom model
Conduction band fraction	0.5			1	Slotboom model
Jain-Roulston coefficient (n-type), A	3.5e-8	8.67e-9		V	Jain-Roulston model
Jain-Roulston coefficient (n-type), B	0	2.57e-7		V	Jain-Roulston model
Jain-Roulston coefficient (n-type), C	0	4.31e-12		V	Jain-Roulston model
Jain-Roulston coefficient (p-type), A	3.5e-8	8.21e-9		V	Jain-Roulston model
Jain-Roulston coefficient (p-type), B	0	2.90e-7		V	Jain-Roulston model
Jain-Roulston coefficient (p-type), C	0	5.77e-12		V	Jain-Roulston model
Band-gap narrowing reference concentration	1	1		$1/cm^3$	Jain-Roulston model
Conduction band fraction	0.5	0.5		1	Jain-Roulston model